FATIGUE TESTS ON TRAILER HITCH AT FAST (FAT-II)

FAST Facility for Accelerated Service Testing

TRANSPORTATION TEST CENTER
PUEBLO, COLORADO 81001

Final Report

This document is available to the public through
The National Technical Information Service,
Springfield, Virginia 22161

PREPARED FOR
THE FAST PROGRAM

AN INTERNATIONAL GOVERNMENT - INDUSTRY RESEARCH PROGRAM

U.S. DEPARTMENT OF TRANSPORTATION
FEDERAL RAILROAD ADMINISTRATION
Washington, D.C. 20590

ASSOCIATION OF AMERICAN RAILROADS
1920 L Street, N.W.
Washington, D.C. 20036

RAILWAY PROGRESS INSTITUTE
801 North Fairfax Street
Alexandria, Virginia 22314

RPI

NOTICE

This document reflects events relating to testing at the Facility for Accelerated Service Testing (FAST) at the Transportation Test Center, which may have resulted from conditions, procedures, or the test environment peculiar to that facility. This document is disseminated for the FAST Program under the sponsorship of the U. S. Department of Transportation, the Association of American Railroads, and the Railway Progress Institute in the interest of information exchange. The sponsors assume no liability for its contents or use thereof.

NOTICE

The FAST Program does not endorse products or manufacturers. Trade or manufacturers' names appear herein solely because they are considered essential to the object of this report.

Technical Report Documentation Page

1. Report No.	2. Government Accession No.	3. Recipient's Catalog No.
TTC-011(FAST-FR84)		

4. Title and Subtitle	5. Report Date
FATIGUE TESTS ON TRAILER HITCH AT FAST-- THE FAT II REPORT.	February 1983
	6. Performing Organization Code
7. Author(s)	8. Performing Organization Report No.
G.J. Moyar* and S.K. Punwani**	Dr-156
9. Performing Organization Name and Address	10. Work Unit No. (TRAIS)
Association of American Railroads	
	11. Contract or Grant No.
	DTFR53-82-C-00282
12. Sponsoring Agency Name and Address	13. Type of Report and Period Covered
U.S. Department of Transportation Federal Railroad Administration Office of Research and Development Washington, D.C. 20590	Final
	14. Sponsoring Agency Code

15. Supplementary Notes

*Consultant to the Association of American Railroads
**Assistant Manager, Mechanical, AAR Technical Center.

16. Abstract

Cracks appeared in a hitch and its underdeck support on one of the three Trailer-on-Flat Cars (TOFC) in the FAST (Facility for Accelerated Service Testing) train consist 3,000 miles after inspection (at 186,000 miles). As a result, a series of static and dynamic (FAST operation) tests was undertaken on a similar car in May of 1981.

It was apparent from the static lateral pull tests that lateral loads of the order of 10 kips would cause relatively high (1,000 με), potentially damaging strains if repeated frequently. These high strains occurred in the plate near the vertical strut weld juncture, due primarily to plate bending caused by the particular strut assembly reaction to lateral load. An asymmetry of vertical and lateral loading response was also observed in this test car.

Following conventional S-N procedures described in the AAR Fatigue Design Guidelines, a fatigue analysis was performed using the cycle-counted strain history recorded from the dynamic tests. Fatigue cracking in the hitch is predicted in the hitch plate at the critical location. The effects of direction of travel, speed, deck support, and material properties were also studied. Deck support modification appeared to have little effect.

From analysis of the dynamic strain and acceleration histories, it is concluded that curve-negotiation forces excite lateral dynamic resonances (≃ 7 Hz) of the TOFC combination, causing high strain cycles in the hitch for normal (45 mph) operation. Slower operation (25 mph) over jointed tangent track can also excite another resonance (≃ 1 Hz), which contributes to fatigue damage of the hitch.

17. Key Words		18. Distribution Statement
Crack Propagation	Rail Car Dynamics	
Fatigue	Strain Gaging	
Flat Car Hitch	Stress Analysis	
Freight Car Design	Welded Structures	

19. Security Classif. (of this report)	20. Security Classif. (of this page)	21. No. of Pages	22. Price
Unclassified	Unclassified	120	

Form DOT F 1700.7 (8-72) Reproduction of completed page authorized

TABLE OF CONTENTS

Section			Page
Executive Summary			x
Acknowledgements			xii
1.0	INTRODUCTION		1
	1.1	Background	1
	1.2	Flat Car Hitch Crack Observations	1
2.0	TEST PROGRAM		6
	2.1	Test Objectives	6
	2.2	Test Plan	6
	2.3	Test Instrumentation	6
3.0	SUMMARY OF STATIC TESTS		13
	3.1	Vertical (Load/Empty) Tests	13
	3.2	Static Lateral Load on Hitch	18
		3.2.1 Static Lateral Pull Tests (Trailer off Hitch)	18
		3.2.2 Hitch Lateral Compliance	25
		3.2.3 Static Lateral Pull on Trailer	25
	3.3	Roll and Twist Tests	29
	3.4	Comparisons to Finite Element Model Predictions	29
4.0	FAST DYNAMIC TESTS		37
	4.1	FAT II Test Consist and Data Acquisition	37
	4.2	Typical Transducer Output	37
	4.3	Quick-Look Maximum Range Summaries	37
5.0	FATIGUE ANALYSIS APPROACH		47
	5.1	Preliminary Considerations	47
	5.2	Assumptions	47
		5.2.1 Critical Stress Environment	47
		5.2.2 Cycle Counting	48
		5.2.3 Typical Fatigue Properties	48
		5.2.4 Cumulative Fatigue Damage Rule	48
6.0	LIFE PREDICTIONS FOR CRITICAL REGION		53
	6.1	Effect of Direction of Travel	54
	6.2	Effect of Speed	54
	6.3	Effect of Deck Support	54
	6.4	Effect of Material Properties	56

TABLE OF CONTENTS (CONTINUED)

Section		Page
7.0	ADDITIONAL FATIGUE ANALYSIS	59
7.1	Life Predictions at Other Gage Locations	59
7.2	Life Predictions Based on Measured Acceleration and Load	59
7.3	Crack Propagation Considerations	60
8.0	LOAD ENVIRONMENT COMPARISONS	63
8.1	Guideline REPOS	63
8.2	TTX Road Tests	63
8.3	FEEST Box Car Tests	70
8.4	FAST Wayside Lateral Wheel Load Environment	70
9.0	DYNAMICS	73
9.1	General Observations from Strip Charts	73
9.2	Resonant Frequencies from PSD Analysis	73
9.3	Comparisons to RDL Test and Computer Model	85
10.0	CONCLUSIONS AND RECOMMENDATIONS	89
10.1	Conclusions	89
10.2	Recommendations	89
11.0	REFERENCES	91

Appendix 1 Instrumentation

Appendix 2 State of Stress Considerations

Appendix 3 Load and Acceleration Stress Conversion Factors

Appendix 4 Data Base Structure

Appendix 5 Summary of Data Conversion Program

Appendix 6 Summary of Data Reduction Program

LIST OF FIGURES

Figure		Page
1	Cushioned Hitch Assembly.	3
2a	Front View of Crack Running 14 inches from Top Left Junction of Plate and Vertical Strut Channel.	4
2b	View of Opened Crack Surfaces at Top Left Junction of Plate and Vertical Strut Channel.	4
2c	Front View of Crack Running 8 inches from Bottom Right Junction of Plate and Vertical Strut Channel	5
2d	View of Opened Crack Surfaces at Bottom Right Junction of Plate and Vertical Strut Channel.	5
3	Sketch Showing Area of Deck Reinforcement	8
4	Gage Locations, Front View Elevated	9
5	Gage Locations, Side View Elevated.	10
6	Accelerometer Locations on Carbody and Trailer.	12
7	Schematic of Static Tests	15
8	Plate Single Strain Gages, Response to Lateral Load on Hitch. . . .	19
9	Plate Rosette Strain Gages, Response to Lateral Load on Hitch . . .	19
10	Structure Strain Gages, Response to Lateral Load on Hitch	20
11	Lateral Load Bridge, Response to Lateral Load on Hitch.	20
12	Plate Single Strain Gages, Response to Lateral Load on Trailer. . .	21
13	Plate Rosette Strain Gages, Response to Lateral Load on Trailer . .	21
14	Structure Strain Gages, Response to Lateral Load on Trailer	22
15	Lateral Load Bridge, Response to Lateral Load on Trailer.	22
16	FAT II Hitch, Lateral Compliance Test Results	28
17	Typical Finite Element Model of Trailer Hitch	30
18a	Back Surface Stress Contours for 10 Kips Uniform Lateral Load . . .	33
18b	Back Surface Stress Contours for 10 Kips Non-Uniform Lateral Load .	34

LIST OF FIGURES (CONTINUED)

Figure		Page
19a	Enlarged View of Stress Contours for Uniform Load	35
19b	Enlarged View of Stress Contours for Non-Uniform Load	36
20a, b,c	Views of TOFC Consist and Instrumentation Car	38
20d	View of Instrumented Hitch	39
21	Maximum Stress Variation in Trailer Hitch	40
22	FAT II Percent Occurrence Spectrum, Gage 5	49
23	Associated Stress Range Histogram, Gage 5	50
24	Typical S-N Curves	51
25	Predicted Fatigue Life as a Function of Fatigue Strength	57
26	Design-Reference Graphs for Preliminary Analysis of Crack-Growth Rates	62
27a	Vertical Acceleration REPOS at TOFC Bolster (Normal FAST Operations)	64
27b	Vertical Acceleration Range Distribution at TOFC Bolster (Normal FAST Operations)	65
28a	Lateral Acceleration REPOS at TOFC Bolster (Normal FAST Operations)	66
28b	Lateral Acceleration Range Distribution at TOFC Bolster (Normal FAST Operations)	67
29	Side Bearing Strikes Per Mile for FEEST Box Car	71
30	Hitch Strain Variation, 41 mph CCW, Run #14, Section 03	74
31	Trailer and Flatcar Accelerations, 41 mph CCW, Run #14, Section 03	75
32	Hitch Strain Variation, 42 mph CCW, Run #14, Section 07	76
33	Trailer and Flatcar Accelerations, 42 mph CCW, Run #14, Section 07	77
34	Hitch Strain Variation, 26.6 mph CW, Run #23, Section 07	78
35	Trailer and Flatcar Accelerations, 26.6 mph CW, Run #23, Section 07	79

LIST OF FIGURES (CONTINUED)

Figure		Page
36	Power Spectral Density of Trailer Lateral Acceleration, 45 mph CCW, Section 07	80
37	Power Spectral Density of Carbody Lateral Acceleration, 45 mph CCW, Section 07	81
38	Power Spectral Density of Trailer Lateral Acceleration, 25 mph CCW, Section 07	82
39	Power Spectral Density of Trailer Lateral Acceleration, 25 mph CCW, Section 18	83

LIST OF TABLES

Table		Page
1	Overview of Test Program.	7
2	Matrix of Static Tests.	14
3	FAT II Static Live Load Strains	16
4	Replaced Poisson Gages (Horizontal) in Vertical Strut Bridges	17
5	Pull Hitch Right C053 (Trailer Car Off)	23
6	Pull Trailer Right C054	24
7	Data Channel Sensitivity of Strain Response, Original Deck Support.	26
8	Data Channel Sensitivity of Strain Response, Modified Deck Support.	27
9	Theoretical Vs Measured Vertical Stresses, Hitch Strut at 21 Kips Vertical Load	31
10	Comparison of Experimentally Derived Stresses to FEM Prediction for 10k Pull to Right	32
11	Max/Min Measurements, 2.1 Laps on FAST, Modified & Unmodified Cars.	41,42
12	"Quick-Look" Digital Data Listings.	44
13	Greatest Overall Min/Max Stress Range (ksi), Hitch Plate Gage #5.	45

LIST OF TABLES (CONTINUED)

Table		Page
14	Effects of Operation, Deck Support, and Properties on Life.	55
15	Relative Life Predictions in Miles.	58
16	Life Predictions for Several Gage Locations	60
17	Life Predictions Based on Load and Accelerometer Transducers. . . .	60
18	Summary of Level Crossing Counts.	68,69
19	Average Lateral Wheel Force (kips) on High Rail	72
20	Summary of FAT II PSD Analysis.	84
21	TOFC Resonant Frequencies (FRATE)	86
22	Resonant Frequencies from RDL Test (Roll Mode Excitation)	87

ACRONYMS, ABBREVIATIONS, AND METRIC EQUIVALENTS

TERM	DEFINITION	EQUIVALENT
A	"A" end of car	
AAR	Association of American Railroads	
ACF	ACF Industries	
ALD	Automatic Locator Detector	
ASCII	(USA) Standard Code for Information Interchange	
ASF	American Steel Foundaries	
B	"B" end of car	
CSB	Center Services Building	
CW	clockwise	
CCW	counterclockwise	
FAST	Facility for Accelerated Service Testing	
FAT	Fatigue Analysis Test	
FATACC	see Appendix 4	
FATLEV	see Appendix 4	
FATPOS	Fatigue Analysis Test: Pecent Occurrence Spectrum (Program)	
FATSEE	see Appendix 4	
FEEST	Freight Equipment Environment Sampling Test	
FEM	Finite Element Model	
FLAP	Fatigue Life Analysis Program	
', ft	foot	0.3048 meter
FRATE	Freight Car Response Analysis and Test Evaluation	
GIFTS	Finite Element Model Program Name	
g	gravitational force	
G	dimensionless acceleration relative to gravity	
Hz	Hertz (cycles per second)	
", in	inches	25.4 millimeters
kip(s)	kilopound(a)	453.59 kilograms
ksi	kips per square inch	
L	Left	
mi	miles	1.6094 kilometers
MGD	Modified Goodman Diagram	
μ	micro	
με	microstrains	
mph	miles per hour	
%	percent	
lb(s)	pound(s)	453.59 grams
psi	pounds per square inch	
PSD	Power Spectral Density	
R	Right	
RDL	Rail Dynamics Laboratory	
REPOS	Road Environment Percentage Occurrence Spectrum	
S-N	"Stress versus Number of Stress Cycles"	
TOFC	Trailer-On-Flat-Car	
ton		0.907 Megagrams
TTC	Transportation Test Center	
TTX	Trailer Train Company Car I.D. prefix	
YS	yield stress	

EXECUTIVE SUMMARY

Cracks appeared in a hitch and its underdeck support on one of the 3 Trailer-on-Flat Cars (TOFC) in the FAST train consist 3,000 miles after inspection (at 186,000 miles). As a result, a series of static and dynamic (FAST operation) tests were undertaken on a similar car in May of 1981. In addition to gaining insight into the cause of cracking, the tests were designed to demonstrate the application of pending railroad industry fatigue design guidelines and collect FAST environmental data for comparison with revenue service.

The experiment was conducted in two phases:

1. The test car, with original construction, was instrumented with an array of strain gages on the hitch and accelerometers on the trailer and car body. Data were gathered from static tests, including lateral load pull tests on the vertically-loaded and -unloaded hitch, and on the side of the trailer. Data were recorded from the transducers as the TOFC operated under several speed conditions, including normal FAST operation (approximately 45 mph) for several laps of the FAST track test loop in both directions.

2. The same program was repeated after the underdeck reinforcement weld was removed under the hitch in an attempt to determine the failure sequence.

It was apparent from the static lateral pull tests that lateral loads of the order of 10 kip would cause relatively high (1,000 microstrain) and potentially damaging strains if repeated frequently. These high strains occurred in the plate near the vertical strut weld juncture, due primarily to plate bending caused by the particular strut assembly reaction to lateral load. An asymmetry of vertical and lateral loading response was also observed in this test car. The uneven vertical load support of the trailer caused higher strains in the right strut; a lateral pull to the right caused greater strains in the plate gages than did an equivalent pull to the left. Considerable plate bending near the vertical strut was also observed. An exploratory Finite Element Model (FEM) computer stress analysis indicated that non-uniform load distribution to the struts and/or twisting of the strut channel would be required to produce plate strains as high as those observed.

A "quick look" tabulation of the dynamic tests on the FAST loop revealed relatively high strain ranges, corresponding to a maximum conventional stress range of 46 ksi, or higher, at a critical hitch plate location. In order to assess the significance of such strain histories on structural integrity, a fatigue analysis was performed using the cycle-counted strain history recorded from these tests, following conventional S-N procedures described in the AAR Fatigue Design Guidelines. Fatigue cracking in the hitch is predicted in the hitch plate at the critical location. The effect of direction of travel, speed, deck support, and material properties were also studied. Deck support modificiation appeared to have little effect.

Life predictions were also made on the basis of data from other strain gages and accelerometers. Fatigue cracking in the hitch head welds was predicted, but no cracking was predicted in the underdeck support weld. Rela-

tively short fatigue life of the hitch plate was also predicted from approximate analyses of the accelerometer data.

An assessment of the FAT II load environment was made relative to data from four tests:

1. Road Environment Percent Occurrence Spectra (REPOS) for 100-ton hopper cars included in the existing AAR Fatigue Guidelines.

2. Previous TOFC road tests from operations over "marginal" class 5 tangent track.

3. FEEST program test results in terms of side bearing strike counts for a 70-ton box car in operation over FAST, as well as general road service.

4. FAST wayside lateral wheel load environment.

From a comparison of these data, it appears that the FAST lateral load environment (average or peak) is probably significantly more severe, per mile, than general revenue service.

In order to understand the particular dynamics of the TOFC combination during FAST operation, several analyses and comparisons were made. These included an examination of selected composite plots of all the transducer outputs for periods of critical strain occurrence, a power spectral density analysis of maximum hitch strain and trailer lateral acceleration for the most interesting periods of operation, and a comparison of previous Rail Dynamics Laboratory (RDL) tests and computer model predictions. From these considerations it is concluded that curve-negotiation forces excite lateral dynamics resonances ($\simeq$7 Hz) of the TOFC combination, causing high strain cycles in the hitch for normal 45 mph operation. Slower operation (25 mph) over jointed tangent track can also excite another resonance ($\simeq$1 Hz), which contributes to fatigue damage of the hitch.

Any conclusions about these tests must be appropriately qualified by considering the FAST mode of operation, the heavy trailer load, and the asymmetrical response of this particular hitch to vertical and lateral load. Nevertheless, it appears that more attention should be focused on the TOFC system lateral response when evaluating structural integrity of hitch designs.

ACKNOWLEDGEMENTS

We wish to acknowledge the assistance of the following persons who have contributed significantly to the successful completion of the various stages of this project:

Testing

Ronald Bidwell served as test engineer and Dennis T. Kido served as assistant test engineer. James P. Jollay provided coordination as acting experiment monitor. All of the above persons who are currently with AAR Pueblo were formerly employed by Boeing Services International, Inc.

At the AAR Chicago Technical Center, William Drish created several data conversion computer programs that greatly facilitated review and analysis of test data. Data base construction tasks were carried out by Francis Loo, Vijuna Scor, Allen Porter, Osman Ahmad, and Daniel Roddy.

Analysis

Mohammed Ghoghawala was primarily responsible for conducting the many computer fatigue and stress analyses and other analytical tasks. Other AAR Chicago staff assistance came from Yun-Long Wang and Vijay Garg, who assisted with the adaptation of a dynamic analysis computer program.

The TTC Data Processing Program group, primarily Michael Reedy, prepared some of the computer graphics. Other TTC support was also instrumental in preparing this report.

Cooperating industry support was especially important to this project. Samuel Halcombe of ACF contributed to test and instrumentation planning and the initial test monitoring effort. Terry L. Pitchford of ASF Industries provided information regarding ASF's road data reduction program that was helpful to our analysis of peak level crossing events.

Finally, we owe special acknowledgement to Eric Wolf and Frank Stec of the Trailer Train Company for their initiative, cooperation, and contribution to many phases of this project--including much of the planning and testing. They provided special data for and constructive criticism of this report.

1.0 INTRODUCTION

1.1 BACKGROUND

The railroad industry has from time to time witnessed the occurrence of cracks on freight cars. More often than not these cracks are explainable simply by reason of poor welding practice. At times, however, despite the best welding practice, fatigue cracking still occurs. In the absence of design for fatigue, the response to fatigue cracks often was to strengthen the component or car detail, either through change in section properties or by using gussets to alter the load path. This sometimes led to more cracks in the original area or cracks at different locations.

In order to provide for an improved response to this threat to structural integrity, the railroad industry has recently adopted fatigue guidelines for the design of freight cars. These guidelines[1]* provide for the design of the car structure, including critical details, through fatigue design techniques employed by industry at large. The implementation of the fatigue guidelines is contingent upon the availability of the Road Environmental Percent Occurrence Spectrum (REPOS) for each car design type. These environmental data consist of load and acceleration-based ranges for the centerplate, sidebearings, and mechanical coupler. The load-based data are used to estimate the strain range values for each critical design detail using conventional or finite element stress analysis. A compendium of experimental fatigue data provides the basis for estimating life. In the case of cars operating on FAST, the strain range is obtainable directly at critical locations. A life estimate for specific design details can be made for cars operating on the Facility for Acceleration Service Testing (FAST) track. For cars experiencing fatigue failures, alternative structural details can be evaluated.

1.2 FLAT CAR HITCH CRACK OBSERVATIONS

Many of the cars which make up the FAST consist have been here since the day the train first rolled around the loop. Obviously, many wheelsets and brakeshoes have been replaced. Cracks in the freight car bodies and other car components have appeared. As a result of some of the cracks observed, it was decided that some mini-tests could be conducted that would be beneficial to the railroad car design community in addition to being directly useful to the particular owners/builders of the car on which the failure occurred. Two Fatigue Analysis Tests (FAT) have been conducted - designated FAT I and FAT II. FAT I was completed and reported on previously[2].

Since the start of FAST, three trailer-on-flat-car (TOFC) units had been operating in the regular consist. During the period from September 1976 to May 1979 they accumulated 189,000 miles, at which time cracks were observed on the "B" end hitch of one of the cars (Car #69, TTAX 160546). Also, under the car deck, the welds attaching a floor reinforcement had failed. Inspection of another car indicated that these same welds were starting to fail.

---

* Numbers refer to references listed at the conclusion of text.

The subject hitch had previously been removed and inspected. A worn pin on the hitch strut was replaced at that time. After 3,000 miles the hitch was again inspected; this time cracks were discovered and the hitch was replaced. Cracks at two primary locations were found:

1. Hitch: Cracked welds in the jaw support (14" and 9 1/2" cracks found in the reinforcing plate attached to the two vertical struts)

2. Under the Deck: Cracked welds at the floor-reinforcing channel.

Figure 1 illustrates the hitch assembly. There were three basic areas of cracks:

a. Head assembly
b. Strut assembly
c. Reinforcement member attachment

Figures 2a through 2d provide several views of the two major cracks in the web plate joining the two channel struts. One crack started in the plate at the top near the left strut and progressed 14 inches down. The opposite side was also cracked, the crack starting in the plate and working its way up towards the top. The cracks appeared to originate at the ends of welds and propagate in, or at the base metal border of, the heat affected zone of the plate material.

The present authors did not examine the actual failed hitch but the results of the hitch manufacturer's metallurgical and fractographic observations and conclusions were made available to the AAR through personal correspondence[3] with the car owner. Their examination of the fractures showed the following conditions existed:

> "The fracture faces were only mildly tinted with rust indicating they had not been exposed to the atmosphere for any prolonged period.
>
> All of the fractures without exception originated and progressed in a fatigue mode.
>
> The topographic features of the fractures indicate the fractures originated and progressed over a relatively short period of time as evidenced by the number of starts and stops and high peaks associated with the progression. - - - While it cannot be determined from the fractures the exact number of cycles involved to failure, the fracture faces indicate the time frame to be relatively short."

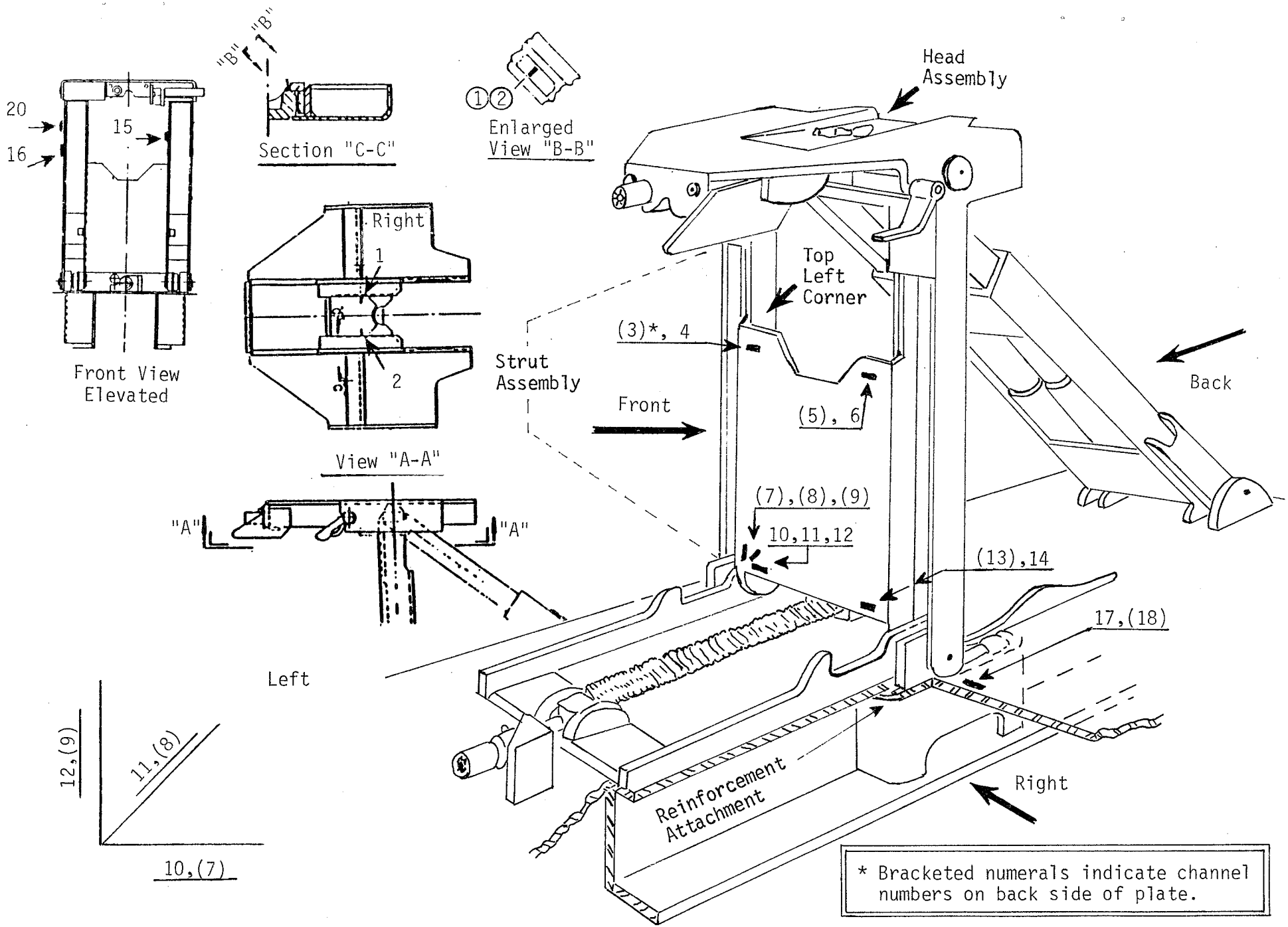

FIGURE 1. CUSHIONED HITCH ASSEMBLY.

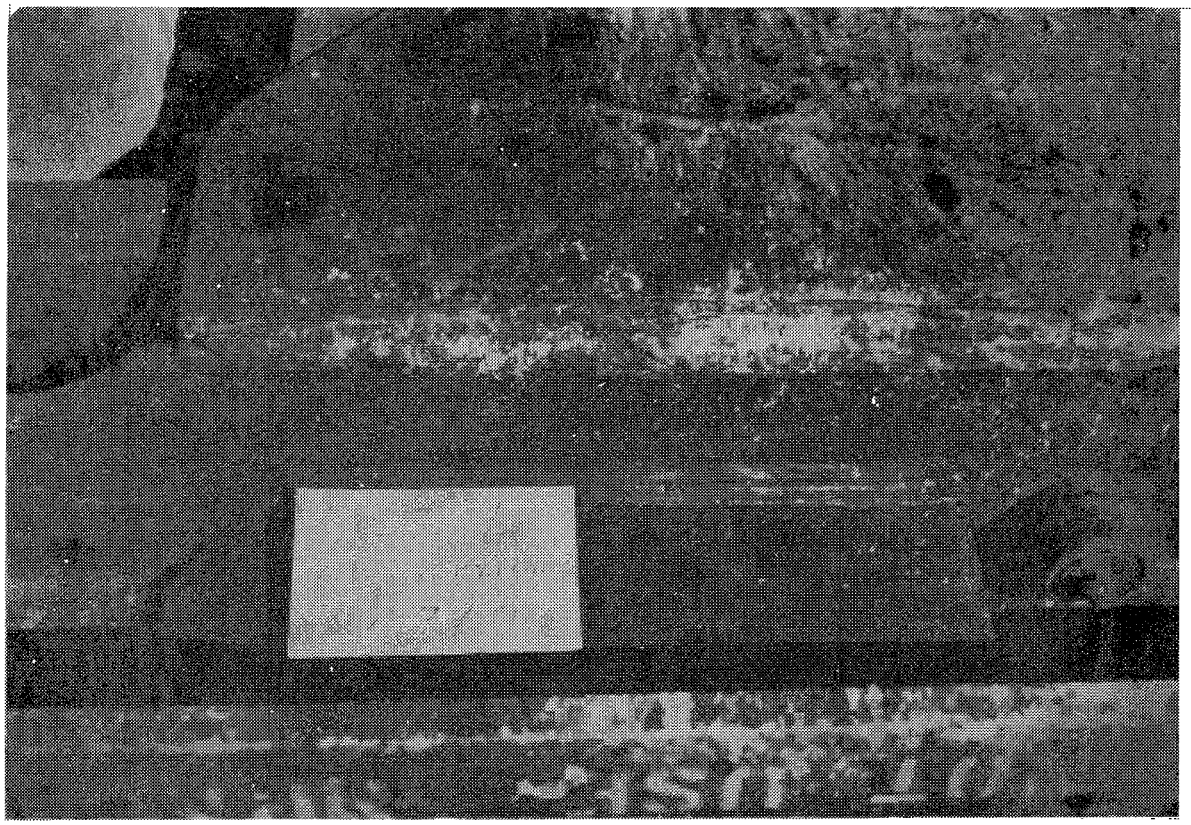

FIGURE 2a. FRONT VIEW OF CRACK RUNNING 14 INCHES FROM TOP LEFT JUNCTION OF PLATE AND VERTICAL STRUT CHANNEL.

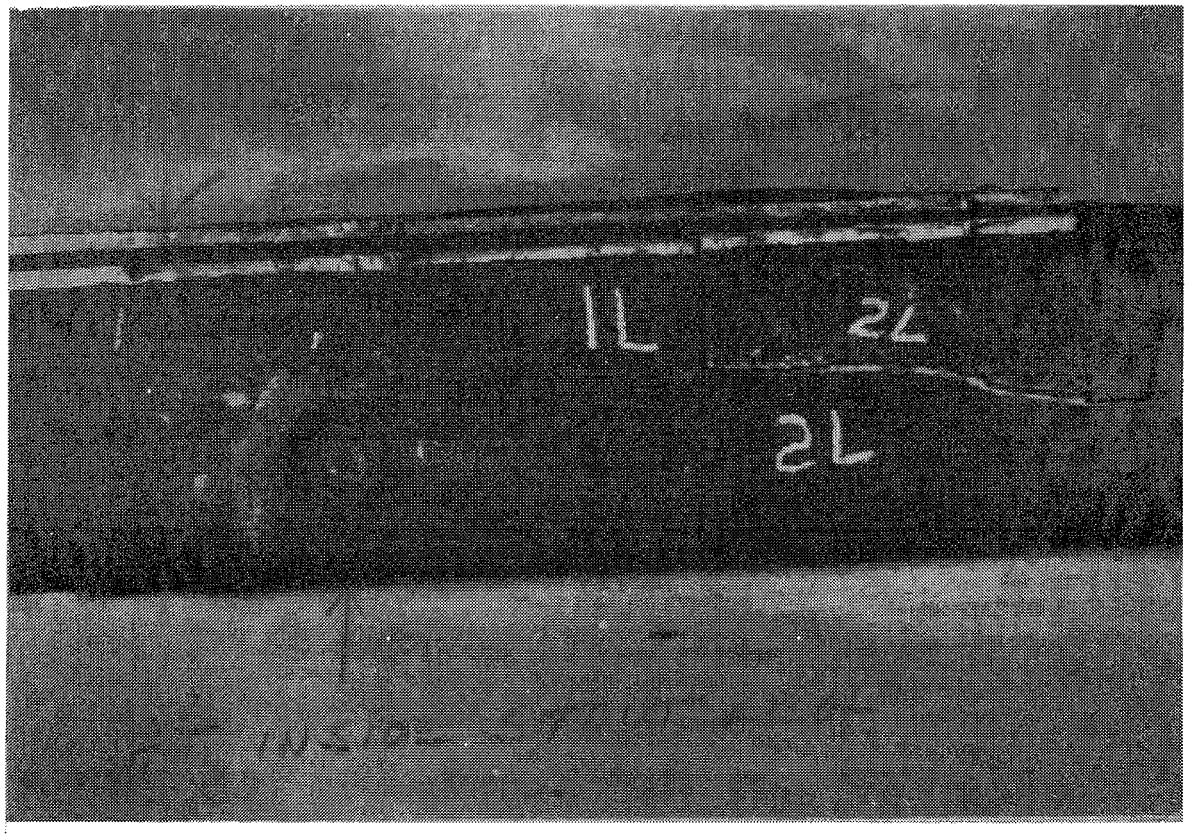

FIGURE 2b. VIEW OF OPENED CRACK SURFACES AT TOP LEFT JUNCTION OF PLATE AND VERTICAL STRUT CHANNEL.

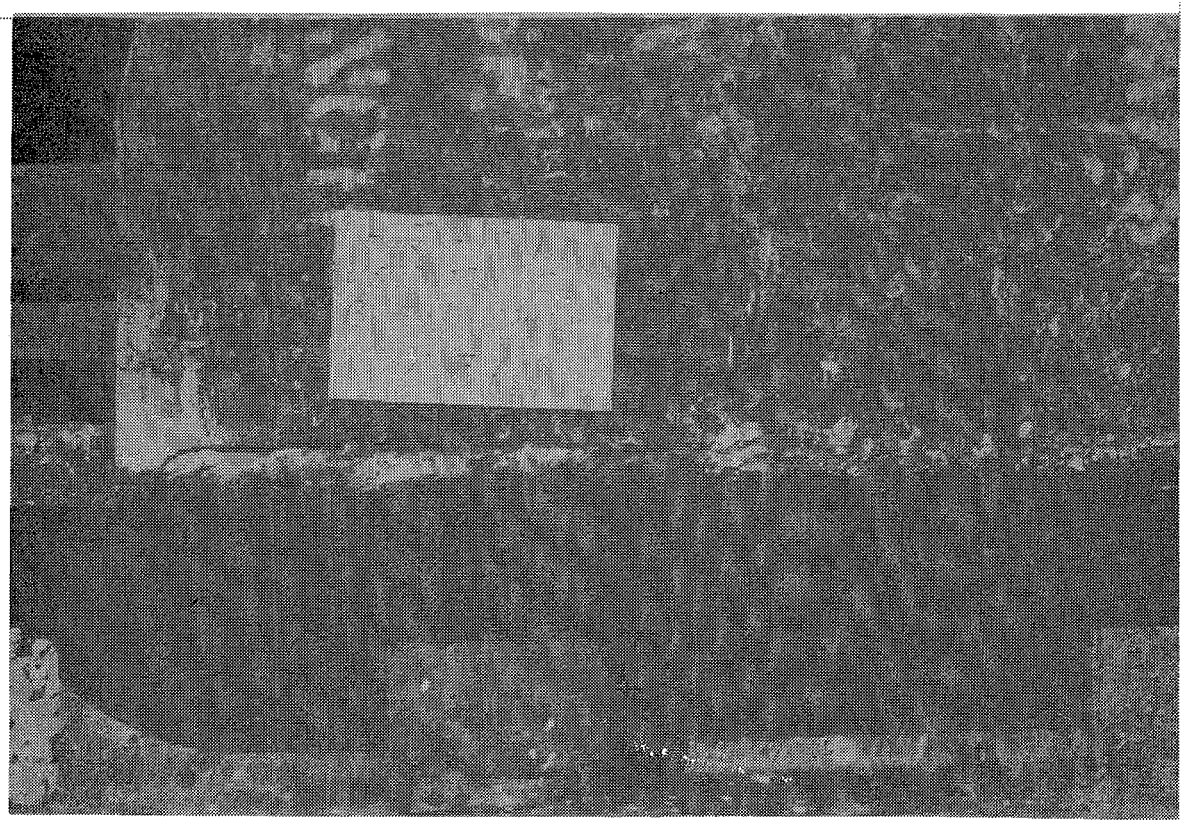

FIGURE 2c. FRONT VIEW OF CRACK RUNNING 8 INCHES FROM BOTTOM RIGHT JUNCTION OF PLATE AND VERTICAL STRUT CHANNEL.

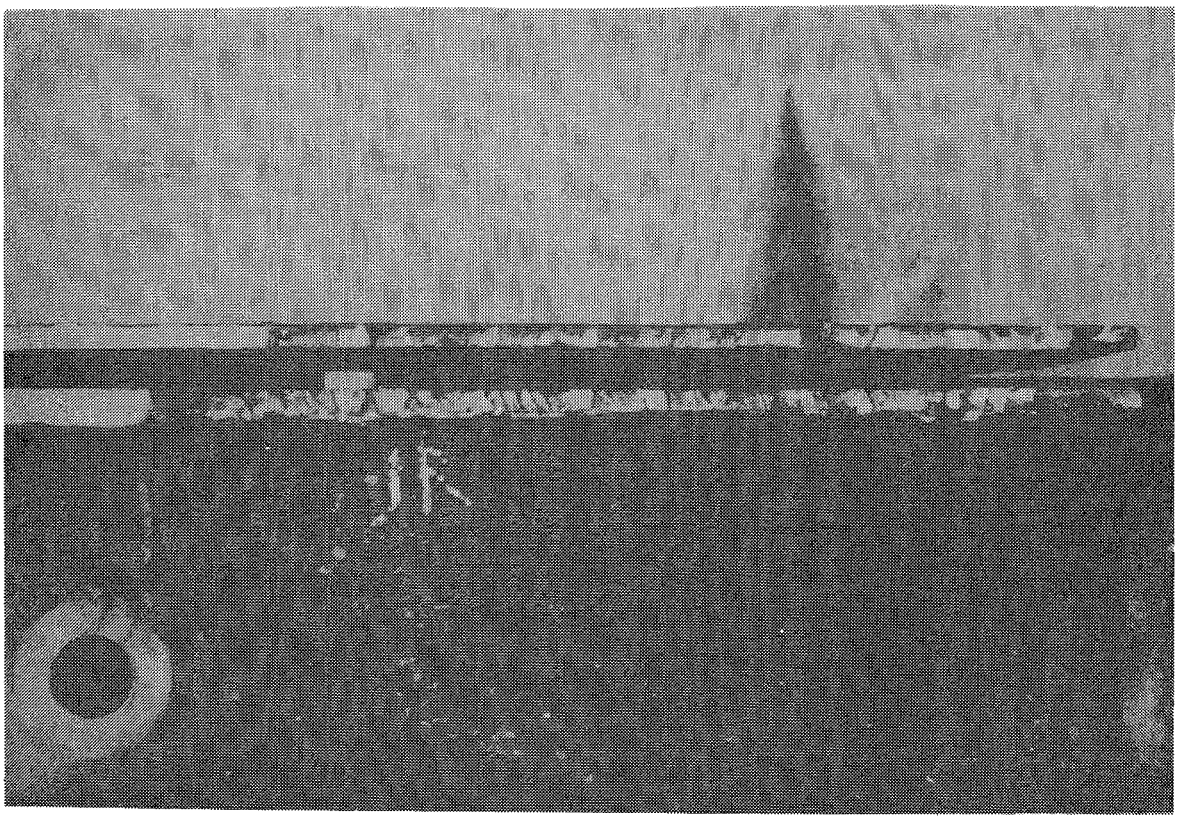

FIGURE 2d. VIEW OF OPENED CRACK SURFACES AT BOTTOM RIGHT JUNCTION OF PLATE AND VERTICAL STRUT CHANNEL.

2.0 TEST PROGRAM

Cracking, when discovered, was severe; therefore, it is difficult to say where the cracks started. Did the failure occur at the reinforcement member below the deck, which allowed the floor plate to be more flexible causing the stresses in the hitch to go up? On the other hand, was the stress level and cracking of the hitch responsible for the subsequent failure of the reinforcement member? These are two structural details that failed, and it is important to determine which failed first in order to recommend appropriate changes to preclude future failures.

2.1 TEST OBJECTIVES

The specific objectives of the experiment were as follows:

1. Estimate the fatigue life of two (hitch and deck) structural configurations on a TTAX car.

2. Collect FAST environmental data for comparison with revenue service data.

3. Demonstrate, through specific case studies on a flat car, the implementation of the fatigue guidelines.

2.2 TEST PLAN

The experiment was conducted in two phases. The test car, with original construction, was instrumented and data were gathered. In Phase II, an underdeck weld was removed and the data collected with the modified car. An overview of the test program is shown in Table 1. Each phase consisted of static and dynamic tests, which are described in detail in subsequent sections.

The static tests conducted were a lateral pull on the hitch, a rock over, and a twist of the car. The dynamic testing took place in the two phases. The dynamic data were representative of normal FAST operation, with additional laps at lower speeds. Specifically, Phase I included 1 lap at 5 mph, 2 laps at 25 mph, and 10 laps at 45 mph, clockwise and counterclockwise; Phase II of the dynamic testing was the same as Phase I except for the removal of the reinforcement channel below the deck. The channel weld was removed in an effort to determine the primary reason for cracking. Figure 3 illustrates the area of deck reinforcement.

2.3 TEST INSTRUMENTATION

Briefly, several gages were placed on the hitch, some of which were wired to read lateral load. Also, some accelerometers were used along with the usual service channels ... speed, Automatic Locator Detector (ALD) markers, etc. Gages were placed on the plate that joins the two struts at the top left and top right, both front and back, where hitch cracks were observed. Gage locations are shown in Figures 4 and 5. These locations were selected by

TABLE 1. OVERVIEW OF TEST PROGRAM.

Phase I (Original test car configuration	Static Tests -	Live Load* Lateral Pull Roll Twist
	Dynamic Tests -	On FAST 5-45 mph
Phase II (Under deck welds removed on reinforcement)	Static Tests -	Live Load* Lateral Pull Roll Twist
	Dynamic Tests -	On FAST 5-45 mph

* Effect of 2 fully loaded trailers.

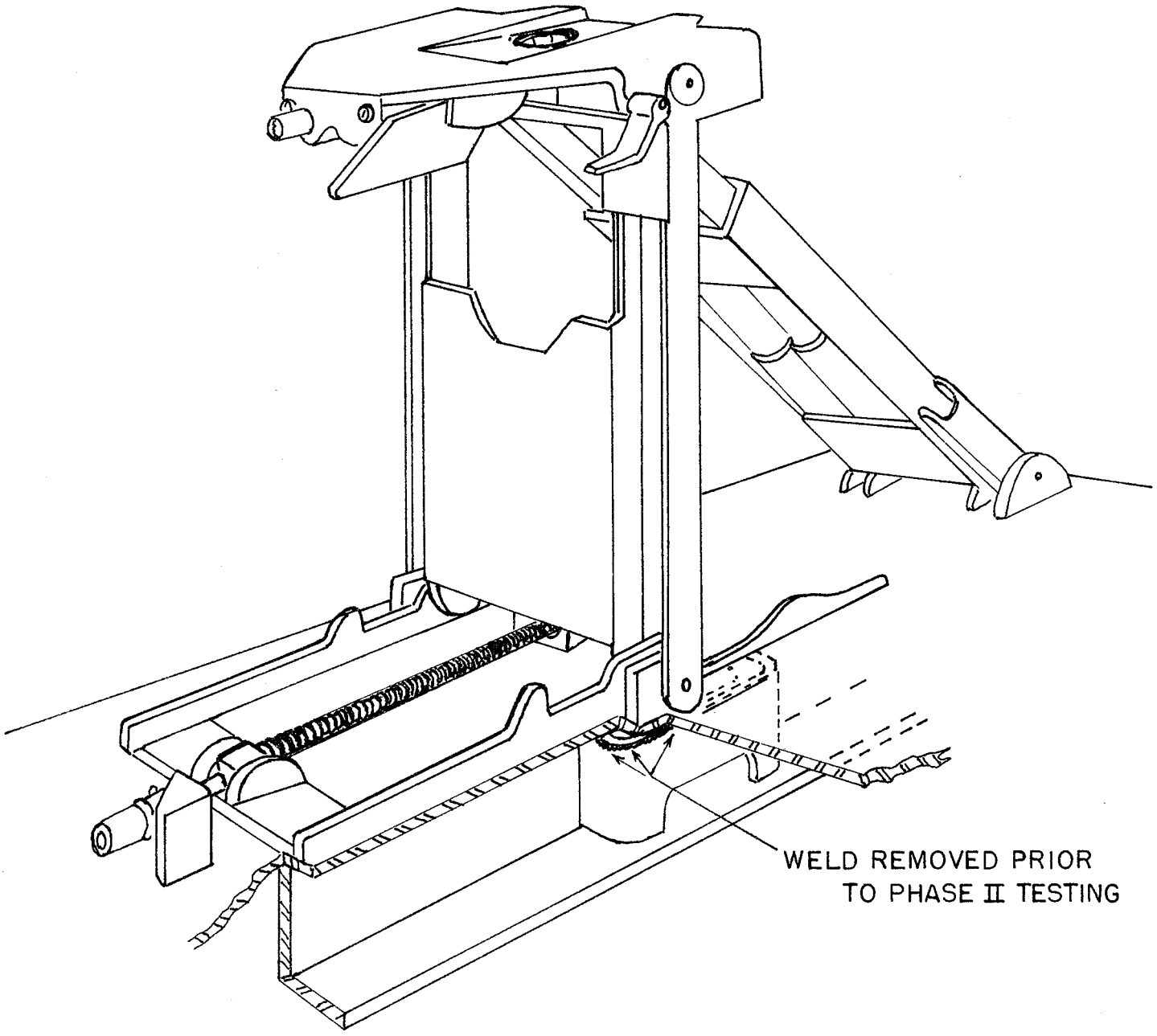

FIGURE 3. SKETCH SHOWING AREA OF DECK REINFORCEMENT.

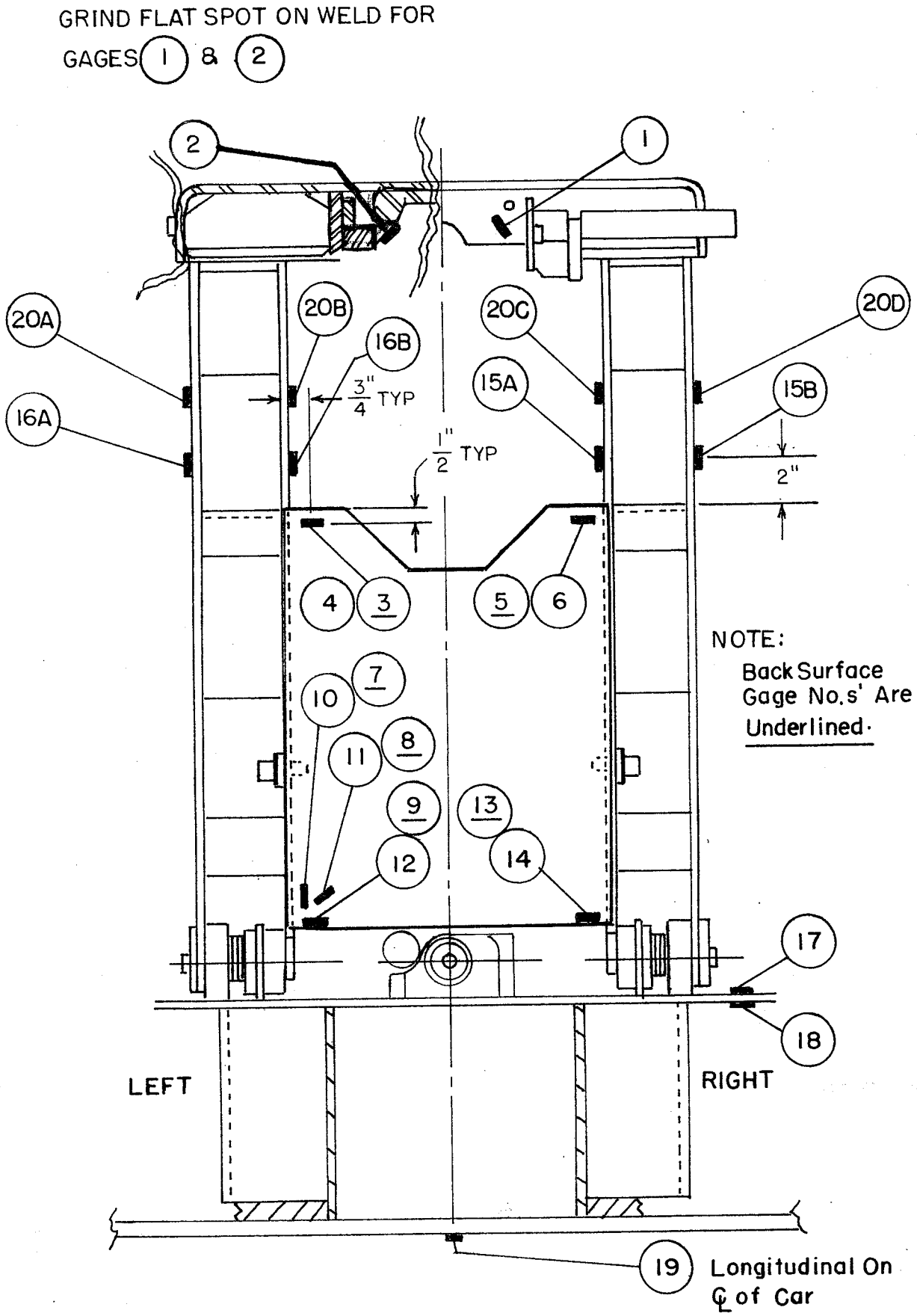

FIGURE 4. GAGE LOCATIONS, FRONT VIEW ELEVATED.

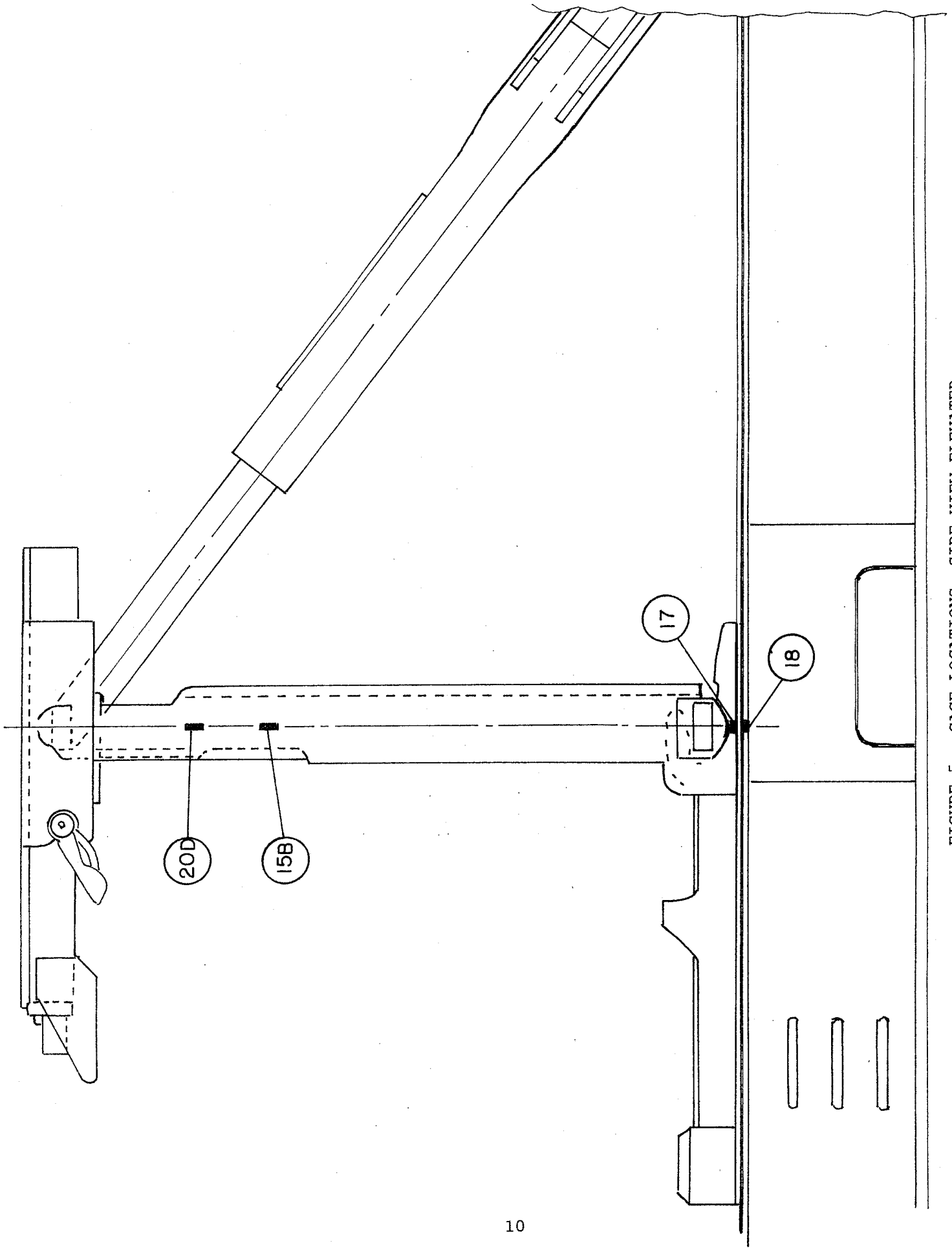

FIGURE 5. GAGE LOCATIONS, SIDE VIEW ELEVATED.

Trailer Train Company (TTX) personnel in consultation with ACF. Also, strain rosettes were applied to the plate at the bottom left both front and back and gages on the other side of the plate both front and back. Gages on the struts, four vertically on each, were wired to measure vertical load. There were also gages on the strut to measure lateral load.

In addition to the gages at fatigue-critical locations, a vertical and lateral load transducer scheme (see Appendix 1), devised in consultation with the manufacturer of the hitch, was used to measure vertical and lateral hitch forces. Also, accelerometers were applied on the car body and the trailer as shown in Figure 6. Trailer mounted accelerometers are as near the center of mass of the trailer as possible on the bottom of the trailer, oriented to measure vertical and lateral acceleration. Accelerometers on the car body included those with vertical and lateral orientation near the center plate, in locations comparable to those suggested in the Fatigue Guideline.

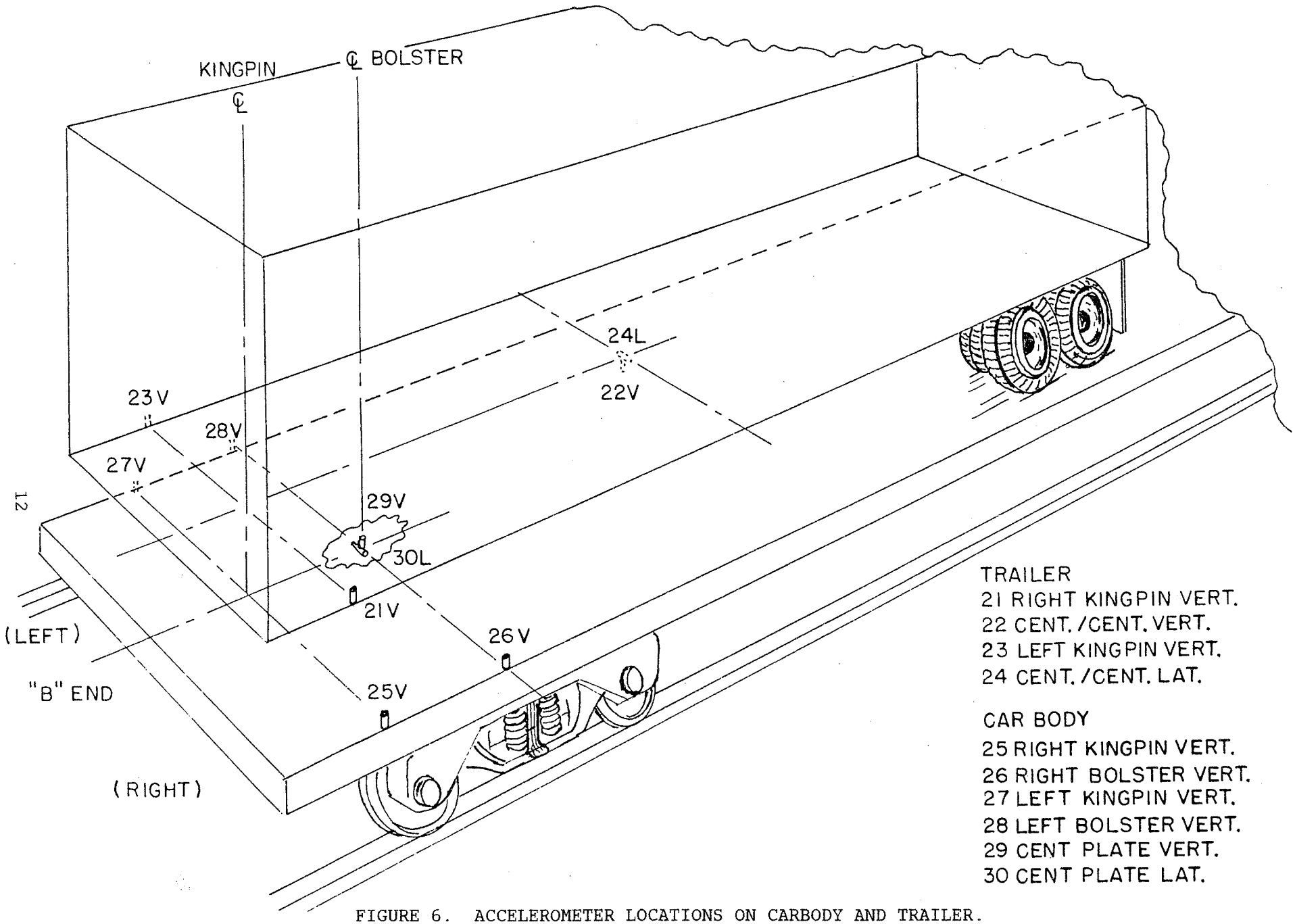

FIGURE 6. ACCELEROMETER LOCATIONS ON CARBODY AND TRAILER.

3.0 SUMMARY OF STATIC TESTS

A series of static load tests was performed on the flat car and B end hitch. These tests were designed to measure the static vertical live load strains in the hitch and flat car, the strain and deflection response of the hitch and deck to lateral loads, and the effect of moderate amounts of car body twist and roll on hitch strains. An overview of these tests is provided in Table 2. The test set up is shown schematically in Figure 7.

3.1 VERTICAL (LOAD/EMPTY) TESTS

The live load strains were obtained by stabilizing and recording the zero signals from the 20 strain gage channels, placing the two fully loaded trailers in position on the 89-ft flat car and recording the resulting strain changes. Each trailer weighed 66 kips, with 21 kips supported at the hitch. The center of the tandem wheels was located some 27 feet from the hitch kingpin.

The test instructions were implemented as follows:

1. With both trailers off, obtain strain output for strain gage data channels.

2. Weigh trailers to obtain load distribution of trailers.

3. Using a lateral load jacking fixture, calibrate the lateral load channel. (This was done by applying a lateral load on the hitch at the kingpin locking plate in 2,000-lb increments from 0 to 16,000 lbs. and recording the output of the lateral circuit.)

4. With trailers returned in place, obtain the data for all strain gage channels.

Table 3 lists the recorded strains before and after trailers were loaded on the car. Table 4 is the result of a repeat test in which minor changes (see Appendix 1) were made in the vertical "load" circuits of the two hitch struts.

From these data the following observations are made:

1. Placement of the trailers on the flat car caused a tensile live load strain of 324 microstrain ($\mu\varepsilon$) in the longitudinal direction of the bottom coverplate of the center sill at midcar (Channel #19; Test C030 - C027). This amounts to a live load stress of about 9,720 psi, which compares favorably to a value of 10,660 psi calculated by the car owner[4].

2. The corresponding strains in the hitch were highest in the head weld, where the average strain was 518 $\mu\varepsilon$ on the right side (Channel #1).

TABLE 2. MATRIX OF STATIC TESTS.

(Test Identification Codes)

		VERTICAL Load/Empty			ROLL		TWIST		LATERAL PULL ON HITCH			
									With Trailer		W/O Trailer	
		Off Car	Off Hitch	On Hitch	Left	Right	Left	Right	Left	Right	Left	Right
ORIGINAL PHASE I	PRE	C027	C025 C028 C029 C034 C036 C039 C042	C030 C032 C035 C038 C043	C044 C045	C046	C047	C048		C040	C021 C023	C024 C026 C031 C041
	POST		C050 C061	C049 C059 C060 C063 C064 C066 C068	C055	C056	C057	C058	C065 C067 C069	C054	C062	C053
MODIFIED PHASE II	PRE		C070 C076	C073 C075 C078	C083	C082	C081	C080	C074	C079	C072	C077
	POST		C050	C049 C053 C059 C065	C055	C056	C057	C058	C064	C054	C061 C062	C051

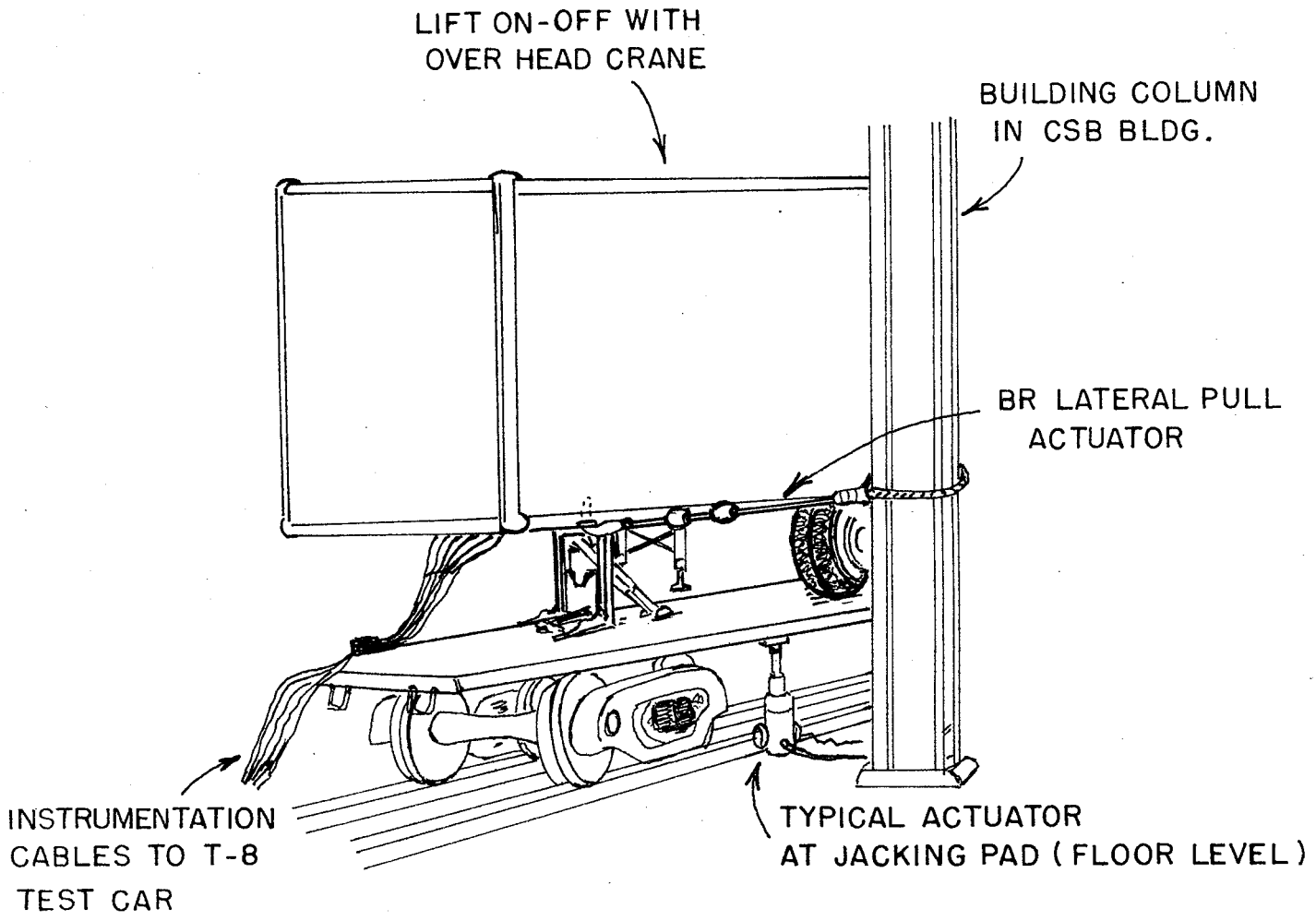

ROLL ACTUATOR @ BR & AR 5" MAX. DISPL.

TWIST ACTUATOR @ BR & L ("B" end, Right and Left)

LOAD / EMPTY USE OVER HEAD CRANE

LATERAL PULL - EMPTY- LATERAL ACTUATOR AT BR TO 10,000# MAX.

LOADED- " " " " " 14,000# MAX.

FIGURE 7. SCHEMATIC OF STATIC TESTS.

TABLE 3. FAT II STATIC LIVE LOAD STRAINS.

(Channels 15 and 16 with Poisson Gages in Place)

Data Channel Number	C027 Trailers Off Car	Change	C028-29 Trailers On Car Off Hitch	Change	C030 Trailers On Car On Hitch	Change (Total) Δμε
1	-92.1	120.3	28.2	482.9	511.1	603.2
2	-7.6	26.8	19.2	312.1	331.3	338.7
3	7.7	-8.0	-0.3	115.5	115.2	107.5
4	104.0	-110.1	-6.1	-32.0	-38.1	-142.1
5	-1.5	-27.5	-29.0	-21.5	-50.5	-49.0
6	-88.6	115.9	27.3	22.4	49.7	138.6
7	145.7	-154.6	-8.9	91.7	82.8	-62.5
8	60.2	-55.9	4.3	-68.5	-64.2	-124.4
9	5.1	-17.8	12.7	-41.9	-29.2	-59.7
10	-67.0	73.9	6.9	44.5	51.4	118.4
11	-46.6	45.4	-1.2	10.3	9.1	55.7
12	19.2	-37.1	-17.9	-5.3	-23.2	-42.5
13	75.4	-111.4	-36.0	88.3	52.3	-23.1
14	-7.0	-3.9	-10.9	-42.0	-52.9	-45.9
15	-5.6	4.0	-1.5	-528.5	-530.0	-524.4
16	8.4	-9.0	-0.6	-79.2	-79.8	-88.2
17	58.0	-10.1	47.9	-66.1	-18.2	-76.2
18	-35.7	8.1	-27.6	64.2	36.6	72.3
19	-8.9	318.4	309.5	6.0	315.5	324.4
20	39.4	-38.6	0.8	-66.1	-65.3	-104.7

TABLE 4. REPLACED POISSON GAGES (HORIZONTAL) IN VERTICAL STRUT BRIDGES.

(Channels 15 and 16 with Bridge Completion Resistors)

Data Channel Number	C042 Trailer Off Hitch Mean (με)	C043 Trailer On Hitch Mean (με)	Δμε
1	0.099	515.041	514.9
2	-2.379	205.503	207.9
3	-5.585	333.246	338.8
4	2.903	-35.678	-38.6
5	-2.647	-40.063	-37.4
6	5.504	31.670	26.2
7	2.126	-00.676	-2.8
8	3.674	-68.740	-72.4
9	16.652	-33.027	-49.7
10	9.894	149.191	139.3
11	1.537	15.138	13.6
12	6.120	-0.285	-6.4
13	11.119	134.769	123.7
14	1.079	-57.039	-58.1
15	-10.058	-388.942	-378.9
16	-27.121	-132.428	-105.3
17	-1.521	-62.667	-61.1
18	-1.221	69.610	70.8
19	-7.714	-4.614	3.1
20	1.336	-168.547	-169.9

3. The load was unevenly distributed to the vertical struts or channels. The strain signal from the vertical bridge circuit on the right strut (Channel #15) was -379 με, while that on the left (Channel #16) was only -105 με (C043 - C042).

4. All the other strains in the hitch plate are relatively low. For example, the most active gage in the FAST test (Channel #5) had a compressive strain of less than 50 με. Actually, the strain was higher in the corresponding back plate horizontal gage on the other side (left) of the hitch (Channel #3). This tensile strain of 339 με (108 με in a repeat test) occurred near the strut with the lower load (left strut, Channel #16).

5. The vertical trailer load caused some compressive strain readout from the lateral load bridge circuit, which was originally intended to suppress vertical load effects. This strain reading was in the range 105 to 170 με.

3.2 RESULTS OF STATIC LATERAL LOAD ON HITCH

With cable and hydraulic actuator, lateral loads were applied as follows:

- Directly - to the vertically-unloaded (trailer off-loaded) hitch; maximum: 14,000 pounds.
- Indirectly - by pulling on the side of the (loaded) trailer, at the bottom and in line with the kingpin; maximum: 5,000 pounds.

Typical results of these tests are graphically displayed in Figures 8 through 11 for the vertically-unloaded hitch, and in Figures 12 through 15 for the trailer-loaded hitch. For clarity, the strain gage data in these figures have been grouped into the following categories: single strain gages; rosette strain gages, structure strain gages, and lateral load bridge. Likewise, the digital data for selected channels from two representative tests are tabulated in Tables 5 and 6.

3.2.1 Static Lateral Pull Tests on Hitch (Trailer Off Hitch)

The following observations are made on the basis of data provided in Figures 8 through 11 and Tables 5 and 6.

1. The horizontal top back plate Gage #5 on the right side of the hitch is the most sensitive to lateral load. From averages of "pull to right" tests, Gage #5 produces a tensile strain of 100 με for a 1,000-lb load. The next most sensitive gages are Gage Channel #13 (front bottom right horizontal) with -70 με and Gage #7 (back rosette bottom left horizontal) with 52 με per kip.

2. A pull to the right causes a positive strain increment in the right strut (26 με/kip) in Channel #15, and a negative strain increment in the left strut (-20 με/kip) in Channel #16.

3. The lateral load circuit has a positive strain increment of 20 με/kip right pull when the hitch was not supporting the vertical trailer load.

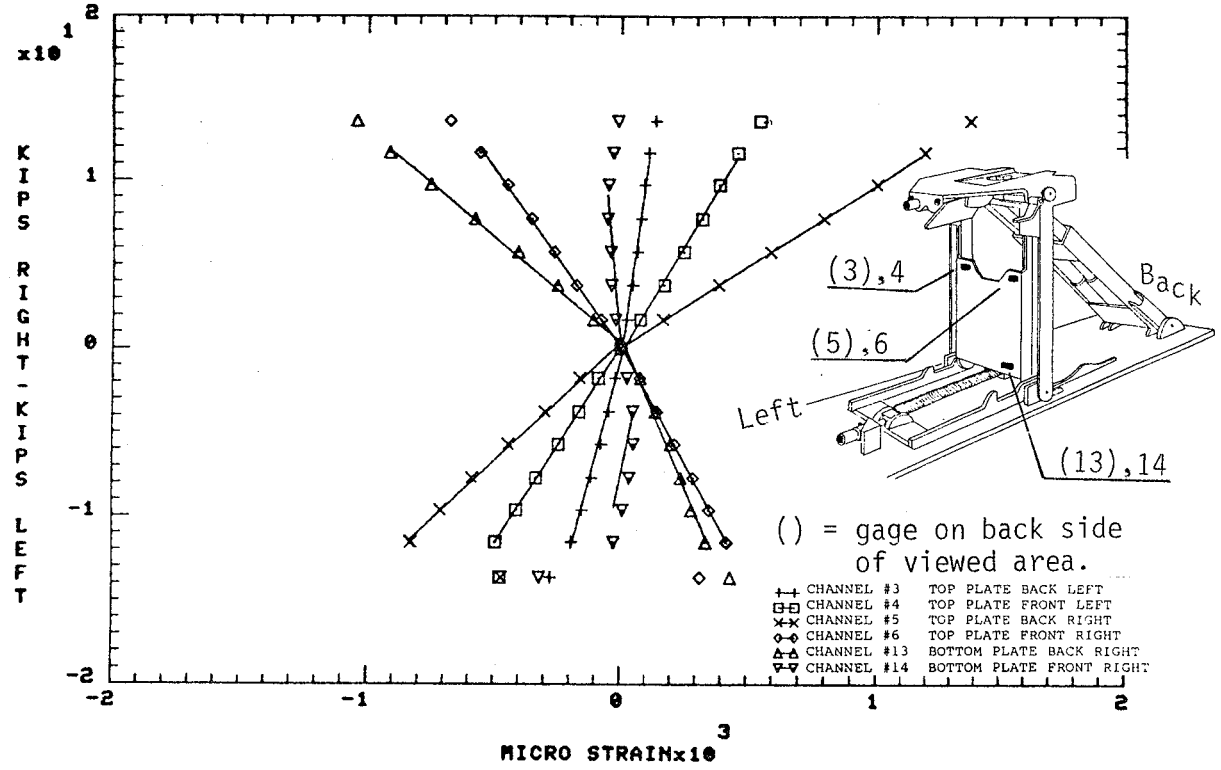

FIGURE 8. PLATE SINGLE STRAIN GAGES, RESPONSE TO LATERAL LOAD ON HITCH.

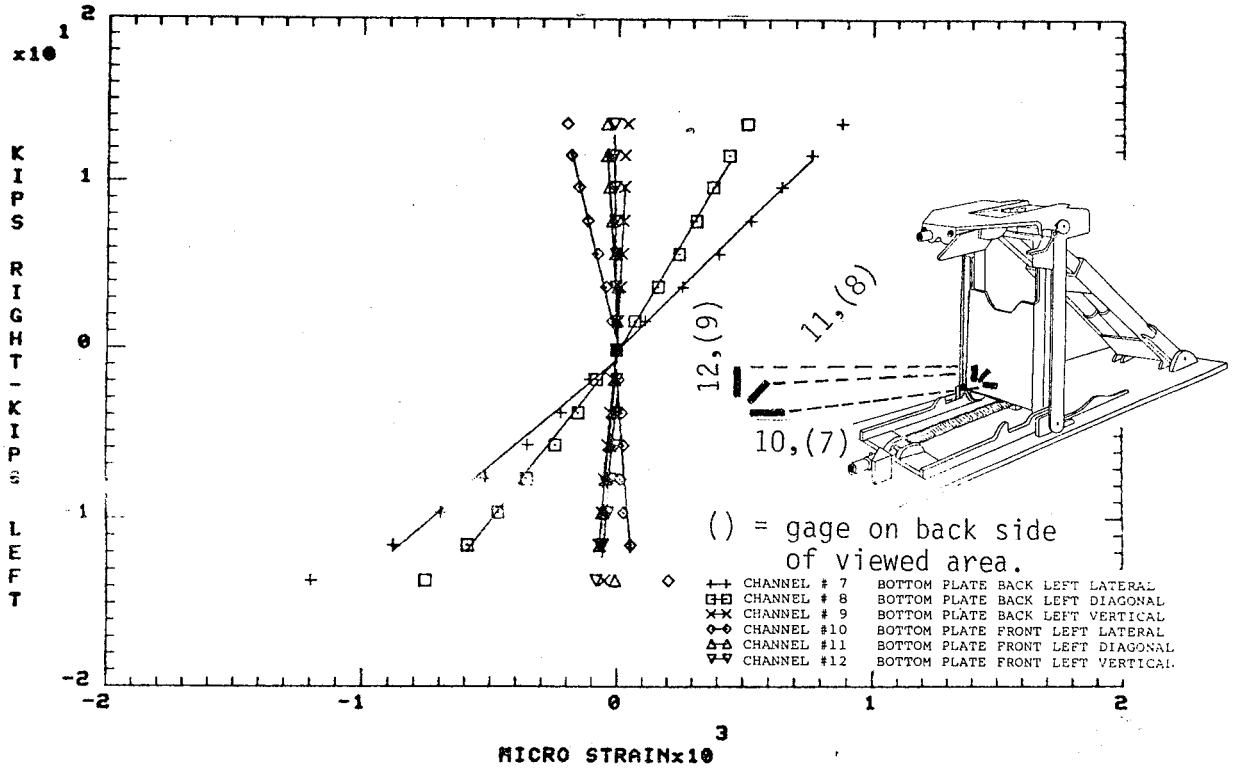

FIGURE 9. PLATE ROSETTE STRAIN GAGES, RESPONSE TO LATERAL LOAD ON HITCH.

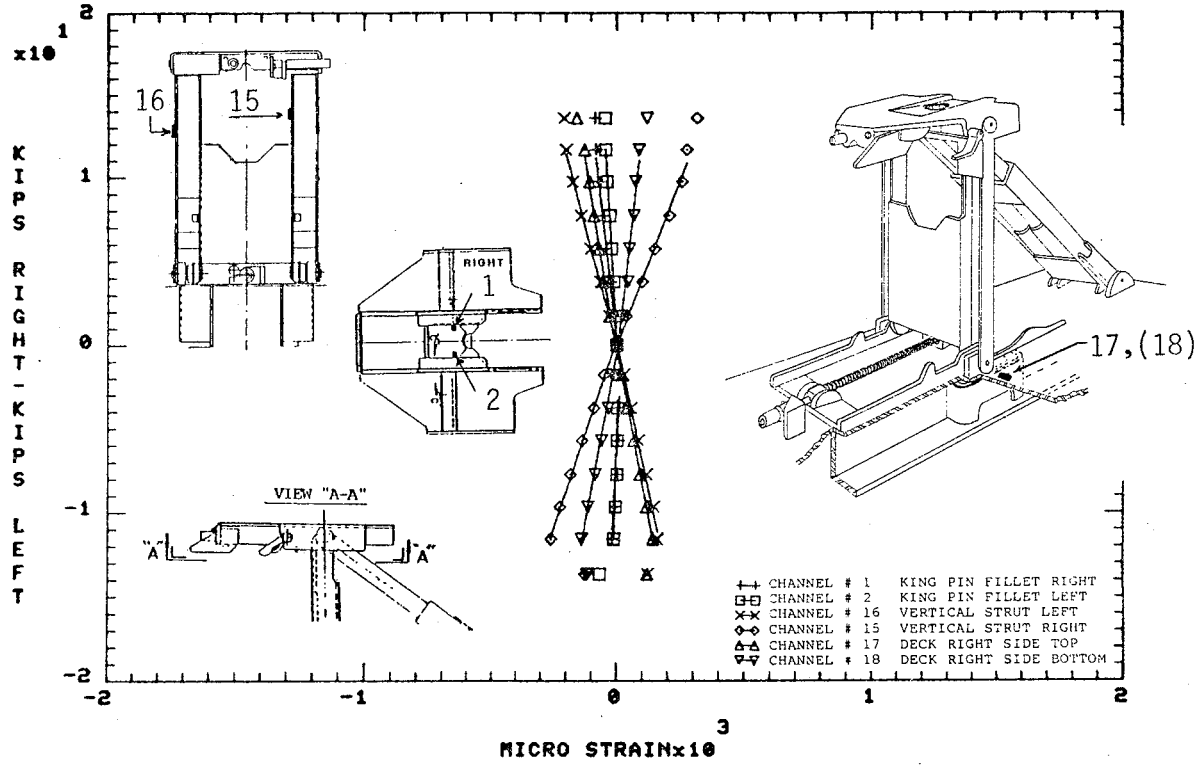

FIGURE 10. STRUCTURE STRAIN GAGES, RESPONSE TO LATERAL LOAD ON HITCH.

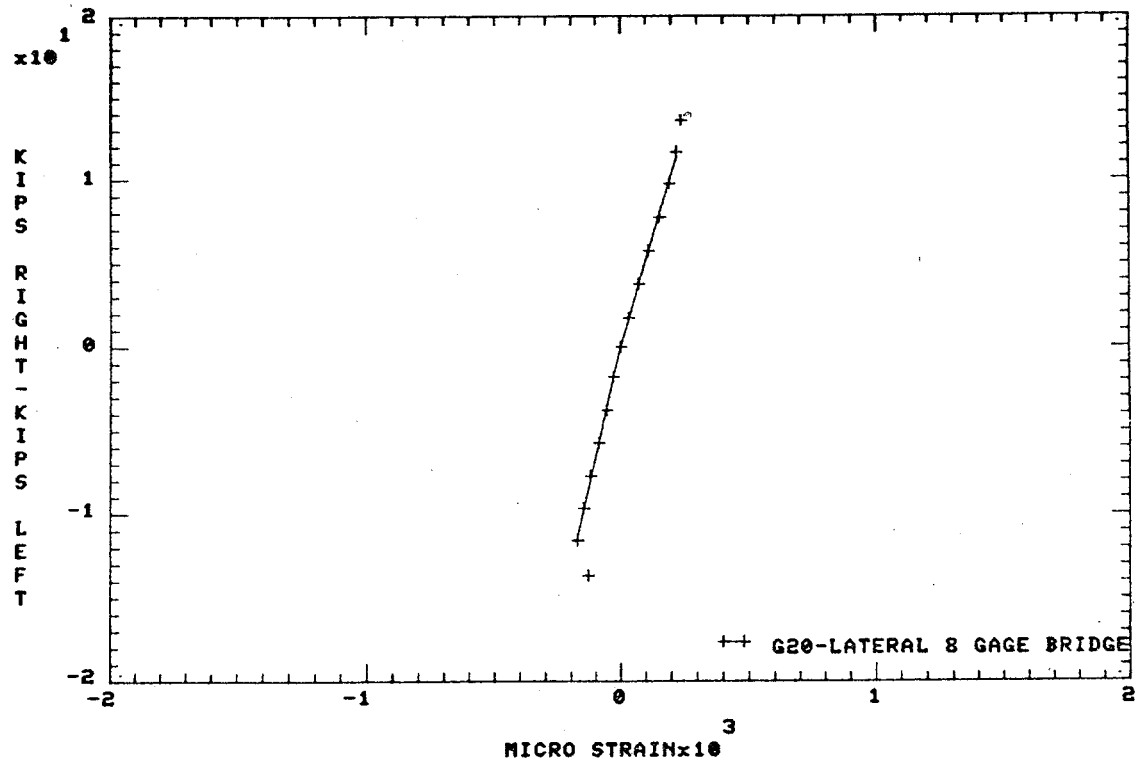

FIGURE 11. LATERAL LOAD BRIDGE, RESPONSE TO LATERAL LOAD ON HITCH.

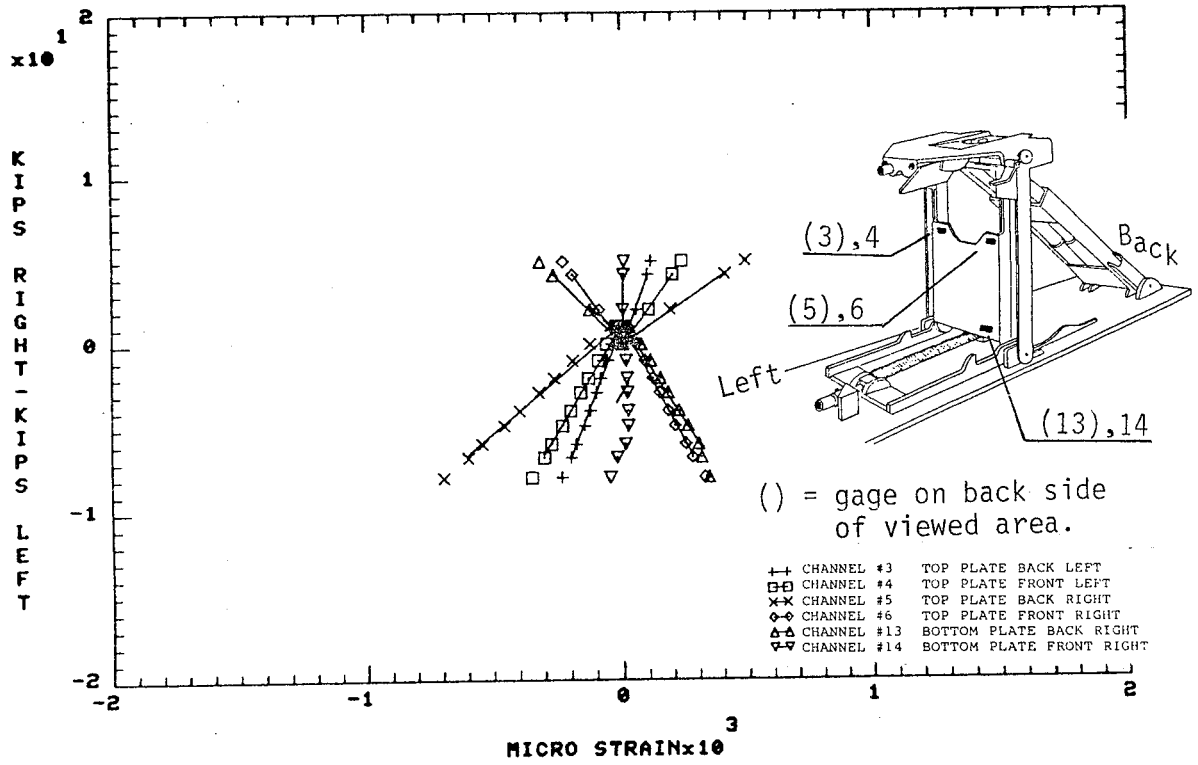

FIGURE 12. PLATE SINGLE STRAIN GAGES, RESPONSE TO LATERAL LOAD ON TRAILER.

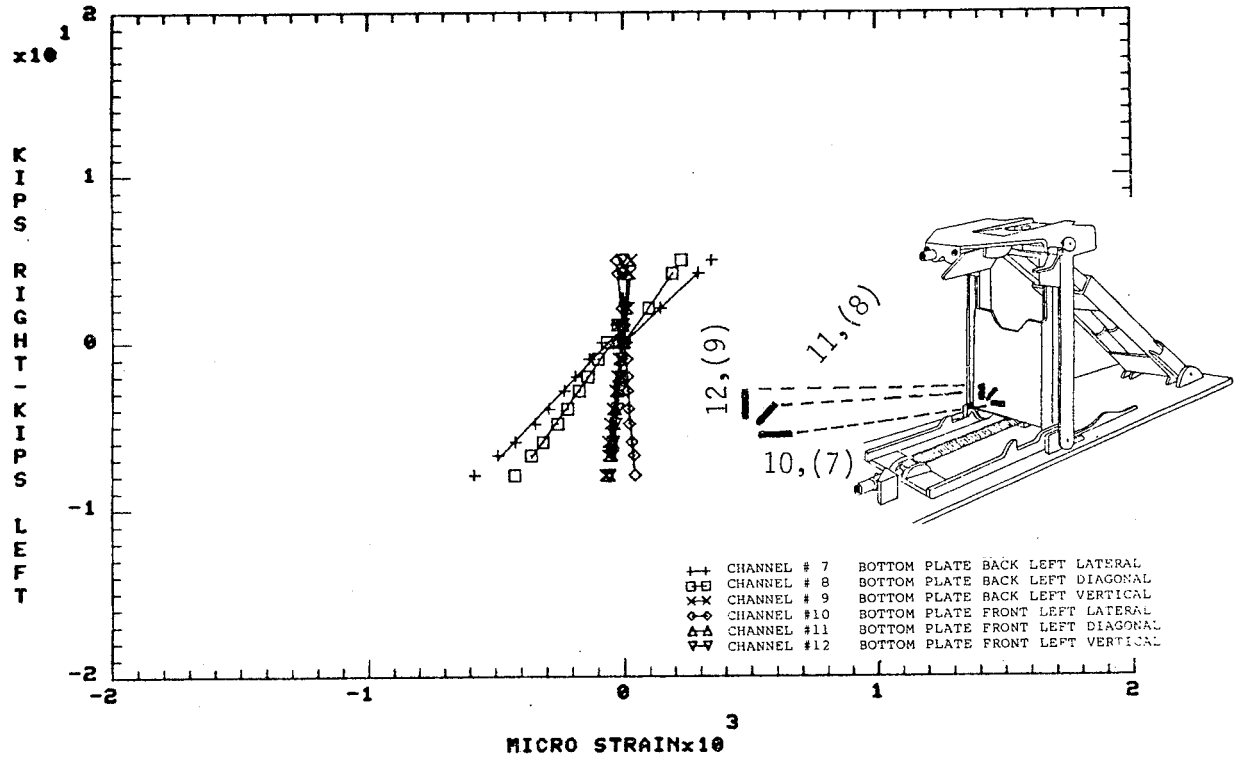

FIGURE 13. PLATE ROSETTE STRAIN GAGES, RESPONSE TO LATERAL LOAD ON TRAILER.

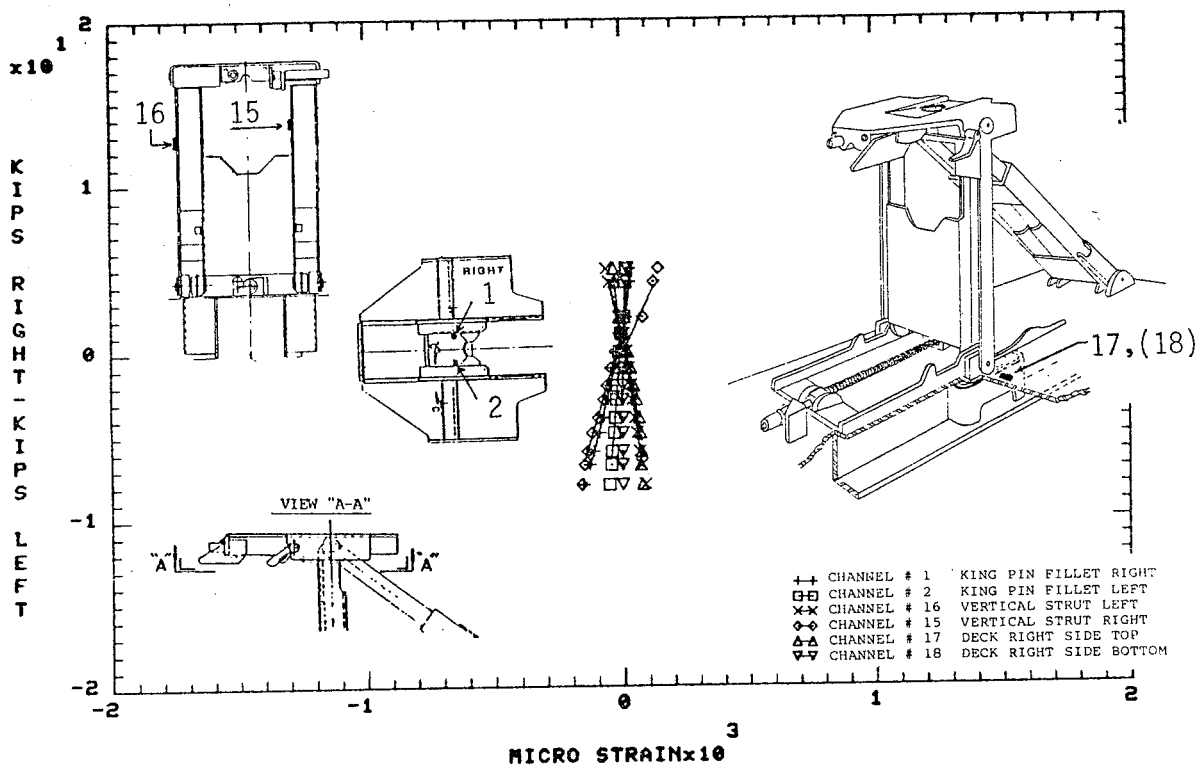

FIGURE 14. STRUCTURE STRAIN GAGES, RESPONSE TO LATERAL LOAD ON TRAILER.

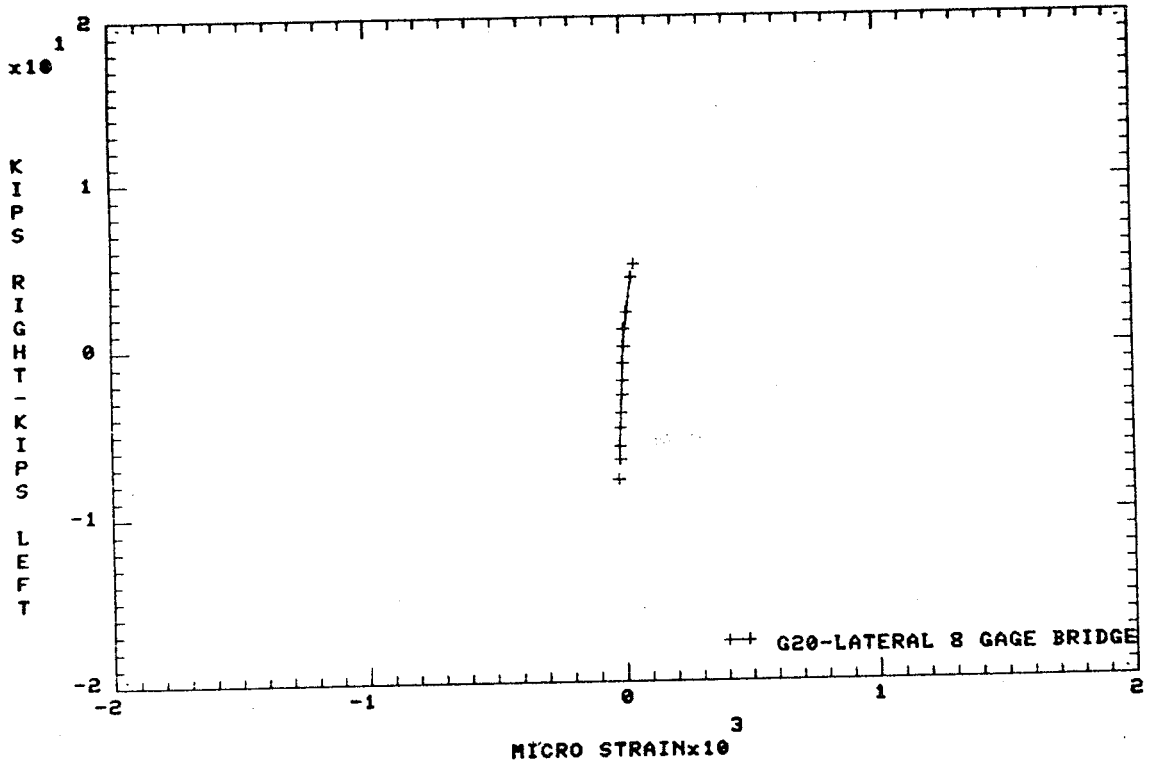

FIGURE 15. LATERAL LOAD BRIDGE, RESPONSE TO LATERAL LOAD ON TRAILER.

TABLE 5. PULL HITCH RIGHT, C053 (TRAILER OFF CAR).

(Strain in με)

Load/Ch.#	1	5	7	13	15	16	17	18	20
0 K	-24.9	22.2	29.7	-52.2	-38.4	-28.4	-5.0	2.5	6.5
10 K	-164.5	1176.9	551.2	-754.0	183.1	-229.4	-10.4	70.3	212.1
0 K	-31.1	168.7	-68.6	7.3	-65.4	-46.3	3.6	-4.5	17.8
2 K	-38.7	336.8	45.5	-100.5	-25.7	-75.1	-23.4	17.3	50.2
4 K	-54.1	559.1	194.2	-242.9	36.6	-109.4	-51.6	39.5	90.3
6 K	-71.1	760.0	338.7	-397.8	87.5	-147.1	-63.9	46.4	129.9
8 K	-88.2	963.3	462.8	-517.5	142.9	-185.7	-85.7	63.5	171.7
10 K	-104.1	1176.4	581.2	-749.5	192.7	-219.4	-102.9	70.8	210.7
12 K	-111.6	1363.6	695.1	-910.8	211.4	-246.2	-122.2	84.2	236.8
14 K	-116.6	1549.1	811.1	-1031.1	252.3	-253.6	-153.3	115.4	254.9
0 K	-31.7	178.6	-46.5	25.4	-64.1	-17.6	5.9	-7.5	11.9

(See Figures 8 through 11)

TABLE 6. PULL TRAILER RIGHT, C054.

(Strain in με)

Load/CH.#	1	5	7	13	15	16	17	18	20
0 K	289.8	101.2	-55.7	170.4	-546.5	-110.7	-18.7	22.0	-14.5
2 K	306.6	290.7	47.6	47.6	-457.7	-122.5	-30.7	28.8	-136.4
4 K	318.0	510.6	237.1	-92.1	-416.6	-162.0	-16.6	37.7	114.8
5 K	319.4	591.3	290.5	-145.4	-397.9	-172.5	-52.7	42.6	-104.5
0 K	361.5	159.1	1.6	143.1	-484.9	-113.0	4.7	-4.4	-135.3

4. A pull to the right causes a small tensile strain in the bottom deck gage (#18) (7 με/kip) microstrain/1,000 pounds.

It is apparent from Figure 8 that considerable bending in the plate is introduced by the lateral loading. For example, Channel #6, which is the gage on the opposite side (front) of the plate from Channel #5 (top plate, back right), even has the opposite sign of strain than that observed in Channel #5.

Also it appears there is a basic right/left asymmetry with respect to gage response. A pull to the right causes a larger strain magnitude in the right side gages than an equal pull to the left causes in the corresponding left side gages.

Removal of deck support does not appear to significantly affect the plate gage responses, although the greater deck flexibility does increase the deck gage strains. The sensitivity of strain response from the various data channels in terms of μin/in/kip lateral load for many of the static tests are listed in Tables 7 and 8.

3.2.2 Hitch Lateral Compliance

In addition to observing the strain response to lateral hitch load, the lateral hitch compliance was estimated from measurements of the lateral movement of the hitch head relative to the car deck. The diagonal distance between a fixed point on the head and a point on the car side sill was measured at 2,000-pound intervals. The results are shown in Figure 16. The relative lateral motion was then calculated from a simple trigonometric relationship.

The lateral compliance of the hitch was approximately 0.039" per 1,000-pound pull. Alternatively, the lateral spring constant appears to be 25,641 lb/inch. It should be noted that because of the way the measurement was made some transverse deck bending flexibility was included. Nevertheless, this value is still 71% greater than the value of 15,000 lb/in. assumed in a recent analysis of TOFC dynamic response[5] following the reference value given in the FRATE model user's manual[6].

3.2.3 Static Lateral Pull on Trailer

In an effort to explore the possible interaction of vertical and lateral loads, some testing was done by applying moderate loads to the trailer side in line with the hitch head. From these tests the following observations are made:

1. The vertical trailer load did not significantly affect the sensitivity of individual plate gages to lateral load.

2. However, the sensitivity of the lateral load circuit is reduced from 20 to 8 με/kip pull right.

3. A pull to the right in the trailer causes a positive strain increment of 28 με/kip to the right strut (#15) and a strain increment of -13 με/kip in the left strut (#16).

TABLE 7. DATA CHANNEL SENSITIVITY OF STRAIN RESPONSE, ORIGINAL DECK SUPPORT.

		PRE DYNAMIC TEST				POST DYNAMIC TEST			
		Lateral Load On Trailer		Lateral Load On Hitch		Lateral Load On Trailer		Lateral Load On Hitch	
Channel Number	Gage Number	C040 Right	Left	C041 Right	C023 Left	C054 Right	C069 Left	C053 Right	C062 Left
1	G1	-7.90*		-2.14	-2.67	5.90	-15.40	-7.30	-1.52
2	G2	-2.23		-1.10	-1.10	3.60	-5.31	-3.75	-0.54
15	G14	61.57		88.06	70.70	28.50	-16.07	24.83	-22.40
16	G11	-45.90		-50.97	47.50	-12.32	8.82	-18.30	15.03
17	G17	-8.15		-10.47	10.30	-6.80	7.56	-10.75	3.98
18	G18	6.10		9.00	-9.30	4.12	0.00	7.48	-5.14
7	7L	55.60		50.69	-53.60	69.26	-58.28	52.15	-98.90
8	7D	35.41		28.72	-37.00	45.50	-42.47	32.84	-53.90
9	7V	5.85		1.54	-4.50	5.76	-6.88	1.81	0.73
10	8L	-13.30		-38.60	4.45	-5.18	4.29	-9.98	26.85
11	8D	2.30		-3.91	-3.12	3.46	-5.80	-3.30	9.07
12	8V	-1.64		-0.76	-2.25	-1.00	-5.76	-2.13	-3.37
3	G3	6.96		9.78	-14.30	22.34	-23.50	9.10	-18.22
4	G4	33.00		33.40	-34.10	47.30	-34.95	39.30	-45.20
5	G5	68.10		100.20	-60.90	98.02	-69.65	100.70	-75.80
6	G6	-28.70		-42.80	31.13	-45.12	32.26	-45.00	40.40
13	G13	-46.20		-56.50	29.40	-63.16	34.02	-76.13	20.30
14	G10	2.58		-7.57	4.88	1.35	-4.77	-6.70	-19.95
20	G20	8.02		15.70	5.60	8.24	-2.40	19.40	-16.08

* Values shown in table indicate strain in micro inch/inch for 1 kip lateral load applied to the right or left.

TABLE 8. DATA CHANNEL SENSITIVITY OF STRAIN RESPONSE, MODIFIED DECK SUPPORT.

		PRE DYNAMIC TEST				POST DYNAMIC TEST			
		Lateral Load On Trailer		Lateral Load On Hitch		Lateral Load On Trailer		Lateral Load On Hitch	
Channel Number	Gage Number	C079 Right	C074 Left	C077 Right	C072 Left	C054 Right	C064 Left	C051 Right	C062 Left
1	G1	-1.10*	-20.90	-3.94	-4.90	-4.00	-16.90	-6.72	-5.80
2	G2	2.63	-6.90	-2.27	-2.20	4.60	-6.87	-3.40	-3.90
15	G14	28.40	-18.30	20.68	-13.87	32.60	-30.56	25.00	-15.39
16	G11	-22.00	11.80	-14.90	13.60	-30.60	5.68	-18.90	10.08
17	G17	-49.70	39.14	-56.60	47.40	-41.50	41.10	-65.30	47.00
18	G18	80.53	-54.70	80.00	-54.80	61.90	-57.38	88.80	-60.00
7	7L	63.12	-68.15	72.60	-60.35	62.00	-63.50	49.80	-54.40
8	7D	34.65	-46.90	29.16	-40.90	36.60	-45.30	33.50	-37.28
9	7V	1.78	-7.26	-1.34	-3.65	0.60	-9.60	2.97	-4.30
10	8L	-23.50	-0.25	-29.00	1.34	-21.40	-1.70	-5.90	-0.50
11	8D	-6.98	-8.30	-14.19	-4.40	-7.08	-9.60	1.79	-5.90
12	8V	-0.50	-5.64	1.32	-1.10	-1.90	-8.90	-1.80	-3.10
3	G3	15.92	-30.00	14.69	-16.55	14.80	-28.40	10.50	-15.97
4	G4	44.40	-38.40	45.90	-32.50	50.90	-44.27	48.20	-31.30
5	G5	107.60	-74.20	92.30	-52.73	113.00	-70.40	111.40	-53.90
6	G6	-50.00	35.20	-50.80	29.60	-52.60	35.70	-56.80	29.60
13	G9	-82.10	28.20	-62.10	18.10	-94.20	27.70	-61.90	19.90
14	G10	3.77	-4.00	-3.76	-2.20	3.00	-3.50	-21.70	0.38
20	G20	15.10	-1.40	18.19	-13.00	21.00	-3.80	20.00	-9.30

* Values shown in table indicate strain in micro inch/inch for 1 kip lateral load applied to the right or left.

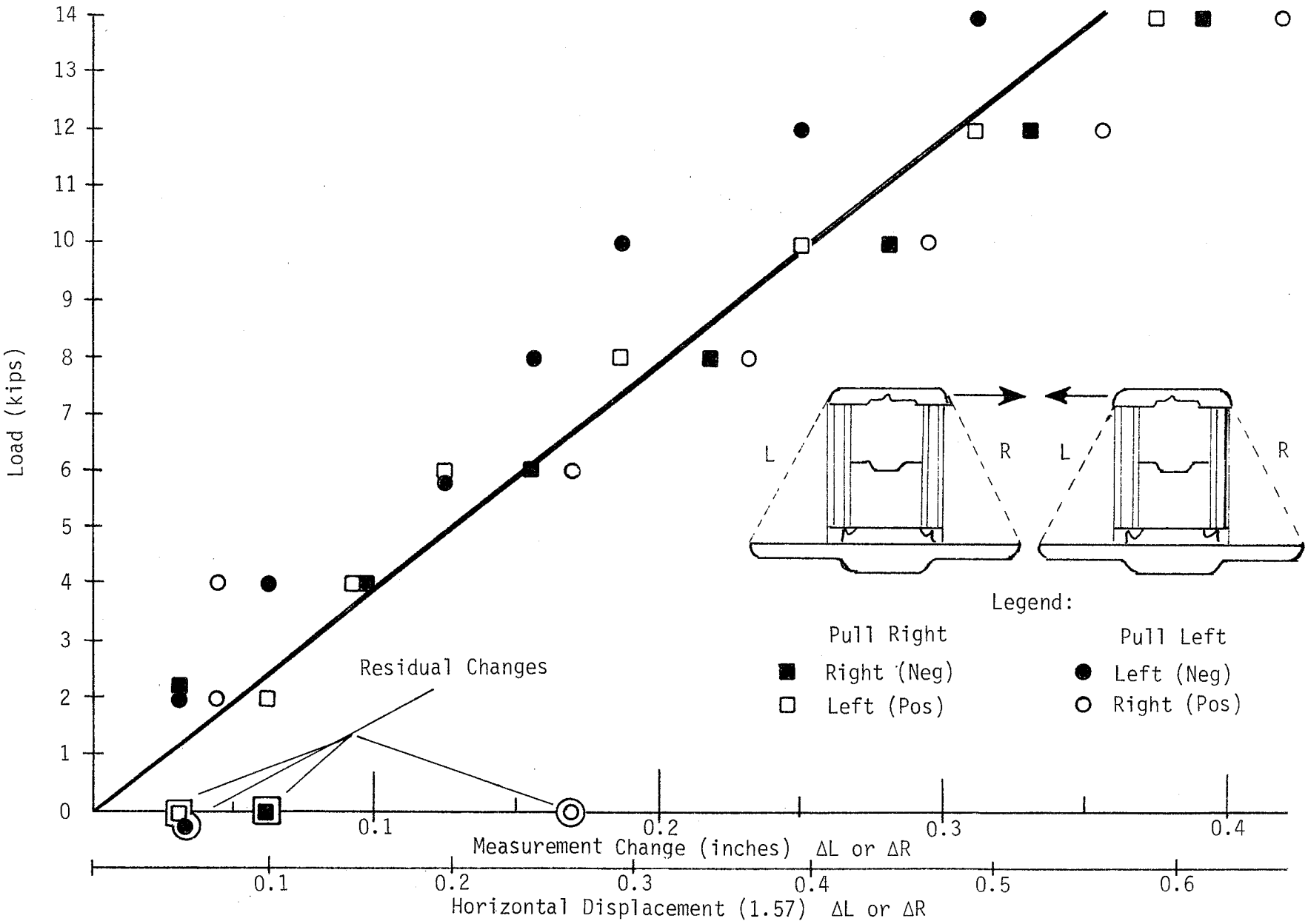

FIGURE 16. FAT II HITCH, LATERAL COMPLIANCE TEST RESULTS.

3.3 ROLL AND TWIST TESTS

A few static tests of the trailer-loaded car were made to measure the response of the hitch strain gages to moderate carbody roll and twist displacements. The purpose of the jacking tests was to calibrate the vertical and lateral load transducer schemes and to obtain an idea of the range involved.

Using jacks located at the two jacking pads at the AR and BR corners, the car was jacked 5 equal displacement increments until the truck springs were fully compressed. At each jacking interval strain levels were recorded, roll of the car relative to the ground measured, and rotation of the trailer (relative to the car deck) was measured. Roll and rotation were measured using inclinometers. This test was repeated by jacking on the left side of the car.

In addition to the roll jacking test, a twist was introduced by jacking at the B-end, Right (BR) and A-end, Left (AL) corners with the same jacks and using the same measurements.

From these tests it was observed:

1. A uniform "roll" of the car produced by jacking both pads on one side, up by 5 inches, caused a strain increment of less than 120 $\mu\varepsilon$ in the plate gages. This was enough roll to raise the center plate edge to top of the 1 1/8 inch high rim.

2. A maximum twist of the car produced by jacking opposite ends of the car, up by 2 inches, caused a strain increment of less than 100 $\mu\varepsilon$ in the plate gages.

3.4 COMPARISONS TO FINITE ELEMENT MODEL PREDICTIONS

It is desirable to have some hitch stress analysis results to compare with experimental values in order to confirm or challenge the credibility of results as well as gain some insight into the actual load distribution or boundary conditions on the hitch. Although a comprehensive stress analysis of the hitch is beyond the scope of this report, a limited effort was undertaken to model the hitch tested using one of the Finite Element Model (FEM) computer programs available on the AAR's computer - the GIFTS program[6].

The FEM constructed for these purposes is shown in Figure 17. Simple four-node plate elements were used. In this exploratory study only a few idealized boundary conditions and load distributions were considered. For simplicity, the hitch struts were assumed to be "built in" to a rigid deck. Any diagonal support reactions were ignored. Furthermore, two extreme load distributions were selected for the analysis of both vertical and lateral loading. In the uniform distribution case, equal lateral or vertical forces were distributed over the upper ends of both the right and left strut channels. For the non-uniform or eccentric loading case, all loads were applied to the right strut, which in tests was observed to be the most heavily loaded strut. Only the pull to the right was analyzed in the lateral load study.

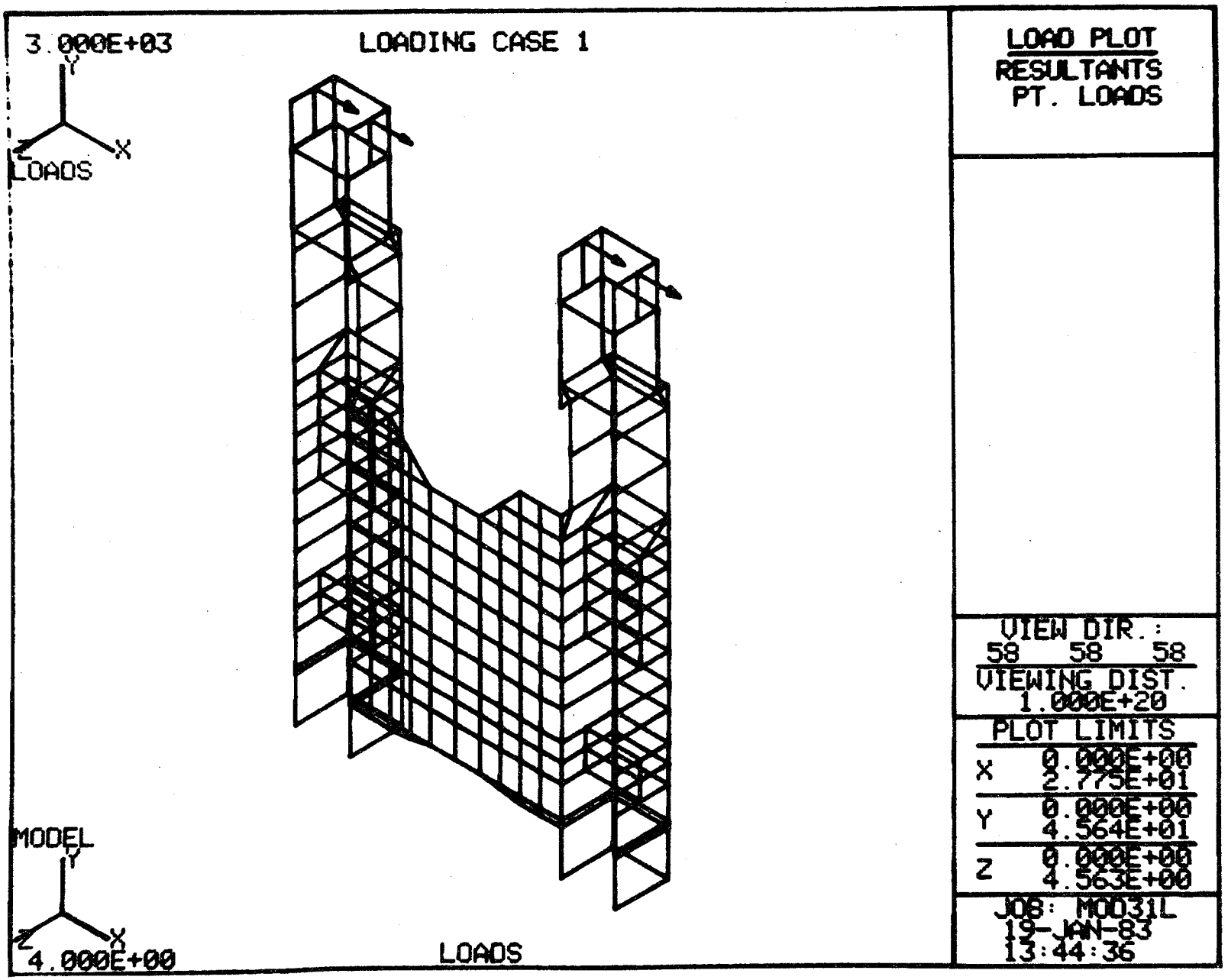

FIGURE 17. TYPICAL FINITE ELEMENT MODEL OF TRAILER HITCH.

From an examination of the FEM results for a uniformly distributed vertical load of 21 kips, it was apparent that the experimentally derived vertical stress values were very high even after the bridge circuits were modified by replacement of the Poisson gages with fixed internal bridge circuit "completion" resistors. Even the case of full vertical loading of the right strut predicted much lower strut stresses than those derived from experimental values listed for Channel #15 (right strut) in Table 4. Comparisons of experimental results versus FEM predictions and direct "strength of materials" computation results are provided in Table 9. From these comparisons it is concluded that the strain values reported for Channels #15 and #16 are unreasonably high, even though they may adequately indicate the degree of eccentric loading in this particular case. This finding casts doubts on the reliability of experimental values from bridge circuit channels. The single gage channel data acquisition and processing still appears credible in light of the good correlation with analysis of Channel #19 (centersill) data reported in Section 3.1 above.

TABLE 9. THEORETICAL Vs MEASURED VERTICAL STRESSES, HITCH STRUT AT 21 KIPS VERTICAL LOAD.

Source	Left Strut	Right Strut
Experiment* (C041)	-2.38	-15.86
Experiment* (C043)	-3.16	-11.37
Strength Theory** (Uniform)	-1.61	-1.61
Strength Theory** (Non-Uniform)	0.00	-2.32
F.E.M. (Uniform)	-2.31	-2.30
F.E.M. (Non-Uniform)	-0.01	-4.60

* Based on measured Strain x 30,000,000.
** Based on strut channel cross section area of 6.5 square inch.

A simple strength-of-materials analysis is not practical for determining stresses in the hitch plate, so the FEM predictions alone were considered and the lateral load cases with no vertical loading were selected for comparison with experimental results. The deflected hitch shapes for uniform and non-uniform load distribution are illustrated in Figures 18a and 18b, respectively. Contours of the back surface maximum principal stress distributions corresponding to these cases are also shown in these figures. An enlargement of the local stress contours in the region of plate gage Channel #5 is also given in Figures 19a and 19b. A direct comparison of FEM predictions and experimental results for selected plate gage locations is provided in Table 10. The correlation of theory and experiment is reasonably good (within 12%) at the most critical location (Gage #5) for the non-uniform loading condi-

tions. However, the amount of plate bending predicted is considerably less than measured.

The size of the finite elements (1.75 inches on a side) in the region of stress concentration is recognized to be relatively large. This "coarseness" of the model may adversely affect the accuracy of stress values predicted in the hitch plate regions near gage #5, for example. In order to evaluate this limitation, a computer run was made with a "refined" plate model for the non-uniform lateral load case. The FEM mesh refinement consisted of the replacement of four adjacent plate elements at the top of the hitch plate/vertical strut junction with one hundred elements.

It was apparent from the results of this analysis that the FEM mesh refinement did not materially affect the conclusions made on the basis of the results such as those presented in Table 10. The predicted amount of plate bending is virtually the same with both models. A thirteen percent reduction in the predicted horizontal stress component is actually predicted for the refined model at the gage #5 location.

TABLE 10. COMPARISON OF EXPERIMENTALLY-DERIVED STRESSES TO FEM PREDICTION FOR 10K PULL TO RIGHT.

Plate Location	Experimental			Lateral Load at Both Strut Theoretical			Lateral Load at One Strut (Right) Theoretical		
	Verti.	Horiz.	Shear	Verti.	Horiz.	Shear	Verti.	Horiz.	Shear
Top Plate Back Right (From channel #5)		30.23		2.34	12.86	-4.87	4.41	25.25	-9.13
Top Plate Front Right (From channel #6)		-13.44		-1.26	-0.55	-0.17	-2.78	-0.40	0.02
Top Plate Back Left (From channel #3)		2.76		-2.50	-13.21	-4.87	-0.38	-0.31	-0.13
Top Plate Front Left (From channel #4)		11.73		1.43	0.91	-0.17	-0.15	0.56	-0.36
Bottom Plate Back Right (From channel #13)		-22.70		-3.70	-18.20	-9.50	0.92	-17.80	-6.00
Bottom Plate Front Right (From channel #14)		-1.52		-1.90	-7.30	-8.51	2.50	-8.10	-5.40
Bottom Plate Back Left (From channel #7,8,9)	7.33	21.69	1.02	3.46	17.72	-9.33	8.00	18.60	-12.86
Bottom Plate Front Left (From channel #10,11,12)	-1.80	-5.10	1.07	2.00	7.34	-8.52	6.56	6.72	-11.74

* Based on measured horizontal strain X 30,000,000.
Stress in ksi

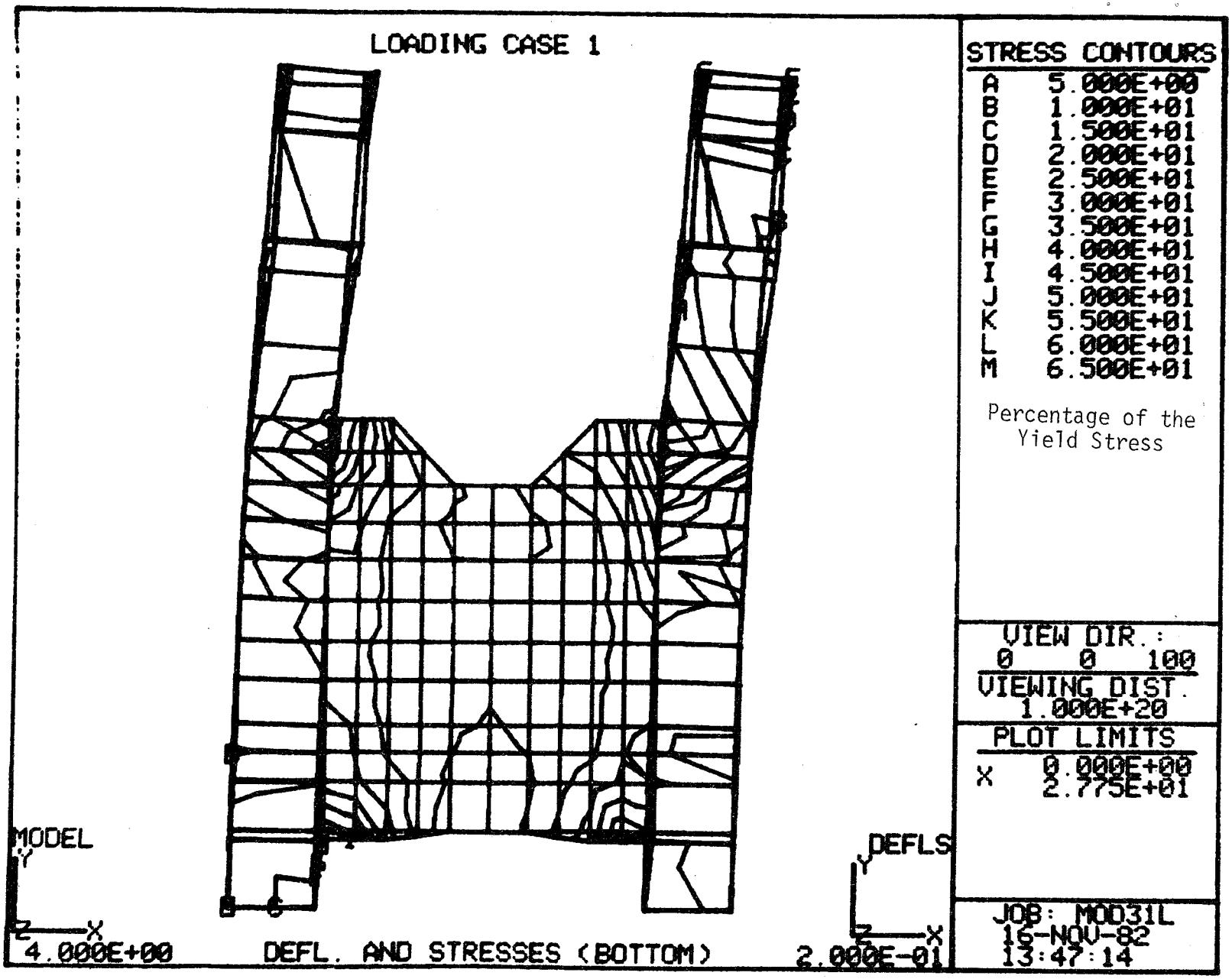

FIGURE 18a. BACK SURFACE STRESS CONTOURS FOR 10 KIPS UNIFORM LATERAL LOAD.

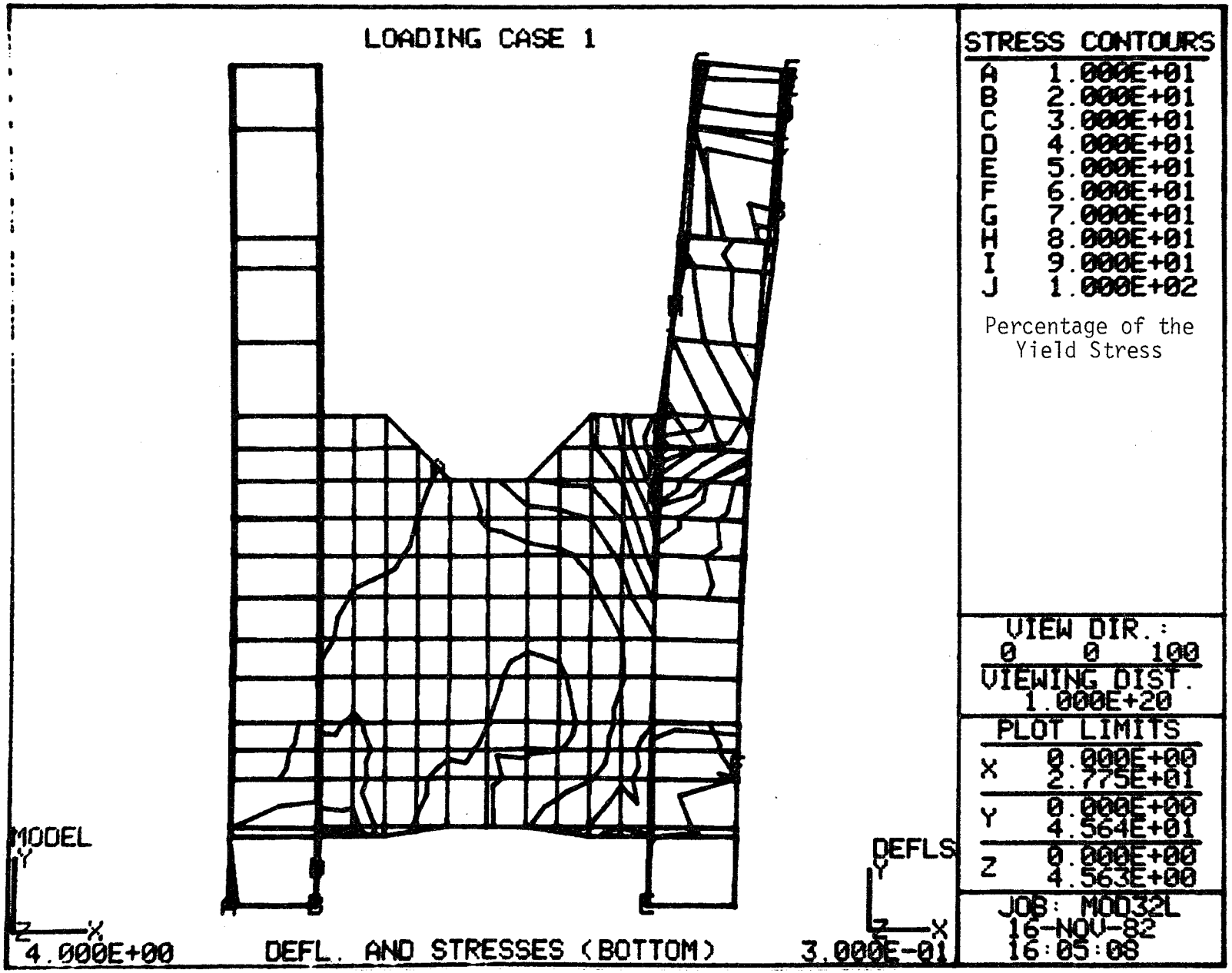

FIGURE 18b. BACK SURFACE STRESS CONTOURS FOR 10 KIPS NON-UNIFORM LATERAL LOAD.

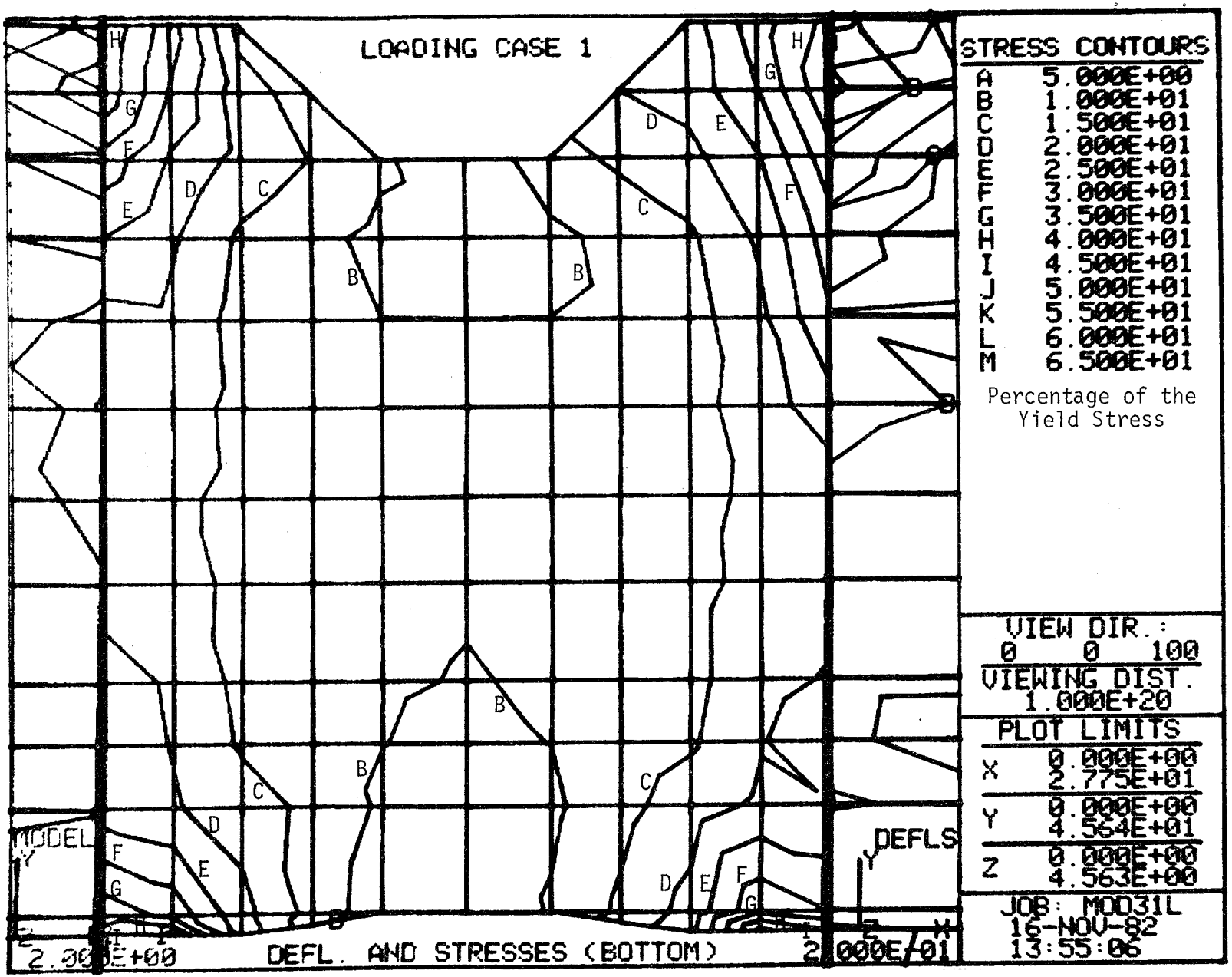

FIGURE 19a. ENLARGED VIEW OF STRESS CONTOURS FOR UNIFORM LOAD.

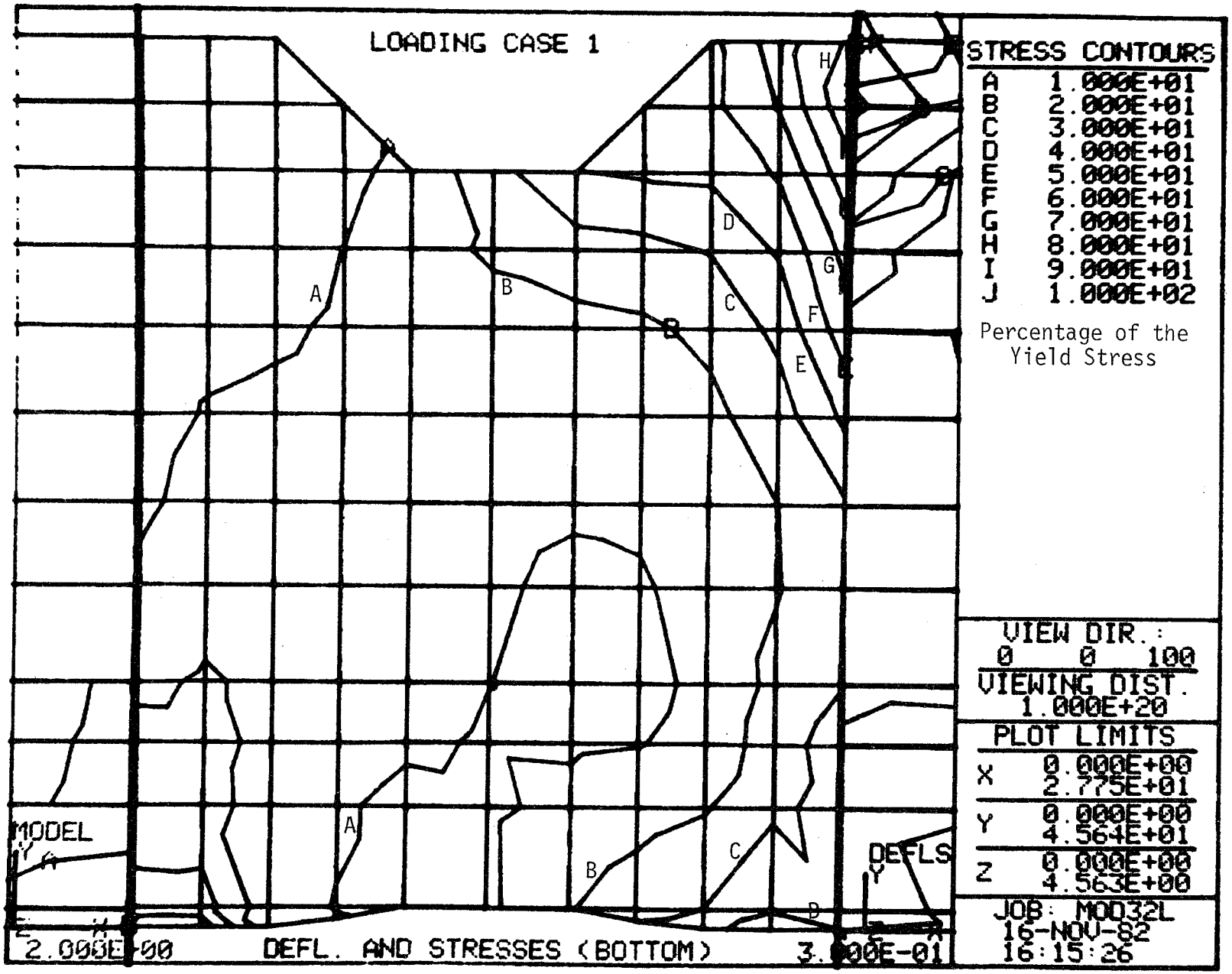

FIGURE 19b. ENLARGED VIEW OF STRESS CONTOUR FOR NON-UNIFORM LOAD.

4.0 FAST DYNAMIC TESTS

4.1 FAT II CONSIST AND DATA ACQUISITION

The test consist included the T-8 instrument car, a 100-ton ballast car, and the test car with the instrumented hitch in the leading position. See Figures 20, a through d.

The T-8 instrument car has an onboard PDP 11/34 computer which controlled the data acquisition, and produced "quick-look" summaries of selected data channels between runs. The sampling rate was 100 samples/sec for all of the dynamic test runs. The data were filtered at 20 Hz, digitized and recorded on digital tape, copied and transmitted to the AAR in Chicago for further data reduction. (Additional detail on test instrumentation is provided in Appendix 1.) "Quick-look" summaries were made for data evaluation on site. These were also useful from an analysis viewpoint.

4.2 TYPICAL TRANSDUCER OUTPUT

Figure 21 shows the response of one of the most active strain channels (in terms of nominal stress) for a period of normal FAST operation over Sections 03 through 09. The strain range for some of the fatigue critical locations was quite high and it is conceivable that a net lateral load may have existed on the hitch during negotiation of certain segments of the loop (Section 07). As noted in the figure, it can be seen that the stress range, on a "once a lap" basis, went as high as 46,000 psi.

4.3 QUICK-LOOK MAXIMUM RANGE SUMMARIES

Prior to any detailed fatigue or dynamic analyses, a portion of the extensive data from the dynamic testing was surveyed in order to identify the most significant transducers and to obtain a quick overview of the effect of the several modes of operation and structural change on the maximum signal range. It was understood that this survey would not be definitive from a fatigue damage standpoint, since the distribution of ranges and numbers of cycles must be evaluated. Nevertheless, it would serve to focus the subsequent fatigue analyses.

Rather than carry out an extensive cycle counting of all strain gage signals recorded throughout the test, an initial computer survey of all channels was conducted, with maximum and minimum values (ranges) of strain noted during a significant portion (over 2 laps) of two test runs at normal FAST speed. These two runs were Run #14, at 45 mph CCW with the original deck support configuration, and Run #21, at 45 mph CCW with the modified deck support. These observed maximums, minimums, and ranges are tabulated in Table 11. It may be seen that the greatest range (nearly 2,000 microinches) occurs for Plate Gage #5. Also note that the deck gage strain range was very small except for the modified car, where greater bending would be expected.

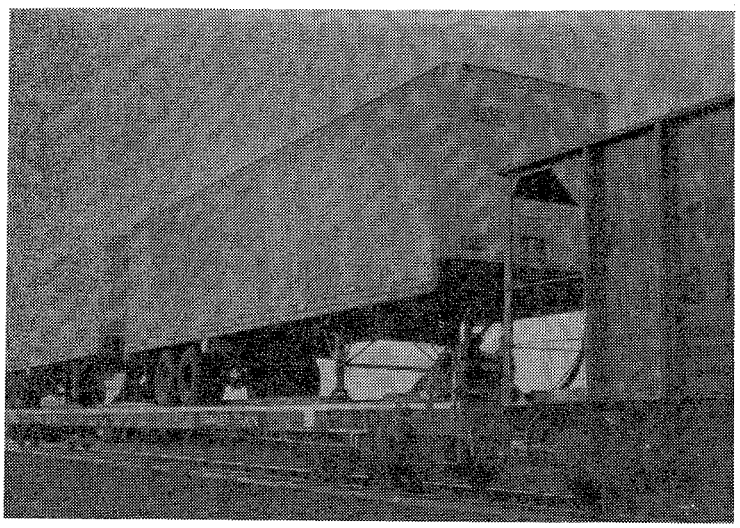

(a)

(b)

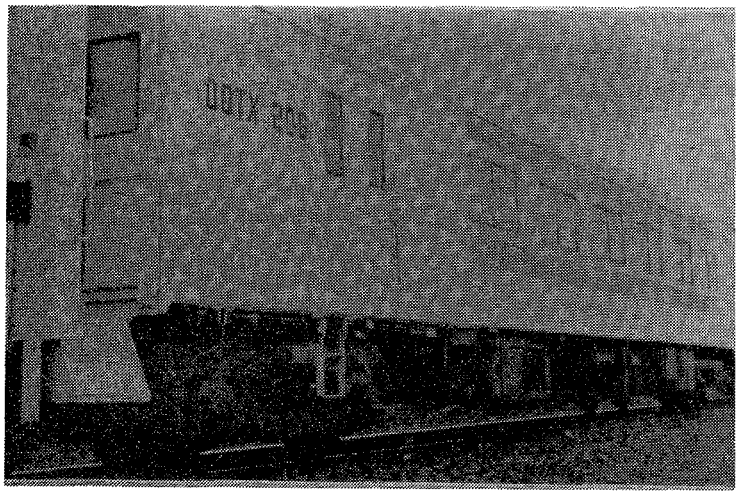

(c)

FIGURE 20. VIEWS OF TOFC CONSIST AND INSTRUMENTATION CAR.

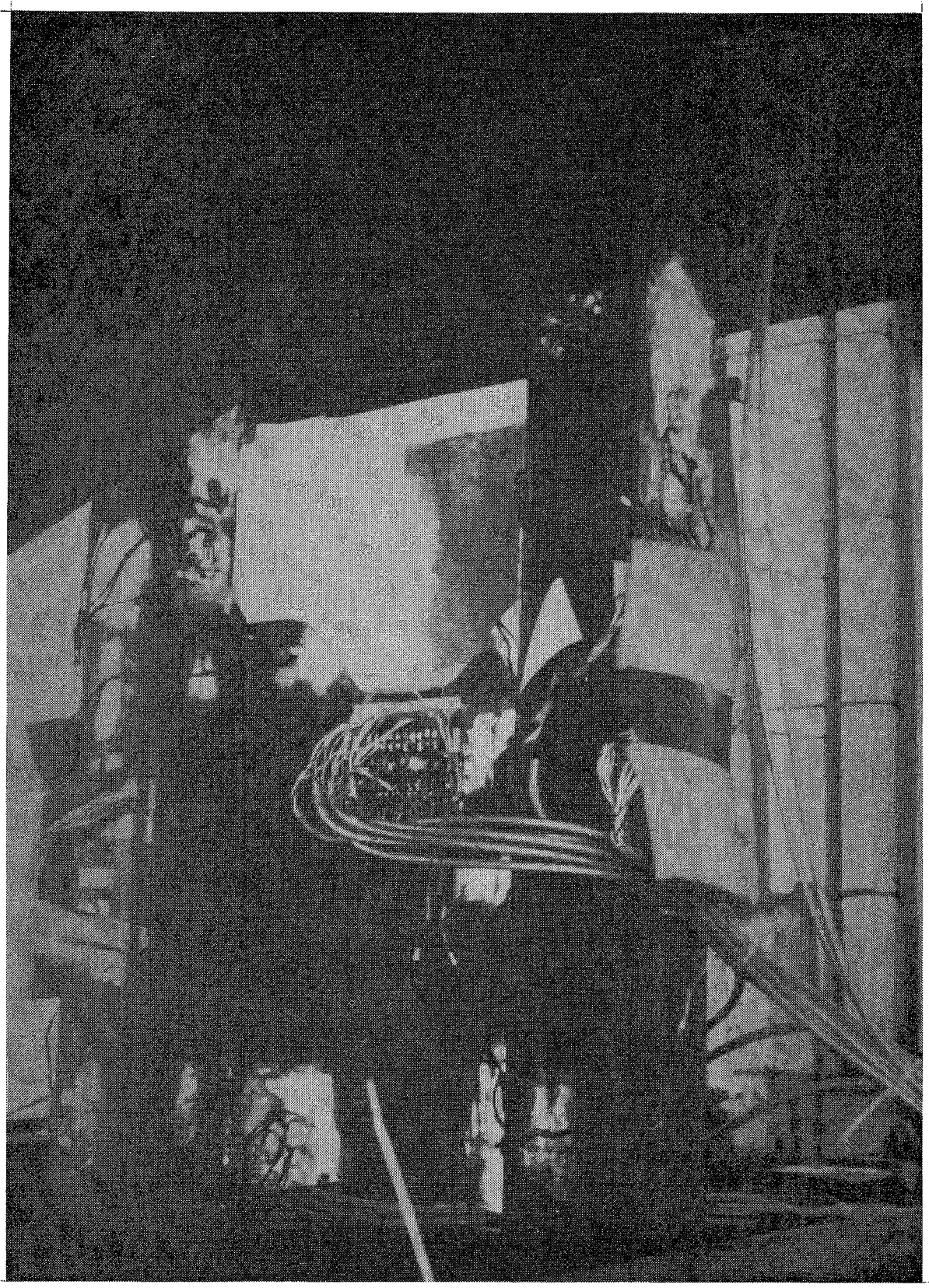

FIGURE 20 (d). VIEW OF INSTRUMENTED HITCH.

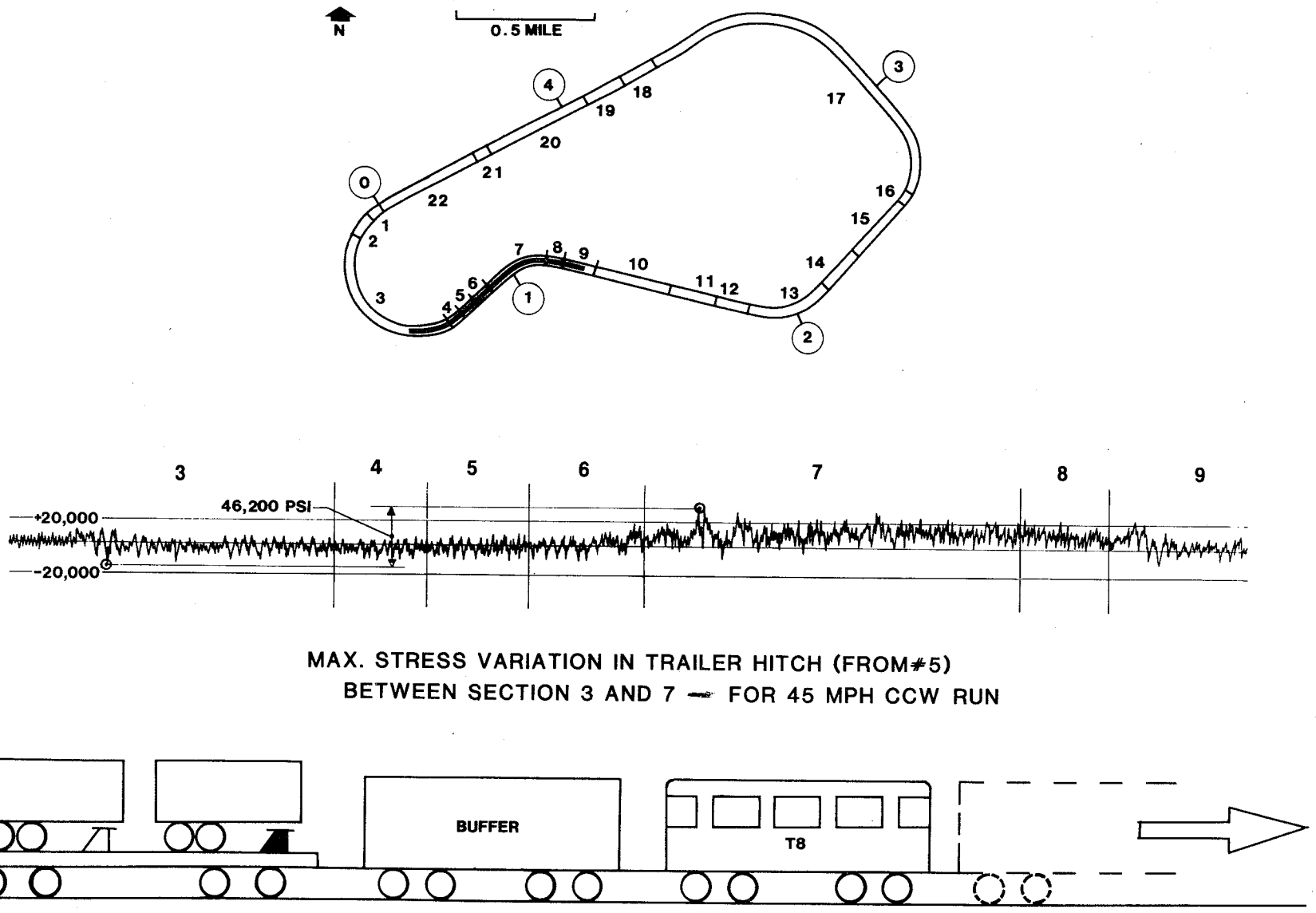

MAX. STRESS VARIATION IN TRAILER HITCH (FROM#5)
BETWEEN SECTION 3 AND 7 — FOR 45 MPH CCW RUN

FIGURE 21. MAXIMUM STRESS VARIATION IN TRAILER HITCH.

TABLE 11. MAX/MIN MEASUREMENTS, 2.1 LAPS ON FAST, MODIFIED AND UNMODIFIED CARS.

	Unmodified Car (R14A00)		Modified Car (R21A00)	
Measurement Channel #	Max. In Micro Inch	Min. In Micro Inch	Max. In Micro Inch	Min. In Micro Inch
1	155.38	-567.69	564.0	-26.916
2	148.04	-185.96	270.38	11.011
3	1772.82	-321.77		
4	403.74	-178.6	303.4	-343.7
5	1008.15	-900.48	544.4	
6	300.97	-418.43	325.4	242.24
7	414	-511.41	616.63	-196.98
8	283.84	-292.41	254.48	-184.7
9	81.07	-4.893	11	-117.45
10	194.53	-113.78	-7.34	-311.98
11	42.82	44.04	-39.15	-162.72
12	42.71	7.34	84.42	26.91
13	440.4	-539.5	705.94	-288.74
14	113.78	-156.605	319.32	13.23
15	411.18	-162.148	145.0	-655.32
16	174.94	-275.339	257.6	-232.51
17	67.39	-105.2194	62.39	-773.24
18	127.242	-37.927	1321.36	91.76
19	89.31	-81.97	99.10	-67.29
20	260.	-52.0	116.235	-237.76

TABLE 11 (CONTINUED). MAX/MIN MEASUREMENTS, 2.1 LAPS ON FAST, MODIFIED AND UNMODIFIED CARS.

	Unmodified Car (R14A00)		Modified Car (R21A00)	
Measurement Channel #	Max.	Min.	Max.	Min.
21	0.3639g	0.339g	0.393g	0.354g
22	0.224g	-0.264g	-0.2272g	-0.2619g
23	0.444g	-0.414g	0.4538g	0.4465g
24	0.377g	-0.368g	0.3778g	0.3851g
25	0.637g	-0.7102g	0.9738g	-0.842g
26	0.736g	-0.476g	0.9786g	-0.68g
27	0.8319g	-0.817g	1.082g	-0.998g
28	0.8981g	-0.637g	0.827g	-0.6742g
29	0.425g	-0.350g	0.542g	-0.372g
30	0.502g	-0.542g	0.7666g	-0.7442g
31	45.1 MPH	26.07 MPH	60.64 MPH*	27.83 MPH

* Momentary speed "spike"

This horizontal plate gage, as well as one of the head weld gages, a deck gage below the hitch attachment at the reinforcement, the vertical strut strain circuit, lateral load circuit, and the two lateral accelerometers were selected for closer study. These transducer ranges were observed for the original and modified car during operation over a tangent section (20) and a curve section (07) and are summarized in Table 12.

For operation throughout the FAST loop, the greatest overall range of strain (Gage #5) for normal operation seems to have occurred between FAST Sections 03 and 07, which included a reverse curve. These ranges (calculated both from the test car analog oscillograph charts and the digital "quick-look" printouts) are presented in Table 13. The values of stress range for operation over this portion of the FAST loop are generally consistent with the maximum strain ranges observed over more than two laps each with the original and modified car.

TABLE 12. "QUICK-LOOK" DIGITAL DATA LISTINGS.

Transducer Ranges		Section 20 unmod	Section 20 mod	Section 7 unmod	Section 7 mod
Head Weld	5 MPH CCW	314	130	---	---
(με)	25 " "	547	477	321	242
(1)	45 " "	359	273	532	510
	25 MPH CW	551	429	362	280
	45 " "	524	392	242	191
Web Plate	5 MPH CCW	443	295	---	---
Horiz.	25 " "	673	715	673	624
(top right	45 " "	758	775	1370	1077
back)	25 MPH CW	711	554	547	520
(5) (με)	45 " "	909	757	846	746
Strut	5 MPH CCW	177	239	---	---
Channel	25 " "	325	522	317	318
Right	45 " "	374	385	361	329
Vertical	25 MPH CW	291	266	227	214
(15) (με)	45 " "	315	331	463	474
Strut	5 MPH CCW	117	158	---	---
Channel	25 " "	271	350	255	307
Left	45 " "	315	316	189	243
Vertical	25 MPH CW	240	239	110	188
(16) (με)	45 " "	276	296	327	325
Deck	5 MPH CCW	34	410	---	---
Bottom	25 " "	50	1030	44	560
(με)	45 " "	62	679	146	775
(18)	25 MPH CW	48	690	46	462
	45 " "	68	774	62	659
Lateral	5 MPH CCW	107	95	---	---
Load	25 " "	258	243	128	180
(με)	45 " "	174	183	309	166
(20)	25 MPH CW	278	167	167	109
	45 " "	232	174	219	229
Lateral	5 MPH CCW	0.37	0.19	---	---
Accel.	25 " "	0.28	0.53	0.51	0.51
Trailer	45 " "	0.37	0.42	0.58	0.65
(g)	25 MPH CW	0.40	0.40	0.35	0.34
(24)	45 " "	0.42	0.41	0.50	0.44
Lateral	5 MPH CCW	0.40	0.29	---	---
Accel.	25 " "	0.45	0.44	0.44	0.43
Car	45 " "	0.49	0.68	0.89	1.28
(g)	25 MPH CW	0.46	0.59	0.37	0.49
(30)	45 " "	0.54	0.56	0.76	0.70

TABLE 13. GREATEST OVERALL MIN/MAX STRESS RANGE (KSI), HITCH PLATE GAGE #5.

	PHASE I UNMODIFIED CAR		PHASE II UNDER DECK WELD REMOVED	
RUN DIRECTION	ANALOG O'GRAPH	DIGITAL 'QUICK-LOOK'	ANALOG O'GRAPH	DIGITAL 'QUICK-LOOK'
CCW	46.2	49.4	37.9	38.0
CW	28.0	33.3	33.7	34.9

5.0 FATIGUE ANALYSIS APPROACH

5.1 PRELIMINARY CONSIDERATIONS

In order to assess the significance, from a structural integrity viewpoint, of a stress history such as that measured by the most active hitch plate gage for 45 mph CCW operation over FAST Sections 03 through 09, it is necessary to perform a fatigue analysis. Such an analysis requires:

a. "Counting" the fatigue-significant stress cycles included in a stress history record;

b. Selecting appropriate fatigue properties for the material and fabricated structural detail of interest;

c. Using a suitable cumulative damage rule to add up the damage or determine the fractional fatigue life "used up" by the spectrum or histogram of stress ranges per unit of service duration.

One approach (illustrated in Section 6.0 of this report) is based on the availability of an experimentally determined stress history in the region of interest. Alternatively, if only component vehicle load or acceleration history are available, then a stress analysis or auxiliary experiments are also required to at least estimate the nominal stress in the critical region. This approach is illustrated in Section 7.0. In either approach, as described in the AAR Fatigue Guidelines[1], the purpose is to obtain a nominal stress spectrum which may be applied to a structural detail for which conventional fatigue properties are available.

5.2 ASSUMPTIONS

The essential assumptions made in the FAT II fatigue analysis are discussed below.

5.2.1 Critical Stress Environment

The practice followed in this test program was to place strain gages within a few plate thicknesses of the expected crack origin and to orient them perpendicular to the direction of expected propagation. The "stress" was then obtained by simply multiplying the strain by the usual elastic modulus.

This may be a gross simplification of a generally complex multiaxial strain environment with strain gradients. The stress index selected should, of course, also depend on the fatigue criterion applicable to the crack initiation or propagation mode of concern. Nevertheless, this simple "stress" is often a satisfactory approximation.

In order to evaluate how satisfactory such a conventional approximation might be in this situation, the variations of the complete state of stress at two critical locations (having rectangular strain rosettes) were studied for periods surrounding minimum and maximum excursions of the most active plate

gage (#5). The details of this study are presented in Appendix 2. It was concluded, upon comparison with principal stresses, maximum shear stresses, and the "fatigue equivalent" uniaxial stress range, that this simple, measured "stress" does in fact provide a satisfactory approximation.

5.2.2 Cycle Counting

A full cycle-counting of this region, using the "rainflow" counting method[7] adopted by the AAR, produced a listing of stress ranges and mean stress, or, in matrix form, a Road Environment Percentage Occurrence Spectrum (REPOS). In the REPOS format, the maximum and minimum load limits of each significant half cycle or reversal are recorded as a percentage of the total number counted.

The "rainflow" program was used to count the cycles inherent in the stress histories such as that shown in Figure 21.

Since mean stress does not have a significant effect on the fatigue properties of many welded structural details, the resulting REPOS may be presented simply as a stress range histogram. As an illustration of these representations of stress environment, the REPOS (Figure 22) and associated histogram of stress range (Figure 23) are given for Gage #5 in the original car structural configuration for all combined clockwise and counterclockwise operation at the nominal 45 mph FAST operating speed. From the REPOS it may be seen, for example, that there are 0.057 percent of the 653.37 cycles per mile, or 37.24 cycles, that have a maximum peak between 3.3 and 6.6 ksi and a minimum peak between -19.8 and -16.5 ksi. For design calculations, the worst case (greatest possible range) assumption is made that the stress cycles in this cell of the matrix have a maximum peak of 6.6 ksi and a minimum peak of -19.8 ksi, or a stress range of 26.4 ksi.

5.2.3 Typical Fatigue Properties

AAR Specification M1001, Chapter VII (Fatigue Design of Freight Cars), does not currently contain a Modified Goodman Diagram (MGD) or fatigue property listing for a reinforced channel-to-plate geometry and loading that is directly applicable to the trailer hitch. However, a possible range of such fatigue properties might be established by considering several of the MGD's that are available for weld-fabricated details. The fatigue properties for all three of the fabricated beams with various attachments and steels included in M1001 (Section 7.4.2 and Diagrams 7.4.2.5.1, -.2, and -.3) can be included within the two S-N curves shown in Figure 24. The fatigue limits for the lower and upper curves are 8 ksi and 13 ksi, respectively. There is no mean stress effect for these structural details and the dependence of fatigue life on stress range (S-N slope) is the same.....k=0.32.

5.2.4 Cumulative Fatigue Damage Rule

The linear damage rule is recommended in AAR Specification M1001. In other words, the fractional fatigue life used at each level of stress range is simply totaled. When this total is unity, the initiation of visible fatigue cracks is expected. The resulting equation for the prediction of miles to

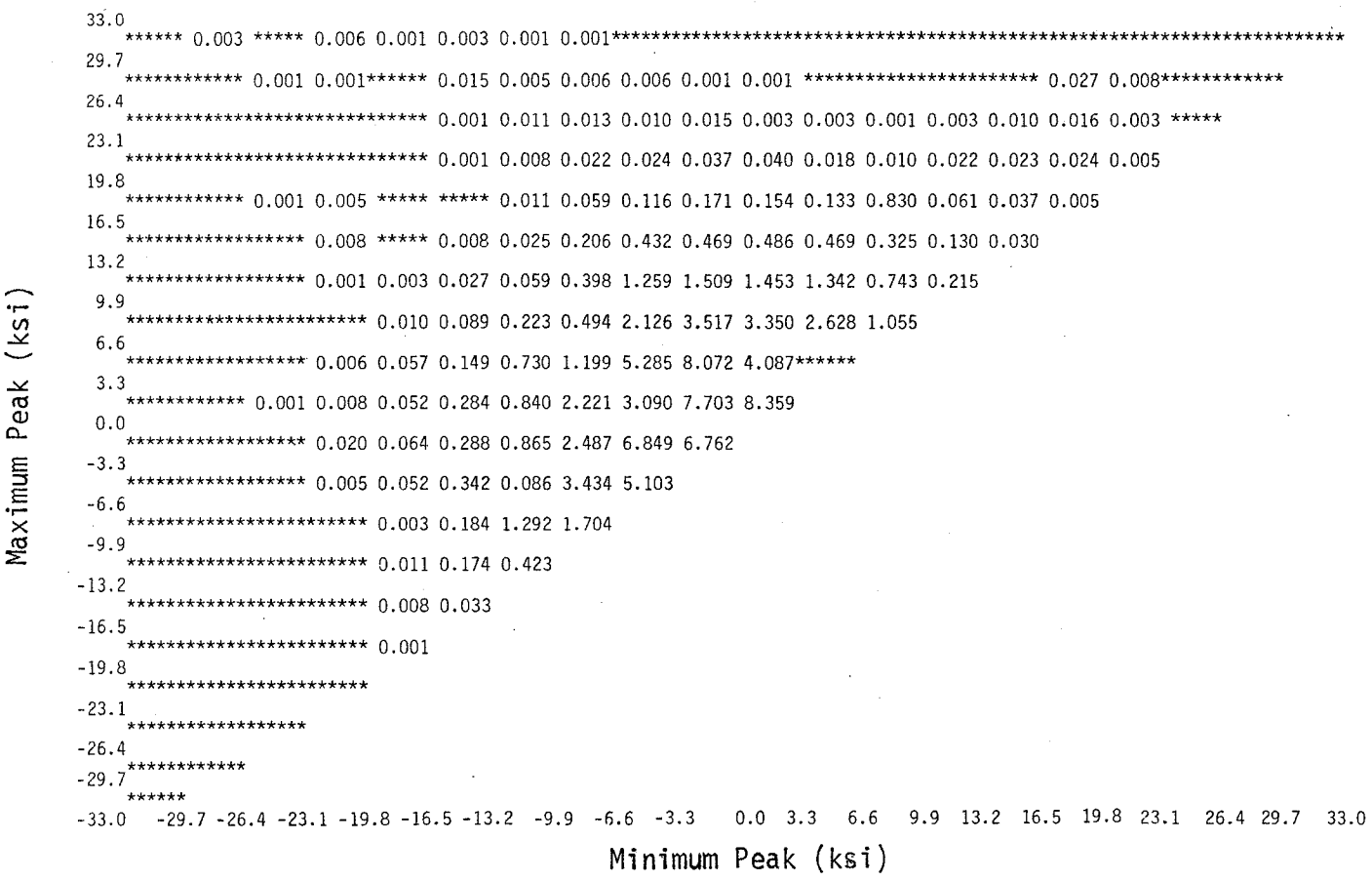

Channel	5	Distance in Miles	90.32	Threshold Level	10.00
Measurement	G5	Elapsed Hours		Total Cycles Counted	59013
Engineering Units	KSI	Average Speed in Mi/Hr		Cycles per Mile	653.37

Miles to Crack
Files Accumulated:
R14A00 R14B00 R14C00 R14D00 R17A00 R17B00 R17C00 R18A00 R18B00

FIGURE 22. FAT II PERCENT OCCURRENCE SPECTRUM, GAGE 5.

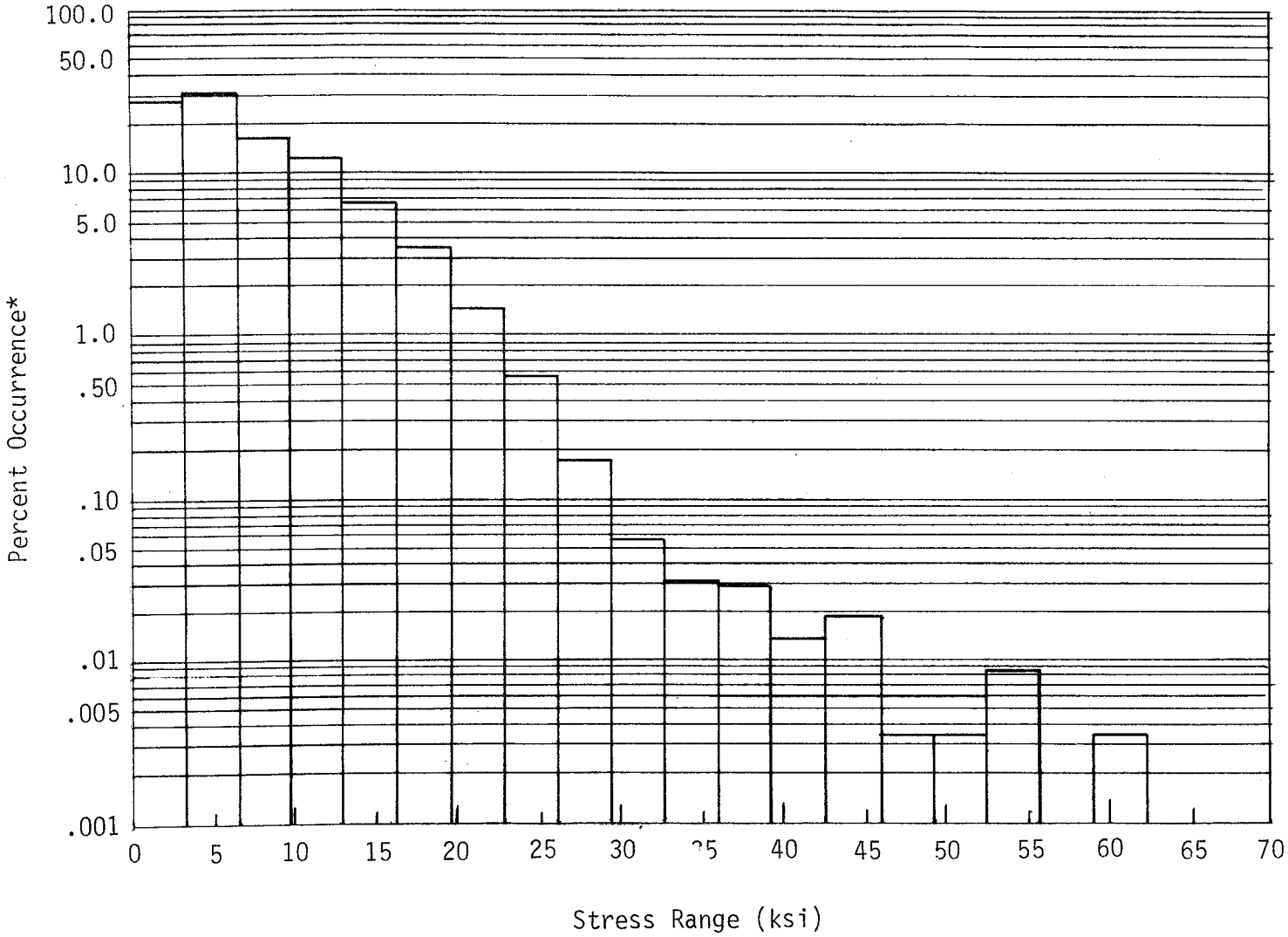

* For unmodified car--45 mi/h, both directions.

FIGURE 23. ASSOCIATED STRESS RANGE HISTOGRAM, GAGE 5.

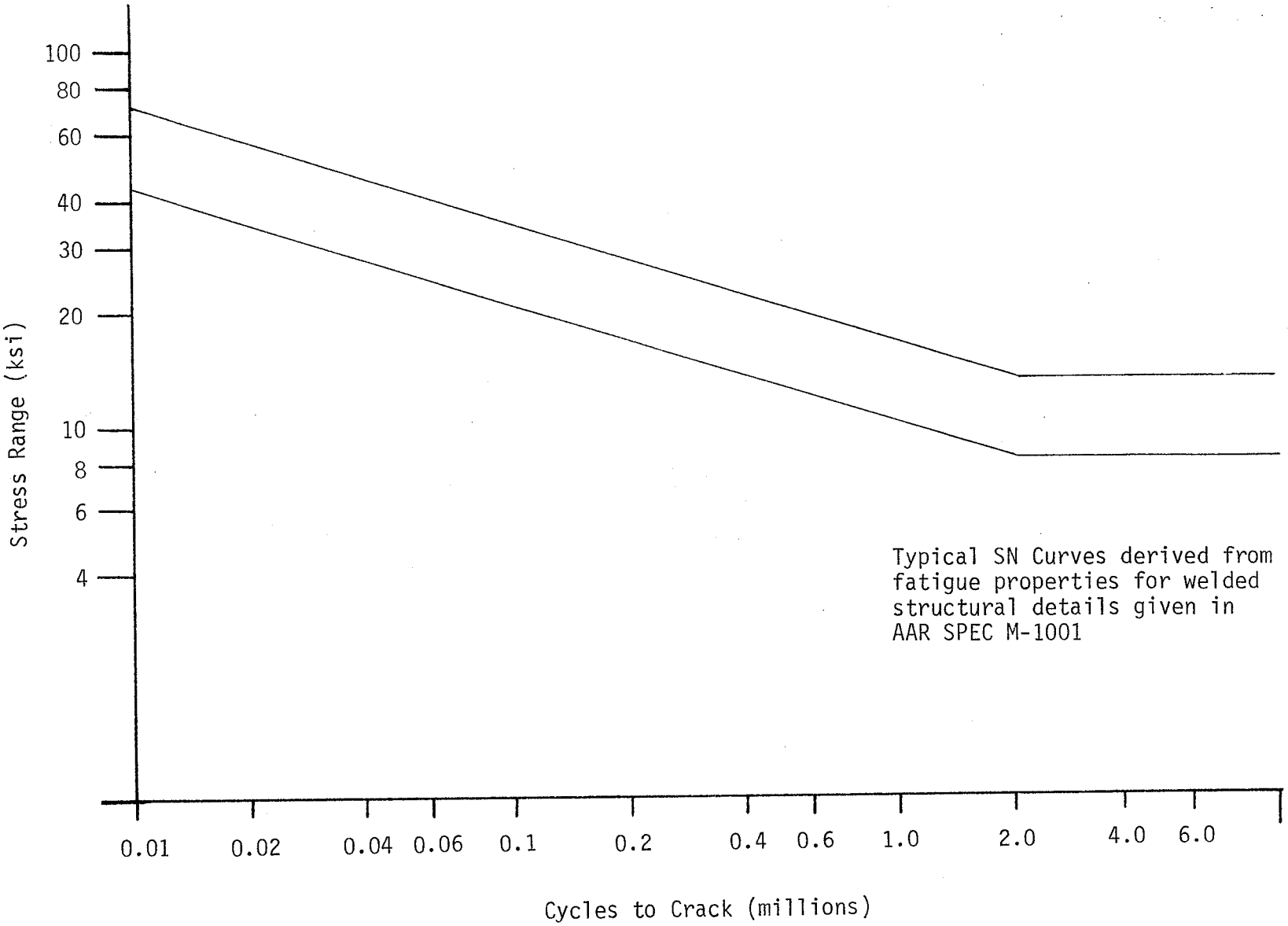

FIGURE 24. TYPICAL S-N CURVES.

cracking and the definition of terms is given below:

$$L = \frac{2{,}000{,}000 \times b^{1/k}}{\sum_{i=1}^{n} m(i) \times S(i)^{1/k}}$$

Where:

b = fatigue limit (strength range)
k = S-N slope (absolute value)
m(i) = number of cycles of stress range S(i) per mile (for all S greater than or equal to b)
n = maximum number of stress range groups or "boxes"

6.0 LIFE PREDICTION FOR CRITICAL REGION

Using the equation given in Section 5.2 and the stress range distribution illustrated in Figure 23, it is possible to predict the FAST laps (or FAST mileage) to first cracking as a function of assumed fatigue limit, b.

As anticipated from the preliminary quick-look strip chart observations and max/min computer surveys, Plate Gage #5 appears to be the best candidate for cycle counting and fatigue analysis. The observed maximum strain range for slightly over two laps with the original car is 1,909 με (57,270 psi) and 1,267 με (38,010 psi) for the modified car. In addition to these min-max surveys, a computer graphics terminal display program, FATSEE, was used extensively to observe the time variation of strain from Gage #5 and other gages in order to verify the ranges and relative cyclic character of the signals.

Therefore, the prediction of early cracking of the original car is reduced to an analysis of strain from Gage #5 for 45 mph in both directions (Run #14 and Run #17 - 18). The combined stress REPOS and stress range histograms for these runs are presented in Figures 22 and 23. For this stress history and the fatigue properties discussed above, the FLAP program predictions for miles to crack are 1,021 miles for an 8 ksi fatigue limit and 5,102 miles for a 13 ksi fatigue limit.

It is clear from this analysis that cracking in the hitch might have been expected early (around 5,000 miles, say) in the FAST operation. Even though cracking was not detected until 180,000 miles of FAST operation, this theoretical prediction is not considered to be unreasonable, bearing in mind that the fatigue methodology and properties are intended to be a conservative design basis for crack initiation. It should also be noted that the test car and hitch had already seen 88,000 miles of revenue service when put to test at Pueblo in late 1976.

First, the stress value used was derived from a measured strain that was in the proximity of a significant strain concentration, and therefore might be expected to be higher than a "remote" nominal stress that might be associated with a structural detail Modified Goodman Diagram or S-N curve. Secondly, the fatigue properties should themselves be conservatively low and would not be expected to be "best fit" values.

Bearing in mind the strong nonlinear dependence of fatigue life on stress or strength level, these conservative predictions are nevertheless encouraging. However, there is more to be learned from such fatigue analyses of the test data than this single prediction.

Some insight into the effect of FAST operation (direction and speed) as well as hitch deck support and material properties may be gained from a comparison of predictions for selected portions of the test runs. In addition, it is possible to explore alternate methods of fatigue estimation based on the data gathered from other transducers on the test car. These issues are explored in the following subsections.

The effect of operation, deck support and properties on life, based on Gage #5 data analysis, may be derived from a consideration of "master" Table 14. The fatigue predictions are made by the use of two programs: FATPOS and FLAP. The FATPOS program is based on the simple life algorithm listed above which depends only on range of stress. The FATPOS calculations were made simultaneously with the cycle counting. Therefore, its predictions are generally less conservative than the FLAP program, which is based on the worst case REPOS cell limits; i.e., stress increment limits. Both values are listed in the table.

An evaluation of the meaning of this master table is provided in the following subsections.

6.1 EFFECT OF DIRECTION OF TRAVEL

From a consideration of range of strain only (Table 13) it might be concluded that the CCW operation is more damaging. Yet, an examination of the master fatigue prediction table, with a view to comparing the results for different directions of travel, reveals that the clockwise direction may be slightly more damaging than the counterclockwise. In order to get a single numerical comparison, a test-mileage-weighted average life in miles is first obtained. Recall that each 25 mph run covered two laps and each 45 mph run covered ten laps. Then, for the given direction (either CCW or CW) multiply each FATPOS life prediction by the appropriate number of laps. Next, add the resulting quantities for all runs in the given direction (for both fatigue strength assumptions). Finally, divide this sum by the total accumulated laps. In this way, the weighted average life for CCW operation is calculated to be 6,602 miles, whereas the corresponding value for the clockwise direction is 5,523 miles.

This is not a strong directional effect. Recall that Gage #5 is on the right side of the car; i.e., inside of the FAST loop during CCW movement, and outside of the loop during CW movement.

6.2 EFFECT OF SPEED

Generally somewhat shorter lives are predicted for the higher, 45 mph speed. In order to obtain a numerical comparison, the same method of weighting discussed above will be used. In this case, the weighted life for all 45 mph runs is 5,174 miles while that for all 25 mph runs is 10,503 miles.

However, in the CW direction with the modified car, nearly equivalent lives are predicted for one 25 mph run as compared to 45 mph, which raises the possibility of a resonance, or critical speed excitation; that will be discussed later.

6.3 EFFECT OF DECK SUPPORT

The weighted average life for all test runs with the car in its original unmodified configuration is 5,819 miles. The corresponding mileage for the modified deck support is 6,305. On this basis there appears to be little effect of the deck support modification.

TABLE 14. EFFECTS OF OPERATION, DECK SUPPORT, AND PROPERTIES ON LIFE.

				Fatigue Life At 8,000 PSI		Miles to Crack At 13,000 PSI	
	Deck Support	Speed MPH	Direction	FATPOS	FLAP	FATPOS	FLAP
R13A00	Original	25	CCW	3929.87			
R13B00	Original	25	CCW	3511.14			
R13A,B	Original	25	CCW	3758.98	2289.49	24077.50	13338.70
R14A00	Original	45	CCW	1507.73			
R14B00	Original	45	CCW	1585.66			
R14C00	Original	45	CCW	1635.75			
R14D00	Original	45	CCW	1867.21			
R14A,B C,D	Original	45	CCW	1634.27	1328.64	8562.95	6517.55
R16A00	Original	25	CW	3153.53	1854.91	19812.61	11188.2
R17A00	Original	45	CW	1323.36			
R17B00	Original	45	CW	1095.51			
R17C00	Original	45	CW	1206.60			
R18A00	Original	45	CW	1266.26			
R18B00	Original	45	CW	1304.87			
R18A,B R17A,B,C,	Original	45	CW	1219.12	851.899	6356.08	4314.99
R20A00	Modified	25	CCW	6574.19			
R20B00	Modified	25	CCW	2942.44			
R20C00	Modified	25	CCW	1798.55			
R20,A,B,C	Modified	25	CCW	3050.41	2480.12	18394.7	13180.30
R21A00	Modified	45	CCW	1764.85			
R21B00	Modified	45	CCW	1757.67			
R21C00	Modified	45	CCW	1786.93			
R21D00	Modified	45	CCW	1622.62			
R21E00	Modified	45	CCW	2114.46			
R21A,B,C D,E				1801.35	1947.73	9833.87	9107.89
R23A00	Modified	25	CW	1695.61			
R23B00	Modified	25	CW	1912.19			
R23A,B	Modified	25	CW	1753.49	1385.19	10019.11	6610.2
R24A,B,C	Modified	45	CW	1866.16	1689.02	10120.42	7955.8

6.4 EFFECT OF MATERIAL PROPERTIES

The effect of fatigue properties is also reflected in the two weighted average lives for 8 and 13 ksi fatigue limits. These values are 1,847 and 10,278 miles, respectively.

A more complete picture of the effect of material property is presented in Figure 25, which plots the predicted fatigue life for one run (#14, CCW unmodified at 45 mph) as a function of fatigue strength from 8 to 20 ksi. The nonlinear dependence of life on stress is reflected by the reciprocal of the assumed S-N slope. In this case, fatigue life is inversely dependent on the cube of the stress ranges above the fatigue limit.

Table 15 presents a comparison of these variables; i.e., operation, support, and properties, as they relate to the test-mileage-weighted life (5,622 miles) over all conditions presented in master Table 14.

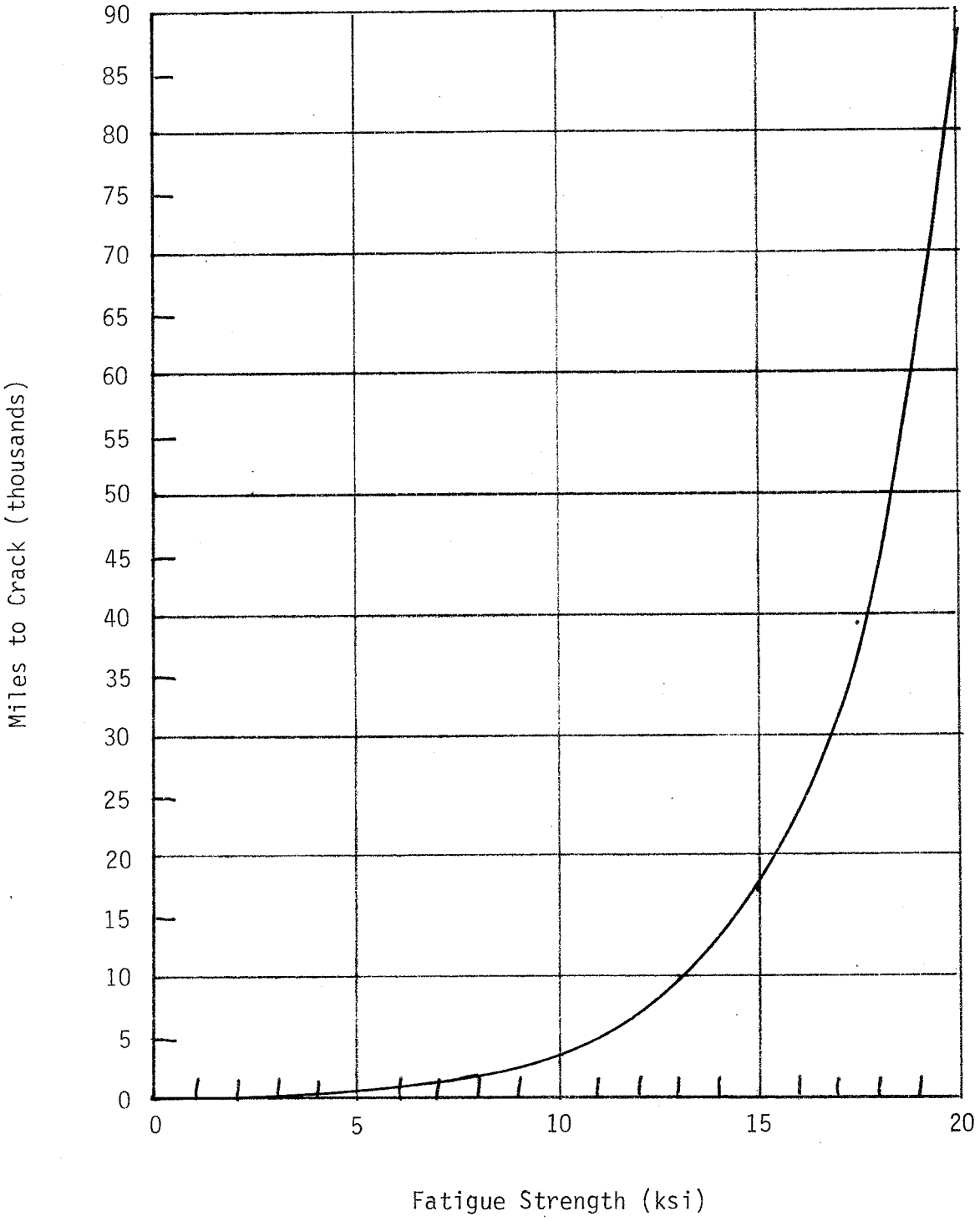

FIGURE 25. PREDICTED FATIGUE LIFE AS A FUNCTION OF FATIGUE STRENGTH.

TABLE 15. RELATIVE LIFE PREDICTIONS IN MILES.

(Test Mileage Weighted Life Over All Cases - 5,622 Miles)

Direction of Operation		
	CCW	1.17
	CW	0.98
Speed		
	45 mi/h	0.92
	25 mi/h	1.87
Deck Support		
	Original	1.04
	Modified	1.12
Fatigue Strength		
	8 ksi	0.33
	13 ksi	1.83

7.0 ADDITIONAL FATIGUE ANALYSIS

In the following subsections the results of additional fatigue initiation analyses, based on other strain gages as well as selected accelerometers, are presented. Some comments on crack propagation analysis are also included.

7.1 LIFE PREDICTIONS AT OTHER GAGE LOCATIONS

Even though plate strain Gage #5 appears to have been placed in the most critical fatigue location, it is of interest to make fatigue predictions at other selected locations, particularly those where cracks were also observed. Accordingly, cycle counting and fatigue predictions were made for the following locations.

1. Gage #7 on the hitch back plate at the bottom left corner (on the diagonally opposite corner and side from Gage #5).

2. Gage #1, a transverse or lateral gage on the hitch head weld on the right side of the hitch.

3. Gage #18, a right lateral gage on the bottom of the car deck near the reinforcement channel.

The predictions were made for data taken from about 2.2 laps of operation of the unmodified car at 45 mph in the CCW direction (Run #14A). As may be verified from master Table 14, the fatigue predictions are not very dependent on number of laps or portion of a test as long as more than one lap is involved. That is, the critical strain ranges for a given configuration and operation are repeatable on FAST, lap after lap.

An intermediate value of fatigue strength (10 ksi) was assumed. These predictions, including that for the Gage #5 location, are given in Table 16.

As expected, the location of Gage #5 is the most critical by a life factor of 3 over the other plate gage locations, and by a factor of 16 over the head gage location. No damage is predicted near the deck/reinforcement gage of the modified car.

7.2 LIFE PREDICTIONS BASED ON MEASURED ACCELERATION AND LOAD

It is theoretically possible to make alternate predictions of fatigue at the critical location based on accelerometer data and special strain gaged circuits calibrated for hitch load. This was done using data from the following:

1. Lateral hitch load-strain gage bridge circuit (Channel #20).
2. Lateral acceleration near the trailer center of gravity (Channel #24).
3. Lateral acceleration of the car body at the hitch (Channel #30).
4. Vertical acceleration at the car center plate (Channel #29).

TABLE 16. LIFE PREDICTIONS FOR SEVERAL GAGE LOCATIONS.
(Based on 10 ksi Fatigue Strength)

Gage Location	Miles	Relative to #5
Gage 5	3,457	1.00
Gage 7	10,640	3.08
Gage 1	57,856	16.74
Gage 18	∞	∞

With all of these transducer channels it is necessary to select a stress conversion factor to relate the signal to stress at the critical plate location. These factors were selected from a consideration of the pre/post test calibration data and from simple rigid body mechanics idealizations for the accelerometers. The details of this derivation of conversion factor estimates are included in Appendix 3. The corresponding predictions of life are listed in Table 17.

In all methods, except that based on car body vertical acceleration, cracking is predicted at lives (miles) not greatly different from that predicted from the directly measured strain. Not much significance should be placed on this "coincidence", however, except that cracking would be predicted in the hitch using data from transducers that are sensitive to lateral load variations on the hitch.

TABLE 17. LIFE PREDICTIONS BASED ON LOAD AND ACCELEROMETER TRANSDUCERS.
(Miles to crack at gage position #5 for 10 ksi fatigue strength)

Transducer	Miles	Relative Life
Strain gage at critical location	3,430	1.00
Hitch Lateral load (strain gage bridge, Channel #20)	760	0.22
Lateral accelerometer near trailer (g/Channel #24)	514	0.15
Lateral accelerometer at car body center plates (Channel #30)	3,674	1.07

7.3 CRACK PROPAGATION CONSIDERATIONS

In addition to the classical S-N fatigue design approach applied above for conservative predictions of crack initiation, principles derived from fracture mechanics technology have increasingly been applied to insure fatigue reliable designs or analysis of crack-growth rates. In his presentation of guidelines for fatigue-reliable design[8], Pellini describes this optional "cracked body design" approach. Generally, these "guidelines are intended primarily for analysis of crack-growth life that remains after a fatigue crack has developed to known size".

Since the conventional S-N analysis employed in the above sections of this report indicates that the stress ranges induced in the hitch by FAST operation could initiate fatigue cracks within a few thousand miles, it might be expected that subsequent crack propagation rates would be relatively high. Pellini advises designers that it is often not feasible to define stress intensity factors for actual cracks in complex regions such as at the toe of welds.

However, some appreciation of these rates and their dependence on stress level and initial crack size may be obtained from examination of a typical crack growth curve for a low-strength steel and simple crack geometry such as one taken from Pellini[8] and reproduced as Figure 26. Certainly, the high nominal stresses measured in this experiment on FAST--as well as the severe geometrical stress concentration factors at the hitch strut/reinforcing plate weld interface--justify the consideration of curves for relatively high (0.9 YS) yield stress.

Many cycles of high nominal stress per mile were observed in the fatigue critical region measured by Gage #5 (see Figure 23, Section 5.0). From this stress range histogram, it may be concluded that about 12%, or 78 stress cycles per mile, have a range greater than 13 ksi, which is a representative fatigue limit from modified Goodman diagrams. These fatigue damaging stress cycles are distributed up to a level as high as 60 ksi at a low frequency of occurrence ($\simeq$.05 cycles/mile). For purposes of simple illustration, let it be assumed that this distribution could be replaced by the application of only 10 cycles per mile of stress range sufficient to cause stresses that are 90% of yield in the critical region.

Further, let it be assumed that the largest non-detectable crack in routine FAST equipment is 0.4". Then, if Figure 26 were representative of the hitch material, geometry and crack type, a crack growth to 2.5" would be expected within 30,000 cycles, or 3,000 miles. As reported in Section 1, crack growth rates must have been even greater than this since, within a 3,000 mile period of FAST operation, cracks progressed from a non-detectable extent to lengths of 9 and 14 inches.

Without question, the actual hitch crack propagation situation is complex, given the various possible modes of propagation and the ways in which existing large cracks can affect the nominal driving stresses. Still, these simplified considerations are sufficient to illustrate what, in fact, was observed--namely, that many cycles per mile of high nominal stress range increase the likelihood that the predicted crack rates will also be very high.

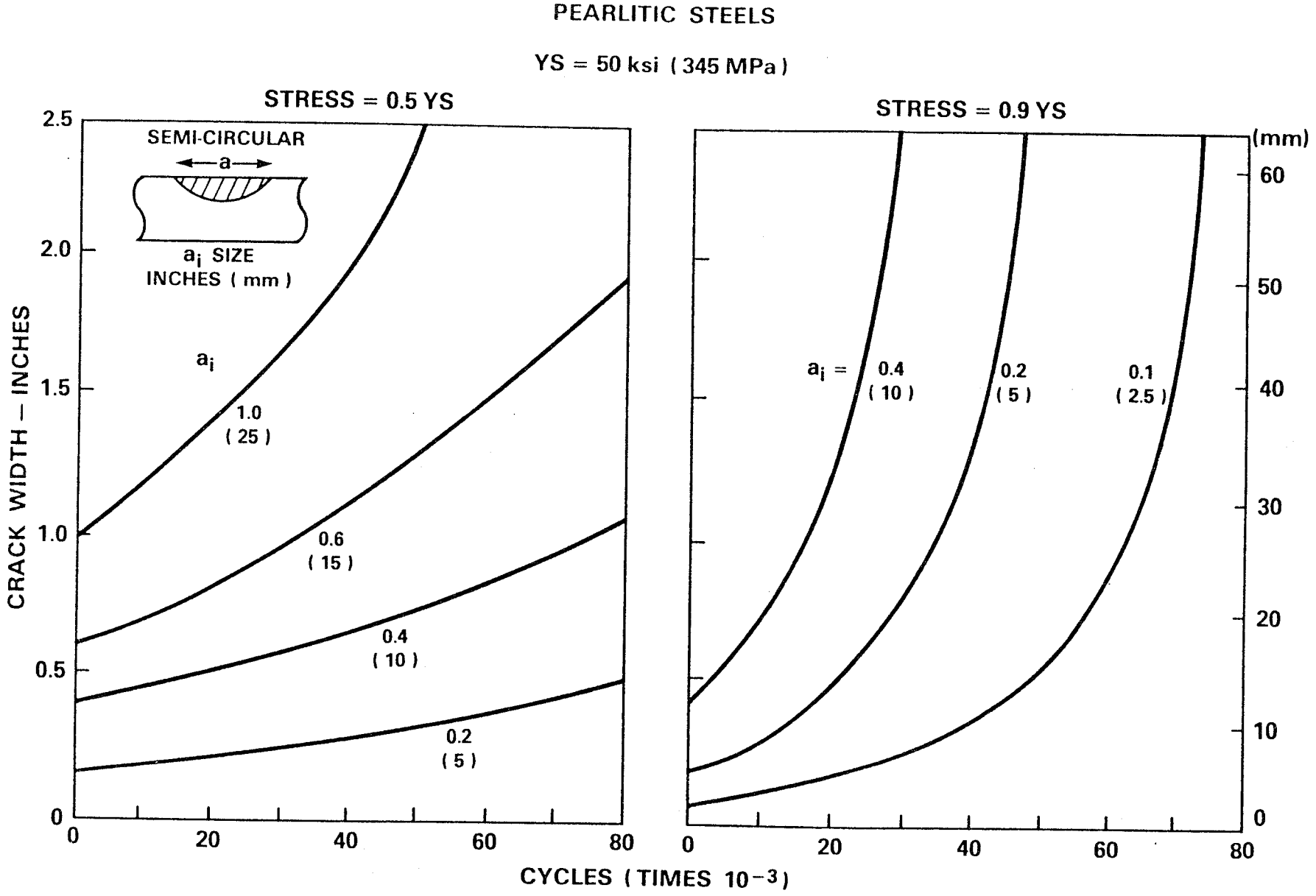

Reproduced from AAR Report No. R-490, Guidelines for Fatigue-Reliable Design of Steel Structures, page 137.

YS = Yield Stress

MPa = MegaPascals

FIGURE 26. DESIGN-REFERENCE GRAPHS FOR PRELIMINARY ANALYSIS OF CRACK-GROWTH RATES.

8.0 LOAD ENVIRONMENT COMPARISONS

8.1 GUIDELINE REPOS

At present there are no REPOS in the AAR manual for flat cars. However, in order to provide a comparison with other car types in the manual, the vertical and lateral acceleration REPOS's at the loaded car bolster are given in Figures 27a and 28a. An alternative representation of the same load environments, in terms of ranges of maximum to minimum load, is illustrated as a bar chart distribution or histogram in Figures 27b and 28b.

If the FAT II flat car body lateral acceleration REPOS is compared to the one available in the AAR manual for 100-ton covered hopper car, certain striking observations can be made. The range of lateral accelerations appears as large for the flat car on FAST as for the hopper car in representative general service. Furthermore, the number of cycles per mile is significantly greater for FAST operation.

These observations may well be expected, considering the high percentage of curve negotiation on FAST and the TOFC lateral dynamics, to be discussed in a later section.

8.2 TTX ROAD TESTS

The only revenue track data available for this type of flat car were provided by Trailer Train Company[9] from operations over "marginal" Class 5 tangent track at various speeds, including 40 and 50 mph. American Steel Foundries performed the road environment data reduction using a mean-level-crossing-peak computer program.[10] Data are available in these terms for the following locations:

1. Bottom car centersill at mid length
2. Vertical deck acceleration at the B end
3. Lateral deck acceleration at the B end
4. Vertical acceleration of trailer on the A end

In order to be able to make some comparison to these data, some of the FAST data for 45 mph were reduced (cycle counted) using a program based on the mean level crossing logic. In Table 18, comparison of the peak level crossing counts per mile are provided for the revenue tangent track, selected FAST tangent track (Sections 18 through 22), and the entire FAST loop for the four transducers in both directions of travel. Unfortunately, there was no lateral oriented accelerometer on the trailer in the revenue tangent track test for comparison to FAST. However, the lateral acceleration environment may be compared for the flat car body. In this case the FAST environment is much more severe, even for the tangent section only. For example, acceleration levels as high as 0.5 g are encountered on FAST while levels less than half of that magnitude are encountered in revenue tangent service. Furthermore, there are many more counts per mile above a significant level (0.1 g say) on FAST. On revenue tangent track there are only 20 counts per mile above 0.1 g while there are an average (CW and CCW) of 141 counts for FAST tangent operation and 277 counts for FAST total loop operation.

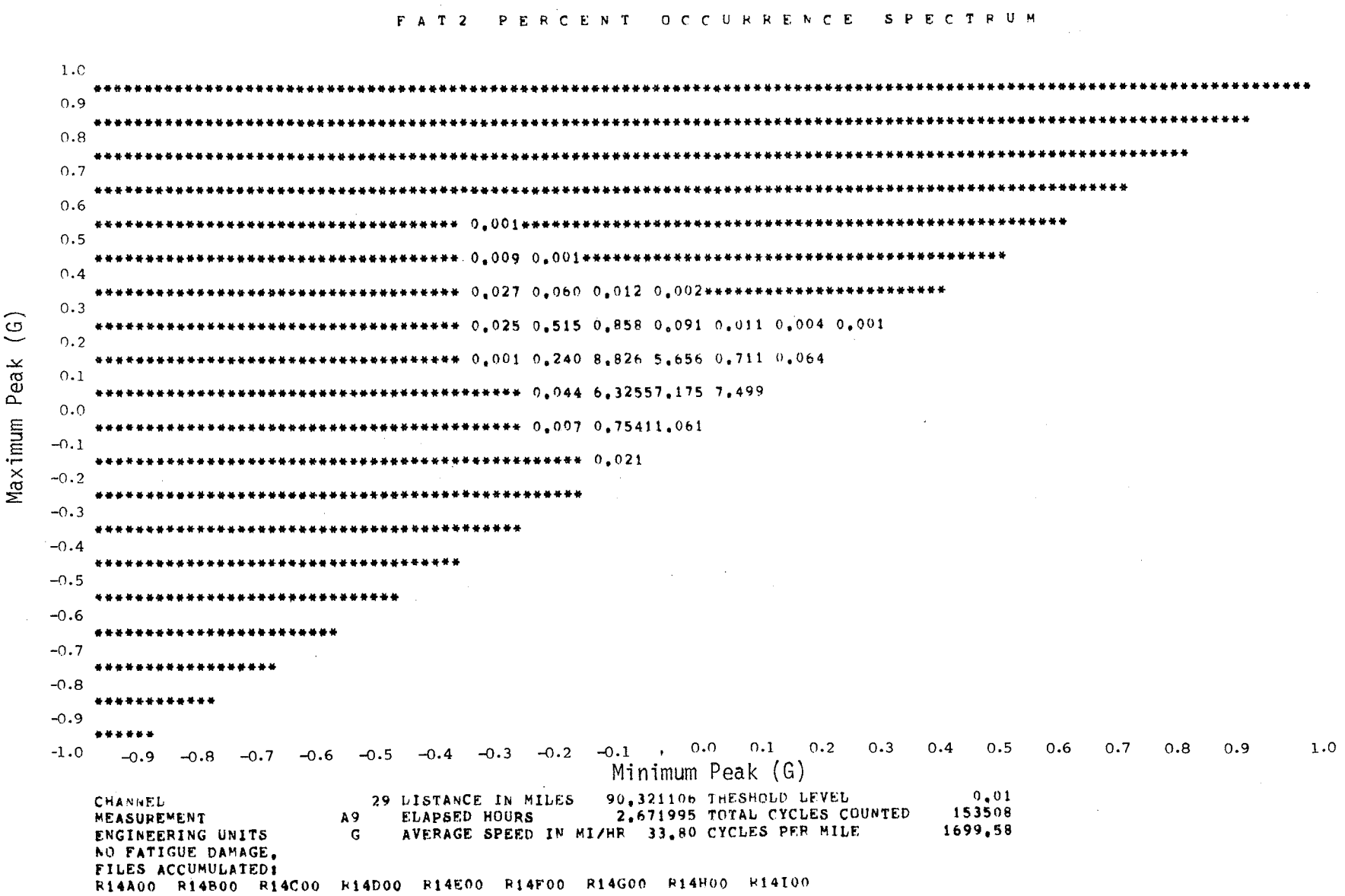

FIGURE 27a. VERTICAL ACCELERATION REPOS AT TOFC BOLSTER (NORMAL FAST OPERATIONS).

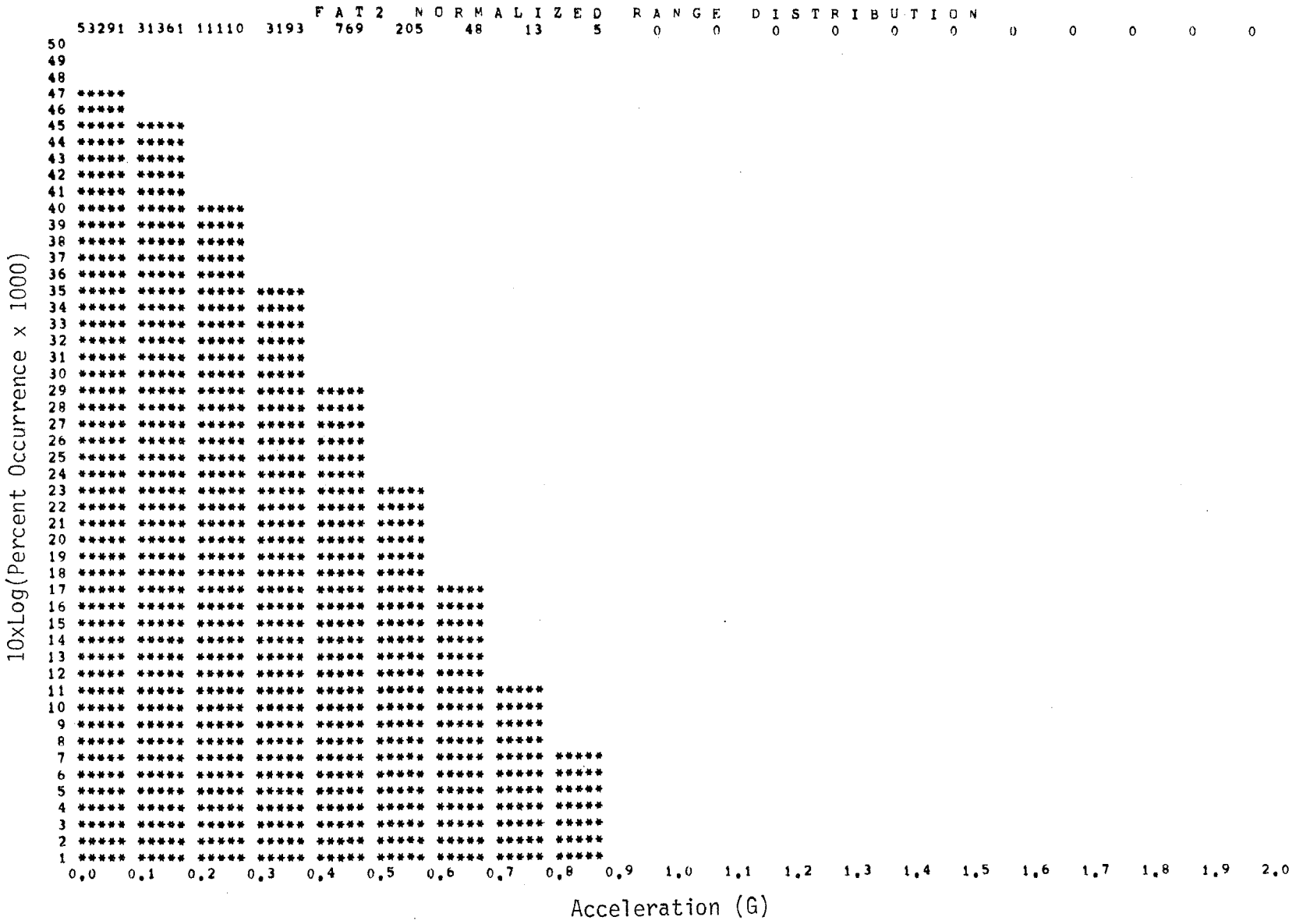

CHANNEL 29 DISTANCE IN MILES 90,321106 THESHOLD LEVEL 0,01
MEASUREMENT A9 ELAPSED HOURS 2,671995 TOTAL CYCLES COUNTED 153508
ENGINEERING UNITS G AVERAGE SPEED IN MI/HR 33,80 CYCLES PER MILE 1699,58
NO FATIGUE DAMAGE,
FILES ACCUMULATED:
R14A00 R14B00 R14C00 R14D00 R14E00 R14F00 R14G00 R14H00 R14I00

FIGURES 27b. VERTICAL ACCELERATION RANGE DISTRIBUTION AT TOFC BOLSTER (NORMAL FAST OPERATIONS).

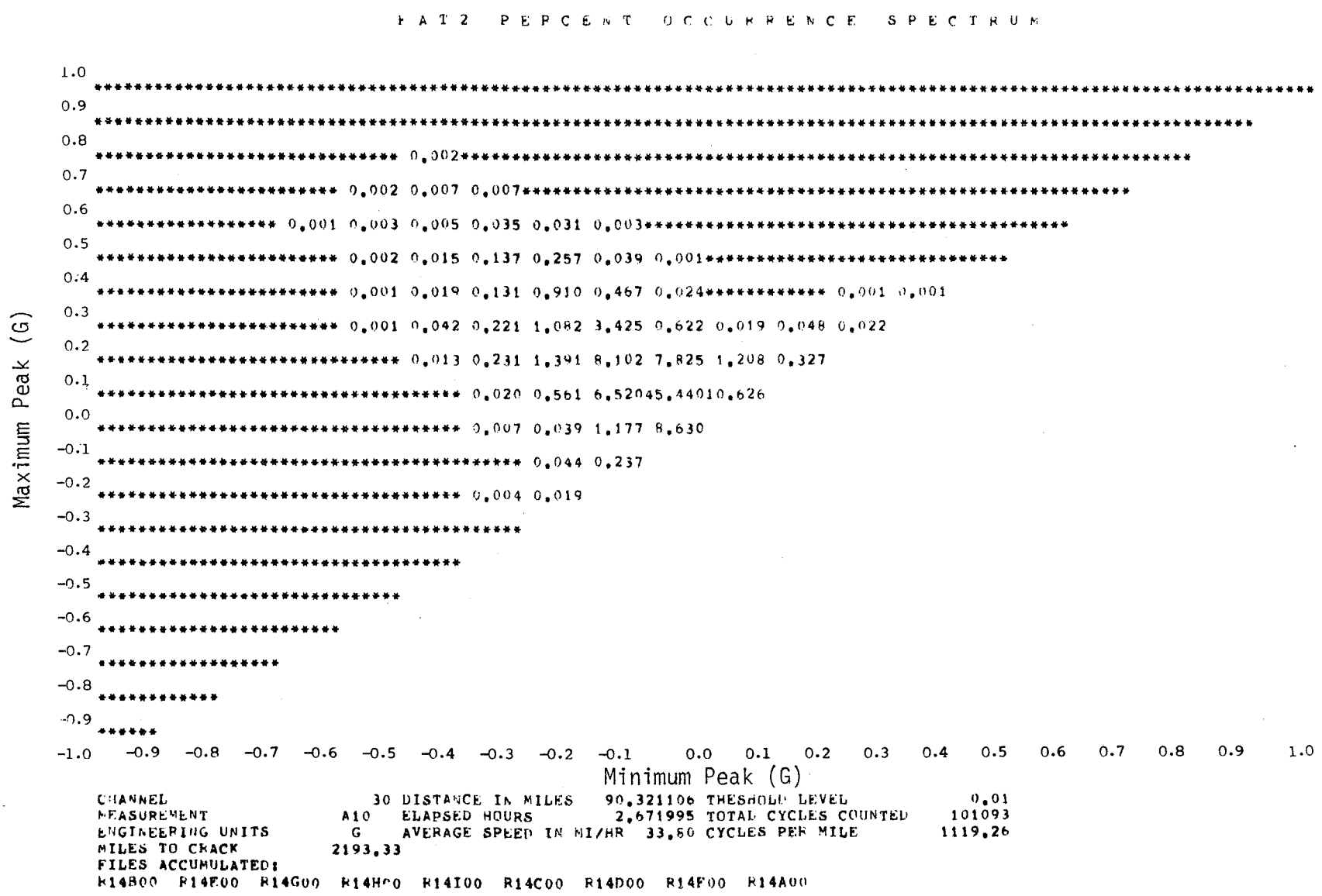

FIGURE 28a. LATERAL ACCELERATION REPOS AT TOFC BOLSTER (NORMAL FAST OPERATIONS).

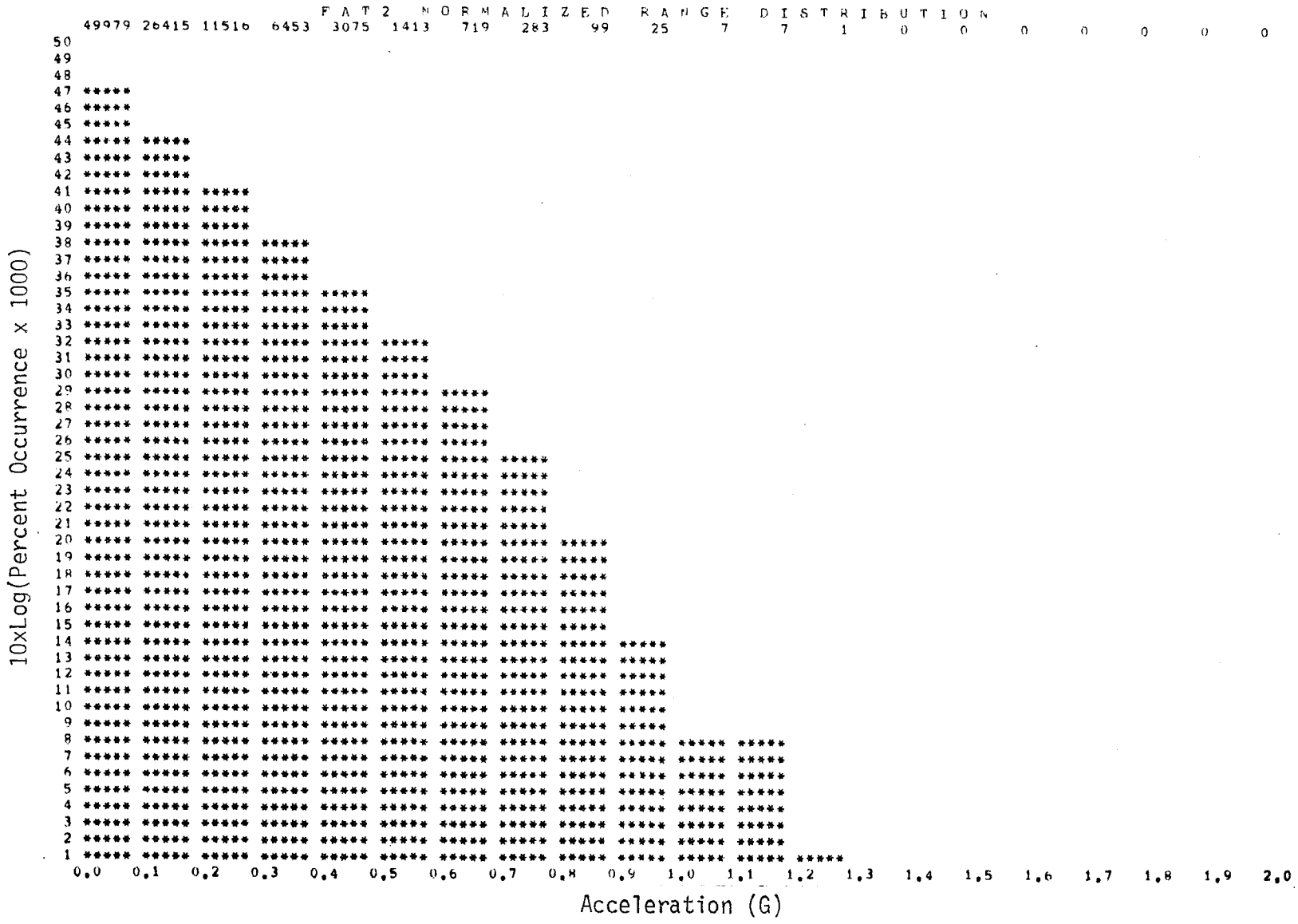

CHANNEL 30 DISTANCE IN MILES 90,321106 THESHOLD LEVEL 0,01
MEASUREMENT A10 ELAPSED HOURS 2,671995 TOTAL CYCLES COUNTED 101093
ENGINEERING UNITS G AVERAGE SPEED IN MI/HR 33,80 CYCLES PER MILE 1119,26
MILES TO CHACK 2193,33
FILES ACCUMULATED:
R14B00 R14E00 R14G00 R14H00 R14I00 R14C00 R14D00 R14F00 R14A00

FIGURE 28b. LATERAL ACCELERATION RANGE DISTRIBUTION AT TOFC BOLSTER (NORMAL FAST OPERATIONS).

TABLE 18. SUMMARY OF LEVEL CROSSING COUNTS.

Strain Level Crossing							Acceleration Level Crossing				Counts/Mile		
Center Sill Longitudinal Strain Mid Car							Car Center Plate Lateral Acceleration						
Strain Level	CCW 45 MPH			CW 45 MPH			Acce. Level	CCW 45 MPH			CW 45 MPH		
X 100	Rev. Tang.	FAST Tang.	FAST Laps	Rev. Tang.	FAST Tang.	FAST Laps	X 0.1	Rev. Tang.	FAST Tang.	FAST Laps	Rev. Tang.	FAST Tang.	FAST Laps
10.0/11.0	0	0	0	0	0	0	5.0/5.5	0	0	0	0	0	001
9.0/10.0	0	0	0	0	0	0	4.5/5.0	0	0	1	0	0	3
8.0/9.0	0	0	0	0	0	0	4.0/4.5	0	0	2	0	0	4
7.0/8.0	0	0	0	0	0	0	3.5/4.0	0	0	4	0	0	8
6.0/7.0	0	0	0	0	0	0	3.0/3.5	0	0	6	0	0	16
5.0/6.0	0	0	0	0	0	0	2.5/3.0	0	0	7	0	3	35
4.0/5.0	0	0	0	0	0	0	2.0/2.5	0	3	10	0	9	66
3.0/4.0	0	0	0	0	0	0	1.5/2.0	2	23	34	2	26	99
2.0/3.0	0	0	0	0	0	0	1.0/1.5	18	95	110	18	123	148
1.0/2.0	2	0	0	2	0	0	0.5/1.0	133	263	294	133	412	241
0.0/1.0	62	224	248	62	239	220	0.0/0.5	275	525	463	275	394	201
0.0/-1.0	1	225	251	1	239	221	0.0/-0.5	112	415	368	112	649	342
-1.0/-2.0	0	0	0	0	0	0	-0.5/-1.0	13	341	305	13	236	212
-2.0/-3.0	0	0	0	0	0	0	-1.0/-1.5	2	113	138	2	56	133
-3.0/-4.0	0	0	0	0	0	0	-1.5/-2.0	0	38	69	0	13	75
-4.0/-5.0	0	0	0	0	0	0	-2.0/-2.5	1	7	29	1	2	33
-5.0/-6.0	0	0	0	0	0	0	-2.5/-3.0	0	2	17	0	1	16
-6.0/-7.0	0	0	0	0	0	0	-3.0/-3.5	0	0	7	0	0	6
-7.0/-8.0	0	0	0	0	0	0	-3.5/-4.0	0	0	3	0	0	2
-8.0/-9.0	0	0	0	0	0	0	-4.0/-4.5	0	0	1	0	0	1
R M S													
Excursion	104.5	100	100	104.1	100	100		0.073	0.095	0.117	0.073	0.09	0.148
Posi. Mean	103.1	100	100	103.1	100	100		0.074	0.079	0.091	0.074	0.09	0.140
Nega. Mean	100.0	100	100	100.0	100	100		0.063	0.089	0.106	0.063	0.07	0.109
Po+Ne Mean	203.1	200	200	203.1	100	200		0.137	0.168	0.198	0.137	0.16	0.250
Base Level	0	0	0	0	0	0		0	0	0	0	0	0

TABLE 18 (CONTINUED). SUMMARY OF LEVEL CROSSING COUNTS.

	CCW 45 MPH									CW 45 MPH								
	TRAILER VERT.			TRAILER LATR.			CEN.PLATE VERT.			TRAILER VERT.			TRAILER LATR.			CEN.PLATE VERT.		
Acceleration Level	Rev. Tang	FAST Tang	FAST Laps	Rev. Tang	FAST Tang	FAST Laps	Rev. Tang	FAST Tang	FAST Laps	Rev. Tang	FAST Tang	FAST Laps	Rev. Tang	FAST Tang	FAST Laps	Rev. Tang	FAST Tang	FAST Laps
0.9/1.0	0	0	0	0	0	0	0	0	0	0	0	0	0	0	0	0	0	0
0.8/0.9	0	0	0		0	0	0	0	0	0	0	0		0	0	0	0	0
0.7/0.8	0	0	0		0	0	0	0	0	0	0	0		0	0	0	0	0
0.6/0.7	1	0	0		0	0	0	0	0	1	0	0		0	0	0	0	0
0.5/0.6	2	0	0		0	0	0	0	0	2	0	0		0	0	0	0	0
0.4/0.5	3	0	0		0	0	0	0	0	3	0	0		0	0	0	1	0
0.3/0.4	11	0	0		0	2	3	2	2	11	0	0		0	5	3	1	2
0.2/0.3	42	0	0		1	16	16	23	25	42	1	0		4	60	16	19	25
0.1/0.2	80	43	32		47	73	78	223	242	80	28	36		70	197	78	206	258
0.0/0.1	131	381	441		530	490	338	973	1120	131	474	428		482	297	338	1224	1054
0.0/-0.1	147	372	432		528	460	351	940	1106	1471	470	420		525	413	351	1220	1060
-0.1/-0.2	78	54	42		47	111	55	274	277	78	41	49		21	125	55	227	268
-0.2/-0.3	23	0	1		0	10	8	14	15	23	0	0		0	14	8	7	14
-0.3/-0.4	8	0	0		0	0	0	1	1	8	0	0		0	0	0	2	1
-0.4/-0.5	2	0	0		0	0	0	0	0	2	0	0		0	0	0	0	0
-0.5/-0.6	0	0	0		0	0	0	0	0	0	0	0		0	0	0	0	0
-0.6/-0.7	0	0	0		0	0	0	0	0	0	0	0		0	0	0	0	0
-0.7/-0.8	0	0	0		0	0	0	0	0	0	0	0		0	0	0	0	0
-0.8/-0.9	0	0	0		0	0	0	0	0	0	0	0		0	0	0	0	0
-9.0/-1.0	0	0	0		0	0	0	0	0	0	0	0		0	0	0	0	0
R M S Excursion	0.196	.116	.111		.112	.129	.132	.132	.130	.196	.110	.113		.113	.157	.132	.124	.125
Posi. Mean	0.183	.110	.106		.108	.119	.127	.122	.121	.183	.106	.107		.114	.159	.127	.117	.123
Nega. Mean	0.160	.112	.109		.106	.122	.117	.124	.122	.160	.108	.110		.103	.127	.117	.116	.122
Po+Ne Mean	0.343	.222	.215		.214	.241	.244	.247	.243	.343	.214	.217		.217	.286	.244	.232	.245
Base Level	0	0	0		0	0	0	0	0	0	0	0		0	0	0	0	0

It also appears that clockwise operation on FAST causes more lateral acceleration peaks above 0.1 g (380 vs. 174). This may be consistent with the finding, given earlier in this report, that clockwise operation is slightly more fatigue damaging.

The car center plate vertical acceleration environment appears to be similar at levels above 0.2 g for both FAST and revenue service. However, the trailer vertical acceleration environment appears to be somewhat more severe in revenue service. This may in fact actually reflect the different location of the accelerometer in these two cases. In the revenue test the accelerometer was on the front end of the trailer, while on FAST it was located at mid-length of the trailer.

8.3 FEEST BOX CAR TEST

A 70-ton box car, which is currently visiting railroads around the country, is equipped with an instrumented truck bolster and load measuring side bearings. It is the car being used to measure the environmental loads in the FEEST program. It measures total vertical bolster load (centerplate and side bearing) and individual side bearing loads. A recording system stores data in various "boxes", as a count, after rainflow counting.

The car made its way from Chicago to Kansas City and to Pueblo. Its short sojourn in Pueblo included 29 laps around the FAST loop with normal CW and CCW operation.

The side bearing load counts are shown in Figure 29. The FAST side bearing counts were multiplied by 4 so that a direct comparison can be made with a Kansas City to Pueblo (600 mile) run. Note the big difference in side bearing loads strikes. This is consistent with the expectation that the "curve environment" at FAST is clearly "accelerated" on a per mile basis. Those elements of the car which are loaded or stressed on curves clearly see an accelerated environment. The centerplate load counts, namely the pure bounce environment, is comparable.

8.4 FAST WAYSIDE LATERAL WHEEL LOAD ENVIRONMENT

Another possible perspective on the lateral load environment on FAST, particularly in the revenue curve section (07), is based on the results of the wayside data collection experiment on FAST[11]. As it turned out, instrumented track data (peak values of lateral and vertical loads in both rails) were recorded and summarized for various cars in the FAST consist. Although included in the summaries, TOFC #TTX 160546 (TTC I.D. #69), which had the cracked hitch, was not individually treated in the report. Nevertheless, some data for this car were included in the computer data base and were retrieved as part of this study. Thus, it is possible to make some observations about the magnitude of lateral rail forces for this car and compare them to the rest of the FAST consist.

For two of the seven instrumented wayside locations in FAST Section 07, the peak lateral wheel force on the high (inner) rail for all four axles was recorded in this data base for several passages of the train consist during

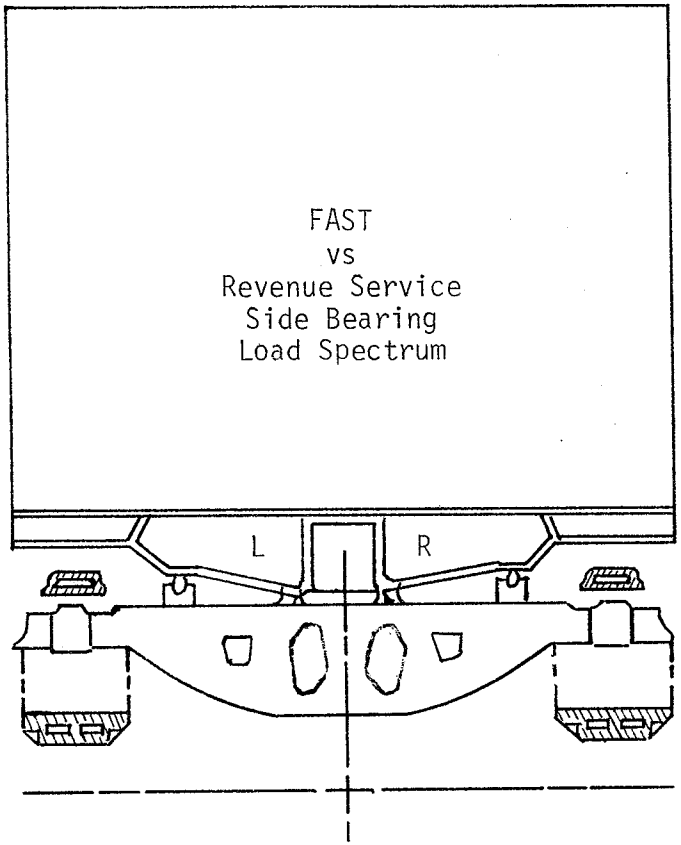

Peak Load Magnitude (kips)

	50	40	30	20	10	10	20	30	40	50
	Number of Side Bearing Strikes in 600 Miles									
KC - Pueblo	0	11	91	483	2029	788	209	43	8	0
FAST	4	9	112	1284	4207	5900	2702	767	39	4

Left ← → Right

FIGURE 29. SIDE BEARING STRIKES PER MILE FOR FEEST BOXCAR.

six series of test runs including TOFC Car #69. The statistical measures of Mean and Standard Deviation were then computed from these data for Car #69 alone and for all 100-ton cars as a group. A comparison of these measures is provided in Table 19. Although the number of data points is limited for Car #69, the average lateral wheel force on the high rail for this car appears to be about the same as the average for all the 100-ton cars.

The highest peak wheel force occurs during the lead axle encounter with the high, inner rail in this (reverse) curve in Section 07 (for all lead axles of 100-ton hopper Cars #5, 13 and 15 in Run #14 - 45 mph CCW, draft lub). The average lateral force on the high rail for all wayside measurement locations in FAST Section 07 is 10.72 kips. The only comparison for the Car #69 lead axle is in Run #15 (45 mph CCW, draft dry), where four observations of lead axle lateral force at two locations on the high rail are tabulated. These values are 11.6, 11.8, 12.0, and 13.0 kips. Since the effect of lubrication of rail was not significant in this situation (as demonstrated in Appendix D of the Battelle report[11]), these values may be compared with the average for all lead axles of the 3 hopper cars in test #14. It should be recognized that the results of measurements at all seven locations in Section 07 are averaged in Run #14 statistics.

Therefore, the evidence from the wayside data collection tests seems to indicate that the lateral wheel/rail force peaks are at least as high for the heavily loaded TOFC Car #69 as for the average 100-ton car in the FAST train consist.

TABLE 19. AVERAGE LATERAL WHEEL FORCE (KIPS) ON HIGH RAIL.

						LOCATION 07-0155		LOCATION 07-0159	
RUN #	MPH	DIR.	OPER.	LUB.	CAR	MEAN	STD. DEV.	MEAN	STD. DEV.
5	30	CW	DRAFT	Y	ALL	2.18	3.16	3.63	3.85
					#69*	1.68	1.97	3.25	3.13
6	34	CW	DRAFT	Y	ALL	2.70	3.62	4.45	4.04
					#69*	2.55	2.90	4.32	3.52
7	34	CW	BUFF	Y	ALL	2.54	3.58	4.39	4.02
					#69*	2.52	2.69	4.58	2.84
8	34	CW	DRAFT	Y	ALL	3.10	3.90	4.97	4.56
					#69	3.43	2.88	5.07	3.51
11	34	CCW	DRAFT	Y	ALL	----	----	5.42	4.06
					#69**	----	----	8.63	3.22
15	45	CCW	DRAFT	N	ALL	6.09	4.65	6.48	4.83
					#69**	6.38	4.79	6.43	3.94

* Based on only 12 observations at each location.
** Based on only 8 observations at each location.

9.0 DYNAMICS

A complete dynamic analysis of the TOFC response to FAST operations is beyond the scope of this report. However, it is appropriate to make some observations of the apparent character (modes and dominant frequencies) of this response for selected periods of operation, as well as to correlate the instantaneous transducer signal with speed and position on FAST.

9.1 GENERAL OBSERVATIONS FROM STRIP CHARTS

Figures 30 through 35 present the dynamic response for all transducers (accelerometers and strain gages) for brief (1.2 seconds) periods during the most significant excursions of the fatigue-critical gage (#5) for various speeds of operation (as detailed on the respective figures).

For 45 mph CCW operation, departing the reverse curve in FAST Section 07, a strongly periodic response is evident at about 7 Hz for Gage Channel #5 as well as the lateral accelerometers on the trailer (Channel #24) and car body (Channel #30). The trailer response is 180 degrees out of phase with the car body.

For one of the 25 mph runs (#23 CW) of the modified car, the predicted fatigue life was relatively low. Also, during the course of the dynamic testing, high speed movies were made of some of the test operations with the modified car at two locations on FAST. From the standpoint of visible lateral dynamics of the trailer relative to the flat car, it was evident from the films that the most critical operating mode was 25 mph, on tangent track in FAST Section 20. Therefore, the data from this run were computer surveyed for max-min response, and fatigue significant periods at curve and tangent track locations were selected for closer inspection.

In Figure 35, a strongly periodic response of the trailer at a frequency of about 4.3 Hz for the 25 mph operation over Section 07 is evident. This periodic response is also seen in strain channels such as #5 in Figure 34. Note, however, that this variation seems to be superimposed on a lower frequency, 1-Hz variation.

9.2 RESONANT FREQUENCIES FROM PSD ANALYSIS

In an attempt to identify those frequencies having the dominant energy content, a power spectral density (PSD) analysis was performed of selected channels (max strain and trailer lateral acceleration) for the most interesting periods (about 40 seconds each) of the 45 and 25 mph runs discussed above.

The results of this analysis are illustrated in the PSD-versus-frequency plots of Figures 36 through 39 and tabulated for nine test conditions in terms of primary and secondary PSD peak and frequency in Table 20. For the frequency region below 20 Hz (data acquisition filter limit) several relative PSD peaks are noted. These dominant peaks are 7.2 Hz for the 45 mph operation in the reverse curve Section 07, 4.2 Hz for the 25 mph operation in the curve

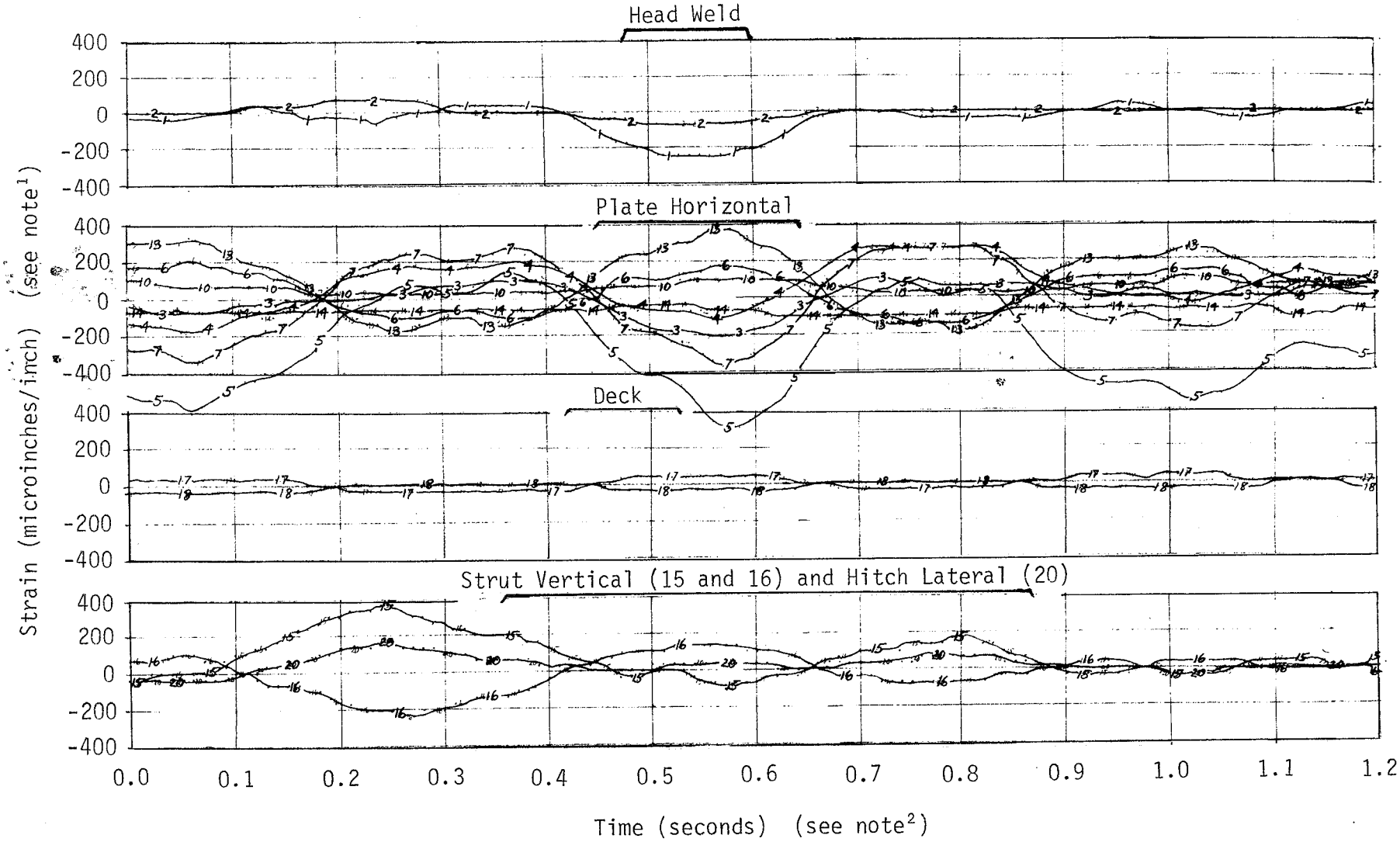

note[1] 200με = 0.588"

note[2] 0.1 second = 1.667"

Location Reference:

Near end of first lap, tie 1900.

FIGURE 30. HITCH STRAIN VARIATION, 41 MPH CCW, RUN #14, SECTION 03.

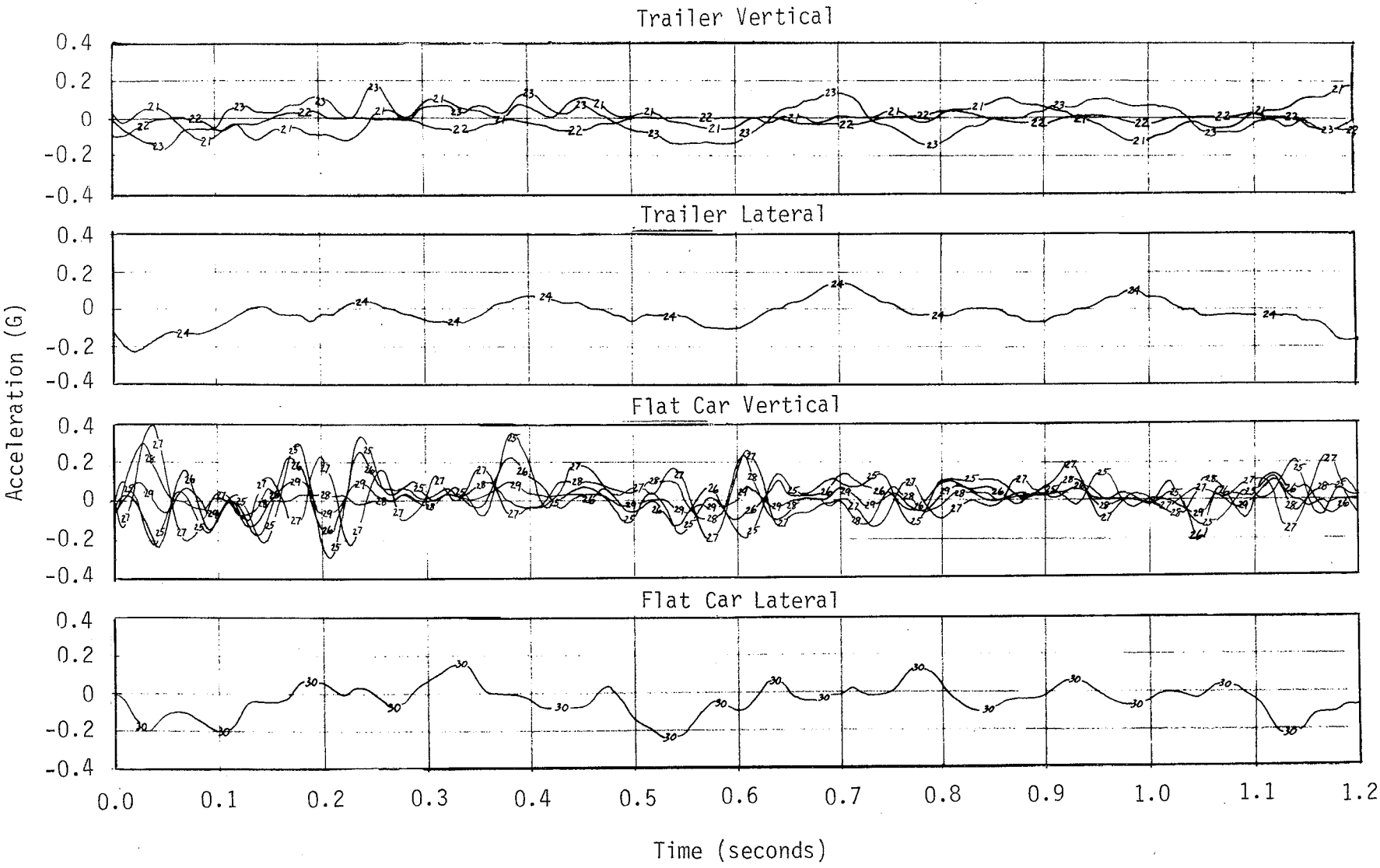

FIGURE 31. TRAILER AND FLATCAR ACCELERATIONS, 40 MPH CCW, RUN #14, SECTION 03.

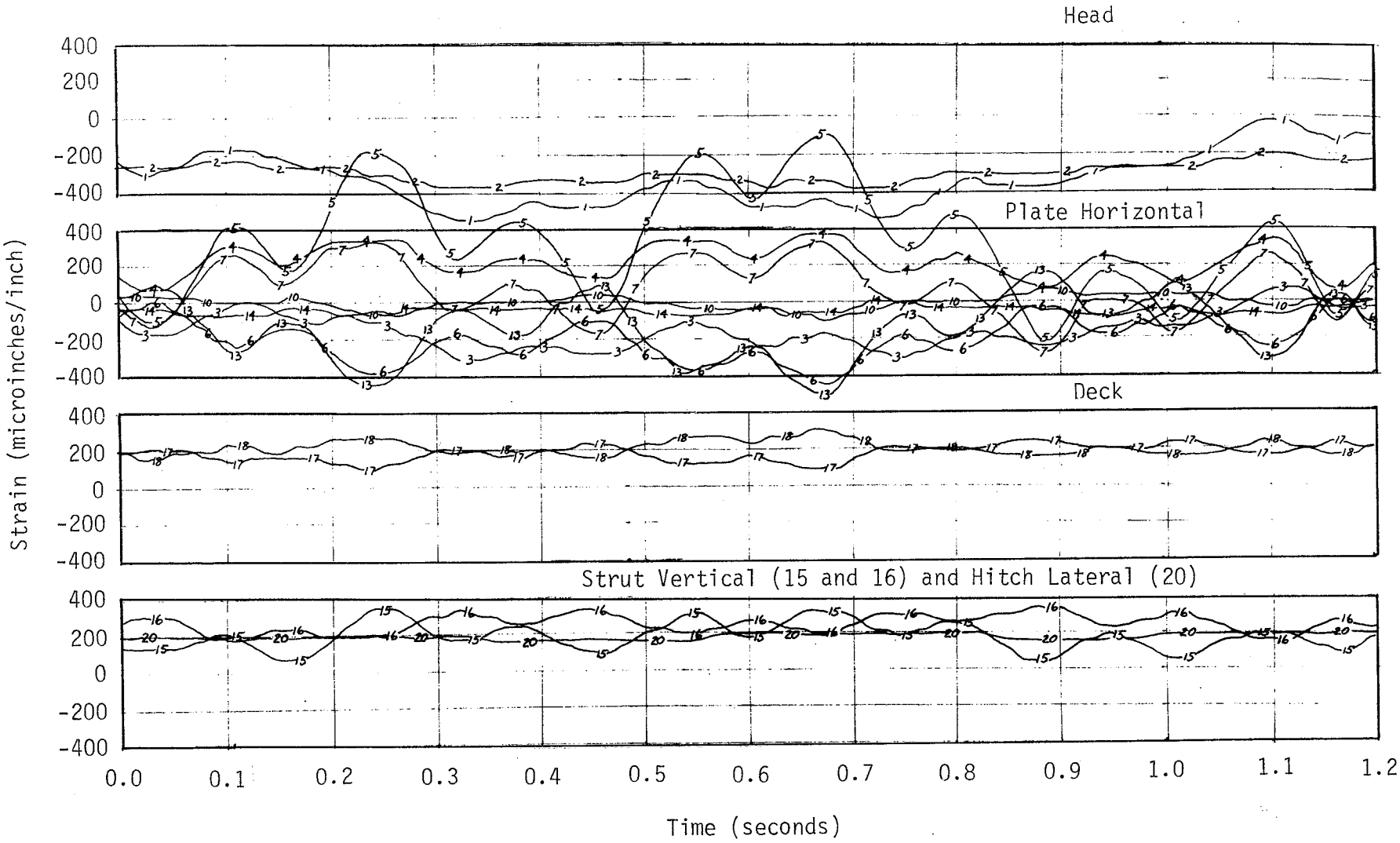

Location Reference:

Near end of first lap, tie 0668

FIGURE 32. HITCH STRAIN VARIATION, 42 MPH CCW, RUN #14, SECTION 07.

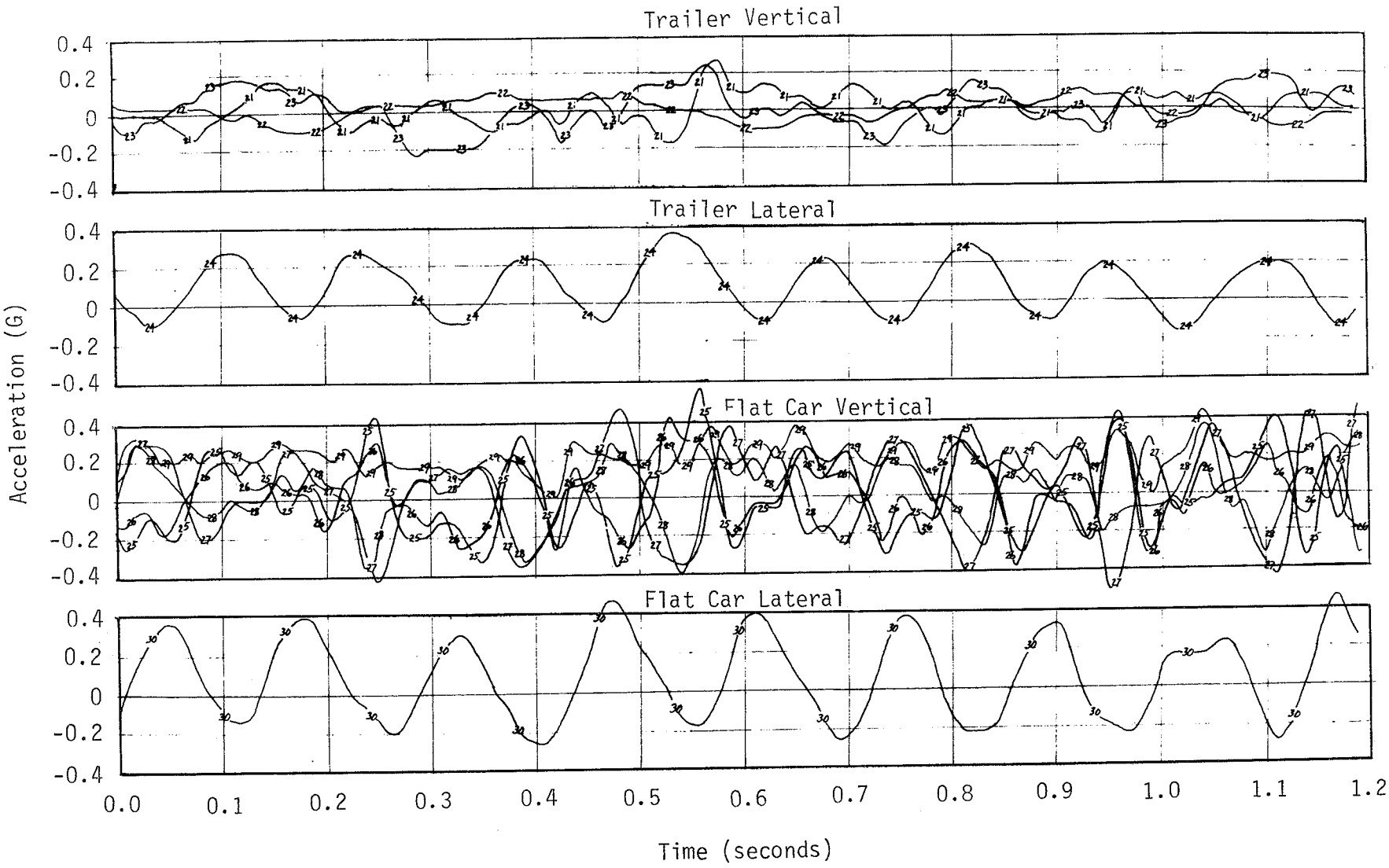

FIGURE 33. TRAILER AND FLATCAR ACCELERATIONS, 42 MPH CCW, RUN #14, SECTION 07.

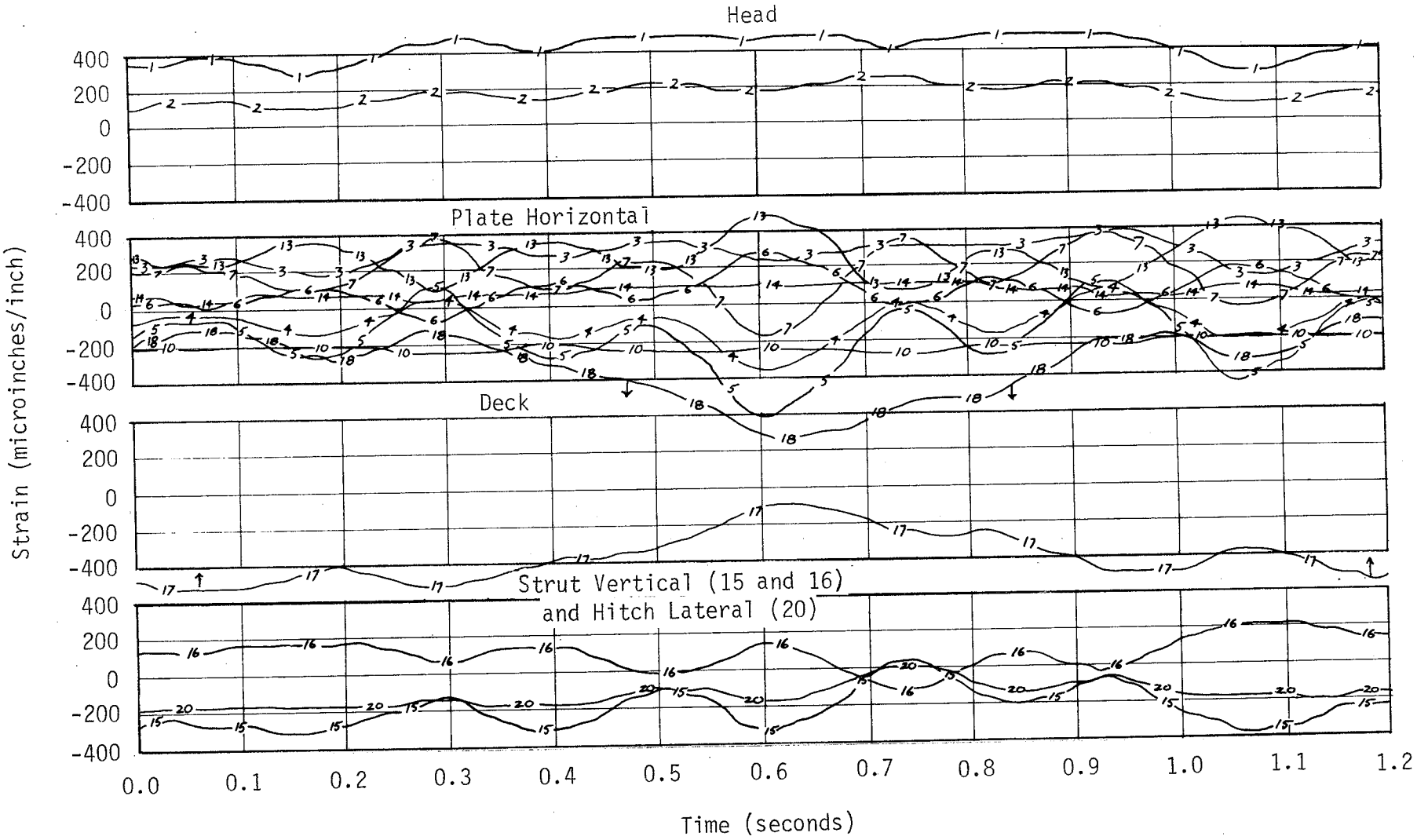

Location Reference:

Near end of first lap, Tie 0546

FIGURE 34. HITCH STRAIN VARIATION, 26.6 MPH CW, RUN #23, SECTION 07.

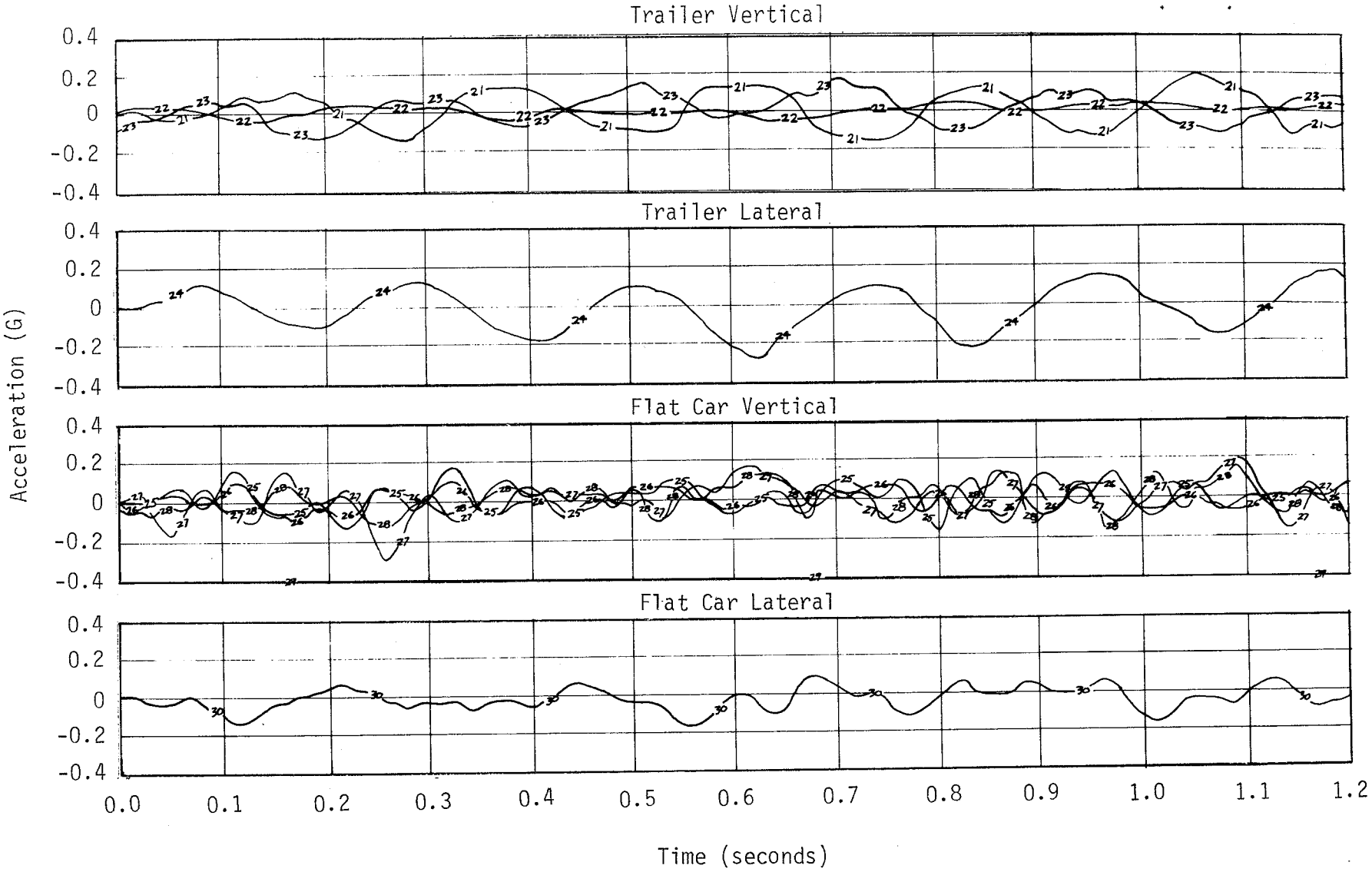

FIGURE 35. TRAILER AND FLATCAR ACCELERATIONS, 26.6 MPH CW, RUN #23, SECTION 07.

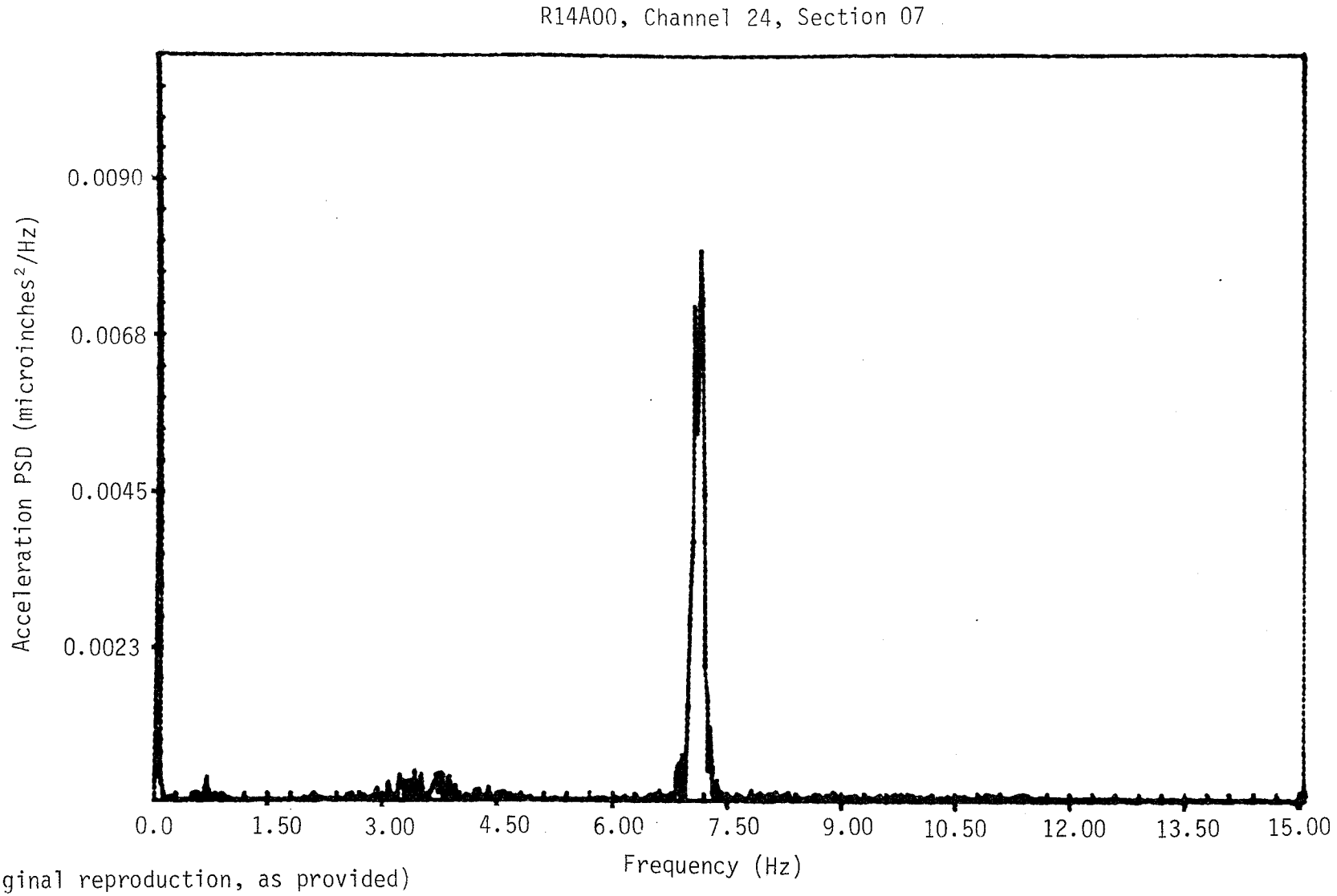

(Original reproduction, as provided)

FIGURE 36. POWER SPECTRAL DENSITY OF TRAILER LATERAL ACCELERATION, 45 MPH CCW, SECTION 07.

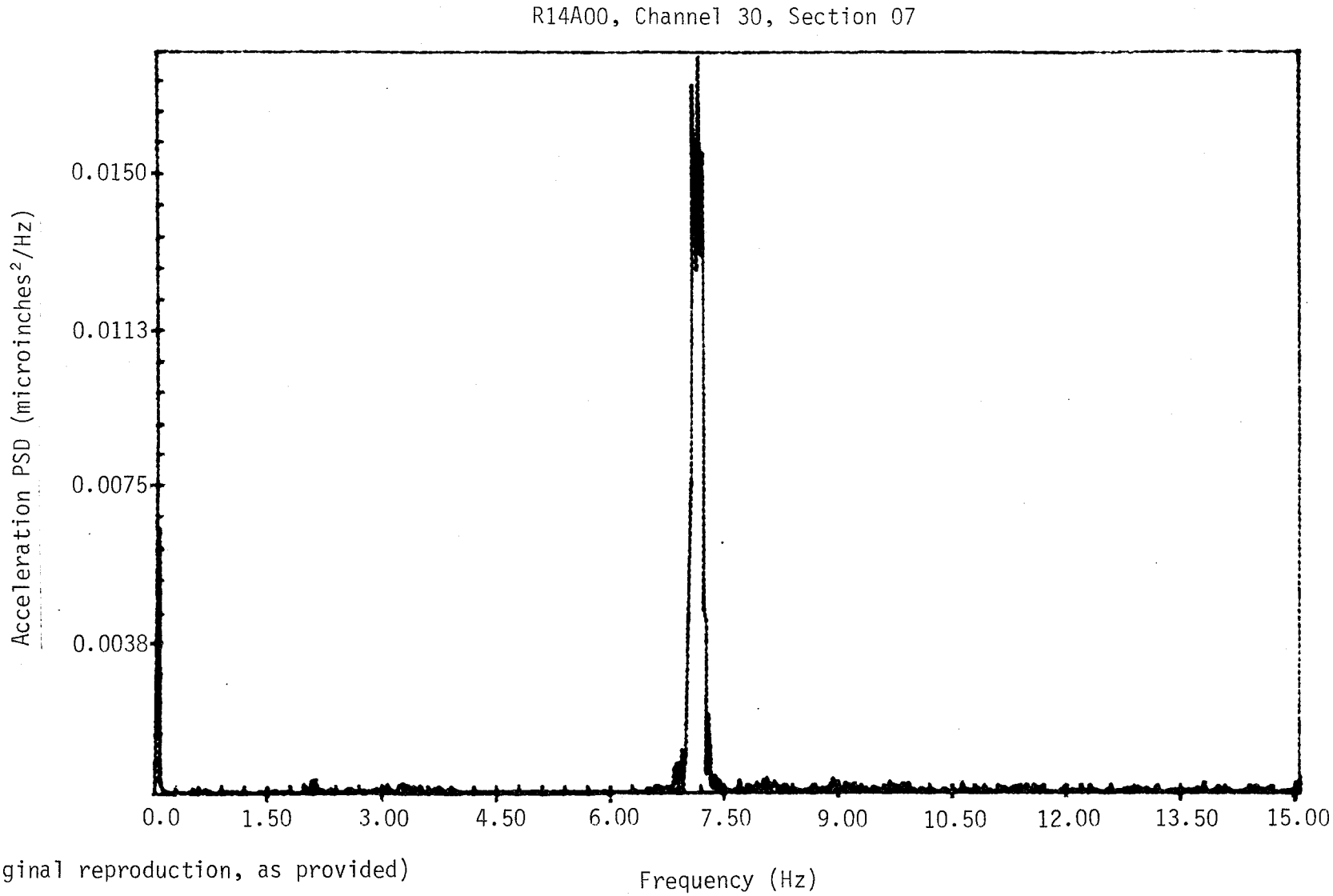

(Original reproduction, as provided)

FIGURE 37. POWER SPECTRAL DENSITY OF CARBODY LATERAL ACCELERATION, 45 MPH CCW, SECTION 07.

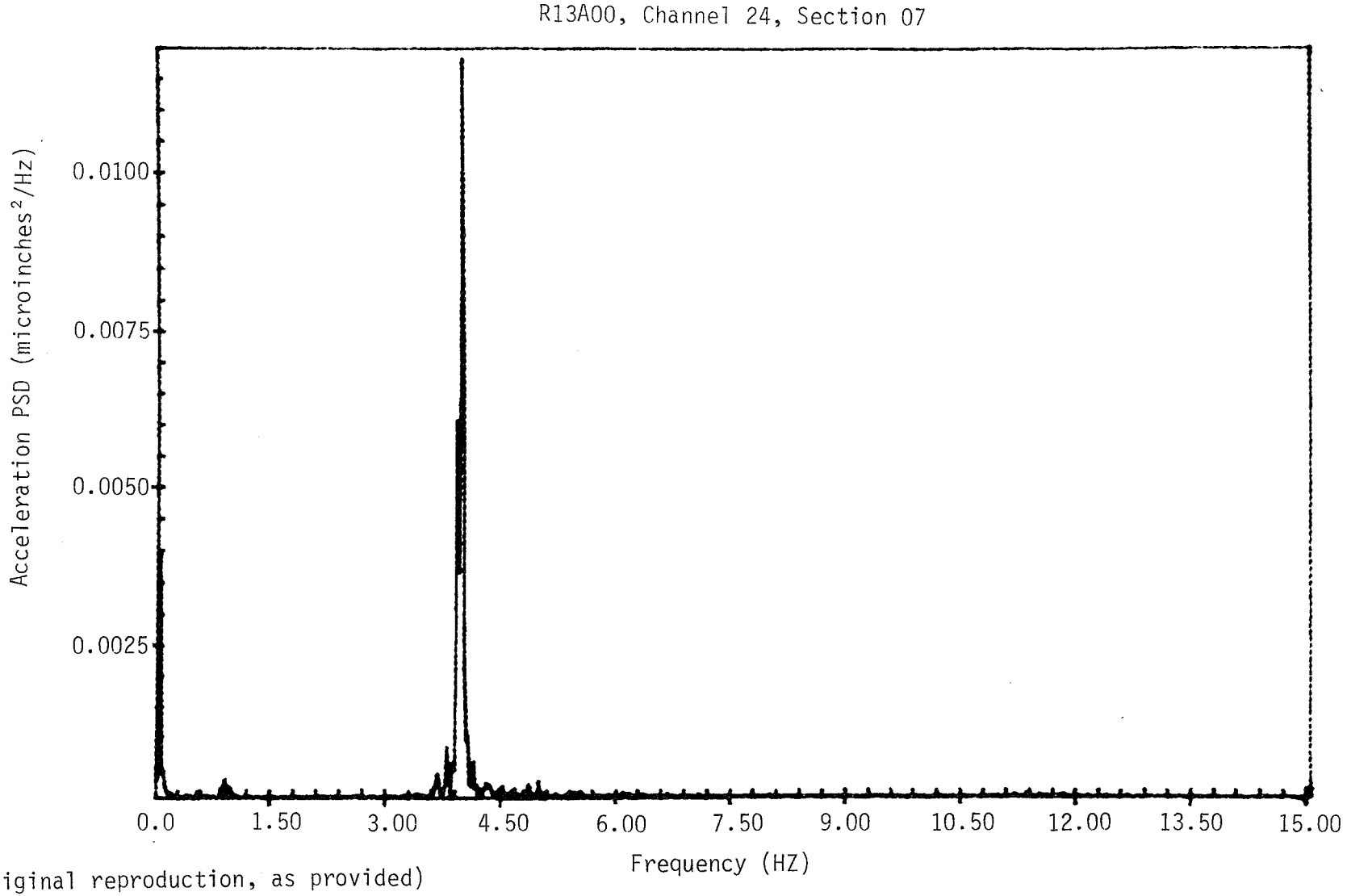

(Original reproduction, as provided)

FIGURE 38. POWER SPECTRAL DENSITY OF TRAILER LATERAL ACCELERATION, 25 MPH CCW, SECTION 07.

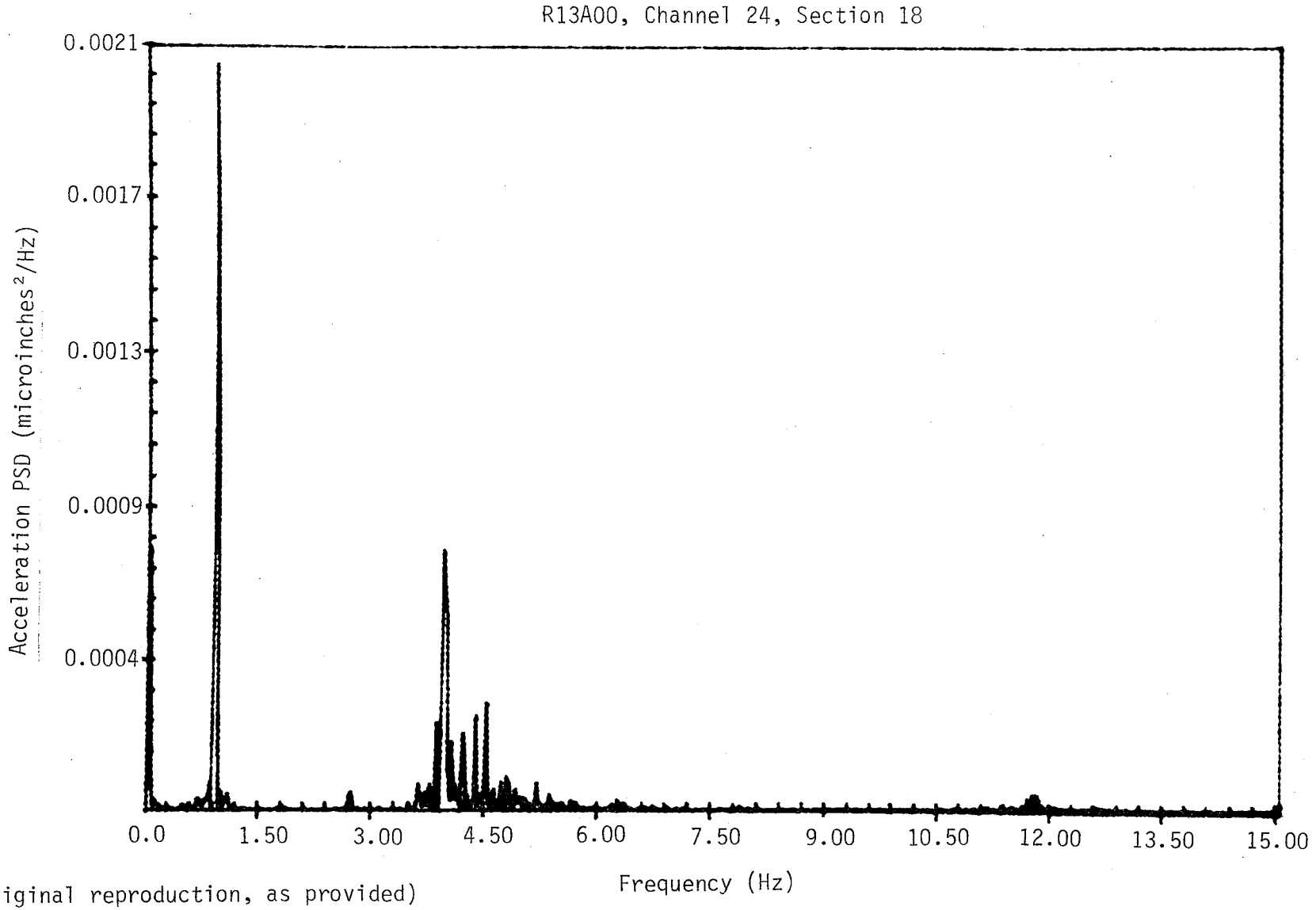

(Original reproduction, as provided)

FIGURE 39. POWER SPECTRAL DENSITY OF TRAILER LATERAL ACCELERATION, 25 MPH CCW, SECTION 18.

TABLE 20. SUMMARY OF FAT II PSD ANALYSIS.

Test Condition					Peak	Max. Strain		Trail.Lat.Acc.		Car Lat.Acc.	
Run #	Car (M or U)	Speed (mph)	Dir.	FAST Sect#	Prime/ Second	Freq (Hz)	Peak X 1000	Freq (Hz)	Peak X 0.001	Freq (Hz)	Peak X 0.001
R14A00	U	45	CCW	18	1	02.67	03.84	04.20	0.84	6.20	0.68
					2	0.84	3.12	6.16	0.62	1.40	0.36
				7	1	7.16	10.68	7.15	8.50	7.15	17.90
					2	0.69	10.50	4.42	0.48		
				3	1	2.41	6.00	6.89	4.10	6.89	7.70
					2	6.90	4.88	4.40	0.48		
R13A00	U	25	CCW	18	1	0.98	16.21	0.98	2.00	11.88	0.19
					2	3.98	0.42	3.90	0.78	3.93	0.17
				7	1	4.05	11.00	4.05	11.80	4.01	3.56
					2	0.90	2.73	0.90	0.40		
R16A00	U	25	CW	20	1	0.88	70.88	0.89	4.40	0.88	0.30
					2	0.54	4.50	0.54	0.27		
				3	1	3.95	8.40	3.96	9.40	3.96	3.38
					2	0.90	3.44	0.90	0.92		
R23A00	M	25	CW	18	1	0.97	63.00	0.97	4.80	0.97	2.00
					2	0.60	11.00	0.60	0.80	2.80	0.12
				7	1	4.35	12.16	4.45	13.00	4.35	1.37
					2	4.71	8.69	4.70	7.80	4.67	0.50

PSD Peak in terms of $(\mu^2)/Hz$ or $(G^2)/Hz$.

sections, and 0.90 Hz for the 25 mph operation in the tangent sections (18 and 20).

The dominant 7.2 Hz frequency observed in the brief, time-variation "snapshots" of Figures 32 and 33, for example, is also evident in the PSD plot. Similarly, Figures 36 and 37 represent the 45 mph case.

9.3 COMPARISONS TO RDL TEST AND COMPUTER MODEL

A series of TOFC vibration tests was performed in the Rail Dynamics Laboratory (RDL) at the Transportation Test Center in past years, beginning in 1976. Also, TOFC dynamic computer models such as the Freight Car Response Analysis and Test Evaluation program[6] (FRATE) have been developed and their predictions compared and parameters adjusted based on these tests. A concise summary of the TOFC resonant frequencies predicted from a recent adaptation[5] of the FRATE model is provided in Table 21.

The dominant frequency of about 7 Hz observed in the FAT II test at 45 mph (Figure 32 and 33) may be a result of the excitation of the trailer yaw resonance predicted at 6.1 Hz by the FRATE model. As noted above in Section 3.2.1, the apparent lateral spring constant measured in this test was 71% greater than the effective value used in the FRATE model. Since resonant frequency is proportional to the square root of the spring stiffness, a 30% greater resonant yaw frequency, or about 8 Hz, might be theoretically predicted.

One of the dominant frequencies of about 1 Hz observed in the FAT II test at 25 mph (Table 20) may be associated with the carbody yaw, trailer roll and yaw at a frequency of 0.90 Hz or the carbody yaw, trailer high center roll at 1.59 Hz. In the TOFC analytical study it was stated that "when the TOFC freight car is traveling on staggered joint rail at speeds in the 20-30 mph range there will be a tendency for the vehicle to respond in its first yaw resonance".

From the RDL test program for roll mode excitation of the loaded TOFC coupled trailer, and carbody roll, resonances were observed at 3.7, 6.2 and 8.4 Hz. A tabulation of these and other resonances excited by the roll test mode on the vertical shaker system[12] is represented in Table 22.

TABLE 21. TOFC RESONANT FREQUENCIES (FRATE).

	Frequency (Hertz)	Description of Reponse Motion
1	.56	Low center roll
2	.90	Carbody yaw, trailer roll and yaw
3	1.59	Carbody yaw, trailer high center roll
4	1.70	Carbody vertical translation and body bending
5	1.76	High center roll
6	2.2	Carbody pitch
7	2.9	Trailer roll
8	4.5	Trailer pitch and carbody bending
9	6.1	Trailer yaw
10	9.0	Carbody second bending
11	10.4	Carbody torsion

TABLE 22. RESONANT FREQUENCIES FROM RDL TEST (ROLL MODE EXCITATION).

Trailer on Flatcar Description	Hertz
Roll with Low Center	.539
Van Trailer Roll	1.131
Carbody Roll with High Center	2.330
Platform Trailer Roll	2.681
Coupled Trailer & Carbody Roll	3.747
Coupled Trailer & Carbody Roll	6.222
Coupled Trailer & Carbody Roll	8.425
Carbody Torsion	12.936

10.0 CONCLUSIONS AND RECOMMENDATIONS

10.1 CONCLUSIONS

Certain tentative conclusions are suggested by the above static, dynamic, and fatigue analyses:

Significant fatigue damage might be expected from measured stress history records such as those illustrated for normal fully loaded operation over the FAST track. Based on conservative fatigue design analyses using measured strains as well as accelerations, fatigue cracking of the hitch plate would be predicted prior to 5,000 miles of FAST operation.

Prior loss of underdeck hitch support does not appear to be a necessary precondition for the occurrence of hitch cracking within the 180,000 miles of FAST operation experienced by the subject flat car before cracks were discovered.

In addition to the 100% fully loaded condition, frequent curve negotiation per mile and the resulting significant lateral load variations appear to be one of the distinguishing features of FAST operation, in comparison to usual revenue service, that contribute to accelerated fatigue life testing of rolling stock.

The lateral dynamic response and resonances of the TOFC excited by FAST operation at both 25 and 45 mph appear to be responsible for most of the hitch fatigue damage.

The vertical load distribution between the two struts of the hitch was significantly unequal in this test and may have contributed to the high strain range in the critical plate area.

10.2 RECOMMENDATIONS

Some follow-up revenue service tests of the TOFC configuration, including curve negotiation, would appear to be justified in order to qualify the extension of these FAST results. Monitoring of only a few selected transducers, with emphasis on lateral load detection, would be adequate as a start.

Subject to such road service test confirmation, more design attention should be focused on the TOFC system lateral response when evaluating structural integrity of designs. This increased attention might be manifested by inclusion of additional data and guidelines in the AAR Fatigue Specification as well as the introduction of appropriate hitch design innovations to modify lateral dynamics and/or reduce critical stress levels. The current AAR specification[13] only requires that the hitch withstand "without damage" a static lateral load of 27 kips.

Although cracking was predicted to occur in the fatigue analysis presented in this report, an apparent discrepancy in predicted and observed miles to crack exists. Several reasons for this "discrepancy", which identify the

elements of conservation built into the fatigue design guidelines, have been discussed. Nevertheless, more work is needed to fully resolve the discrepancy.

Further fatigue analysis method development is needed in order to provide more explicit and reliable design guidelines for complex welded structures that appear to defy the nominal stress approach. A pertinent practical example of such an alternative approach that uses local off-notch or "hot spot" measured strains at weld toes has recently been published[14]. This approach makes application of the technology on weld fatigue that has been developed in connection with welded tubular structures in offshore drilling platforms and uses hot-spot strain-life curves provided by the American Welding Society. Future rail vehicle and component fatigue tests should incorporate some hot spot strain measurements to facilitate the evaluation of this method.

11.0 REFERENCES

1. Association of American Railroads, "Fatigue Design of Freight Cars," Chapter VII of Manual of Standards and Recommended Practices, Section C - Part II, Specifications for design, fabrication and construction of freight cars M-1001, Volume 1, Revision of March 1, 1979.

2. Moyar, G. J. and J. E. Burns, "Freight Car Fatigue Analysis Test on FAST." Department of Transportation Report no. FRA/TTC-80-04, July 1980.

3. Personal communication between E. J. Wolf (Trailer Train Co.) and S. K. Punwani (AAR).

4. Personal communication between E. J. Wolf (Trailer Train Co.) and G. J. Moyar (consultant to AAR) dated 7/1/82.

5. Kachadourian, G., "TOFC Lading Response for Several Track Profiles and Hunting Conditions." Department of Transportation Report no. FRA/ORD-80/3, April 1980.

6. Kachadourian, G., N. E. Sussman and J. R. Anderes, "FRATE Volume 1: User's Manual." Department of Transportation Report no. FRA/ORD-78/59, September 1978.

7. Simon, R., R. Proszowski and A. M. Zarembski, "RAINFLOW Counting Program -- User's Manual," AAR Report R-274, August 1980.

8. Pellini, W. S., "Guidelines for Fatigue - Reliable Design of Steel Structures," AAR research report R-490.

9. Personal communication between Punwani (AAR) and Wolf (TTX) on road test data.

10. Personal communication between S. K. Punwani (AAR) and ASF personnel on peak level crossing program.

11. Tuten, J. M. and H. D. Harrison, "Final Report on FAST Wheel/Rail Loads Wayside Data Reduction to FRA," Battelle Lab. report of September 30, 1980.

12. Kachadourian, G. and N. E. Sussman, "Validation of FRATE - Freight Car Response Analysis and Test Evaluation." Paper presented at ASME 1977 Winter Annual Meeting, November 28, 1977.

13. AAR Manual of Standards and Recommended Practices, Section I, Specially Equipped Freight Car and Intermodal Equipment. Specification M-928-80 Highway Trailer Hitches for Freight Cars (1980 Revision).

14. Leever, R. C., "Application of Life Prediction Methods to As-Welded Steel Structures," ASME International Conference on Advances in Life Prediction Methods presented at The Materials Conference, Albany, NY, April 18-20, 1983.

APPENDIX 1. INSTRUMENTATION

The instrumentation used for each of the two-phase dynamic test program, as well as the preliminary static tests, included strain gages and accelerometers. Some of the strain gages were single gages on rosettes while others were wired in accordance with vertical and lateral measuring schemes. These are described in detail.

Figures 4 and 5 show all measurement channels wherein strain gages were used. Channels #15 and #16 were multiple gages wired in a circuit to measure the vertical load on the right and left struts, respectively. Early in the experiment, so-called "Poisson" gages were included in the bridge circuit in place of the circuit-completion resistors shown in Figure A1.1 for the vertical struts. However, the electrical resistance of these gages varied unaccountedly during initial testing and they were subsequently replaced by the circuit-completion resistors. Channel #20 also used multiple strain gages to measure lateral load on the hitch. The wiring diagrams for these three transducer bridge circuits is shown in Figure A1.1. The single gages (Channels #1 and #2, for example) were applied at locations where cracks had occurred or at locations where it was felt that the stress pattern was not clear. Accelerometers were applied, as shown in Figure 6, in order to gain an understanding of the dynamic behavior of the car and trailer.

ALD markers on the FAST track were used for ground reference. Speed and time code data were also recorded on separate channels. The T-8 instrument car was used for data collection. The data acquisition system utilized a PDP 11/34 computer. Data were filtered for 100 Hz low pass and digitized at 256 samples/sec. The digitized data were stored in binary format. Selected channels of data were examined for "quick look" purposes, using the "quick look" program available on the system. This permitted examination of selected channels of data over previously delineated track sections. Minimum, maximum and mean values were printed out.

The static tests also utilized the same transducer channels, except for ALD markers and speed. Applied force, as measured by a load cell, was also recorded by the data acquisition system of the T-8 instrument car. The "quick look" output was also employed for the static tests.

The strain gages were 120 ohm and the accelerometers were the Kestter piezo-resistive type with ± 5g range. Generally, 10 volt excitation was used. A digital count of 8196 was used over the transducer range.

The vertical and lateral force transducer schemes, as shown in Figure A1.1, did not function as well as had been anticipated. The principal problem was the crosstalk between vertical and lateral load applications.

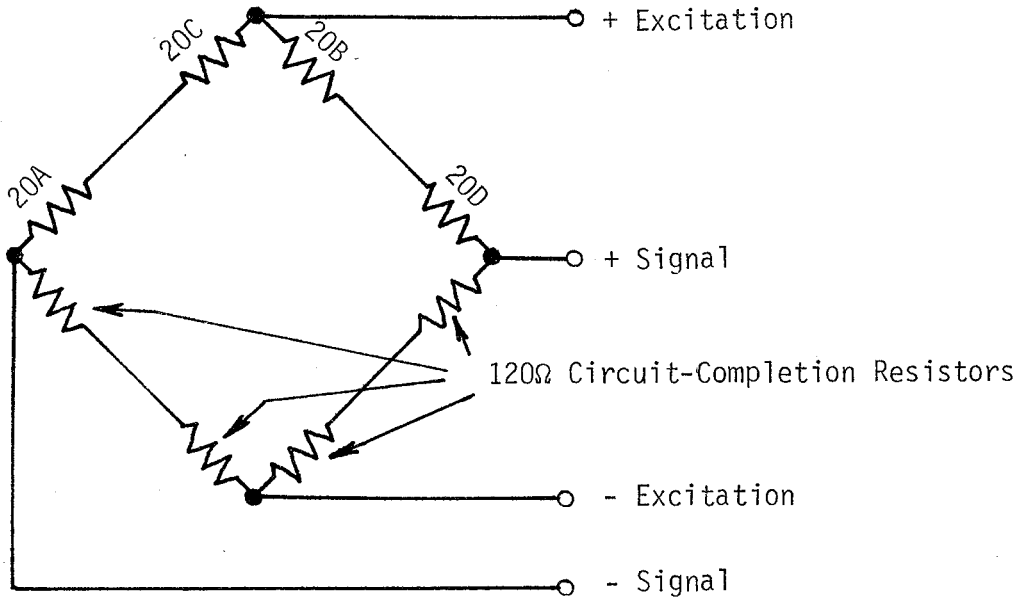

Lateral "Load" Bridge

Vertical Strut "Load" Bridges

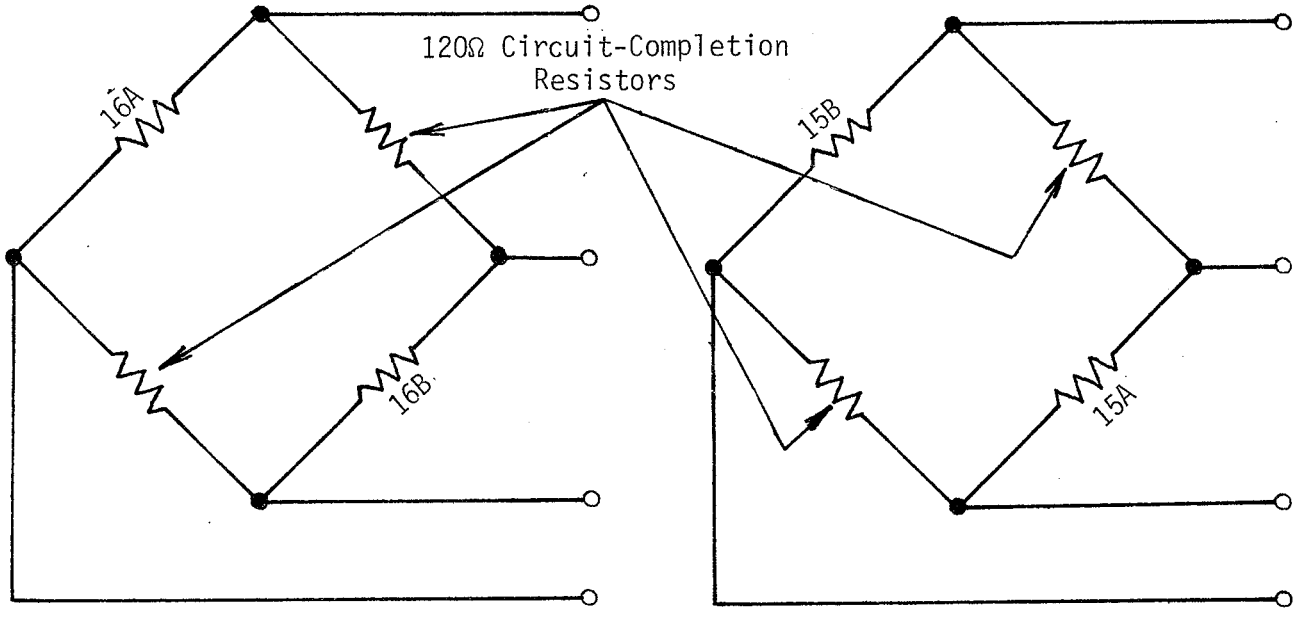

Left Strut

Right Strut

FIGURE A1.1. TRANSDUCER BRIDGE CIRCUITS.

APPENDIX 2. STATE OF STRESS CONSIDERATIONS

The great bulk of fatigue data is based on uniaxial stress or loading tests. However, even when data from fatigue tests of actual structural details are available to establish Modified Goodman Diagrams, it is important to consider the state of stress and its variation near the critical region of the actual design in comparison to the tested configuration.

A conventional method of design evaluation in a biaxial situation involves placement of a single strain gage perpendicular to the expected route of crack propagation or in the direction of maximum principal stress. Then the strain measured by this gage is simply multiplied by the elastic modulus to obtain an approximation of the significant design stress. This often provides a reliable index of stress except when the principal stress components have opposite signs or when there is significant shear in a plane perpendicular to the plate surface in the region of expected crack initiation. In this case the approximate uniaxial or conventional stress would be unconservative if uniaxial fatigue data were being used because the maximum range of shear stress has a dominant effect on crack initiation.

In order to test for the possibility of this situation and assess how satisfactory the conventional assumption would be, the output from the lower left hitch plate location, where full (3-leg) rectangular rosette strain gages were placed, was examined during several time periods. For example, the biaxial stress components derived from Hooke's general elastic law, as well as the "so called" effective stress, are displayed in Figure A2.1 for the same 1.2-second time period previously selected for the display of horizontal gage strains shown in Figure 32. Note that the horizontal and vertical stress components are in phase and usually of the same sign. The orthogonal shear stress (acting on horizontal and vertical planes) is relatively low. In effect, the horizontal and vertical gages are nearly aligned in the principal directions. Since these components are of the same sign in most cases, the shear stresses on planes perpendicular to the plate surface are relatively small, even for those planes at or near the plane of maximum stress (about 45 degrees from vertical or horizontal). The greatest shear then occurs in planes that are oriented at 45 degrees to the plate surface and have a magnitude equal to one-half the maximum principal stress. This is a situation similar to simple uniaxial stressing.

In the legend notations of Figure A2.1, the maximum range of the stress component for this time period is given parenthetically following the stress component name.

The given plane selected for display of shear stress is one of the 45 degree planes perpendicular to the plate surface that bisects the vertical and horizontal directions. The range of this stress is 6.80 ksi. Note that the range of the maximum shear stress is only one-half this range. This is because only the positive direction shear stress was plotted as "maximum shear stress".

Since the greatest range of normal stresses (horizontal) is approximately 20 ksi, the corresponding range of shear stress on the plane at 45 degrees to

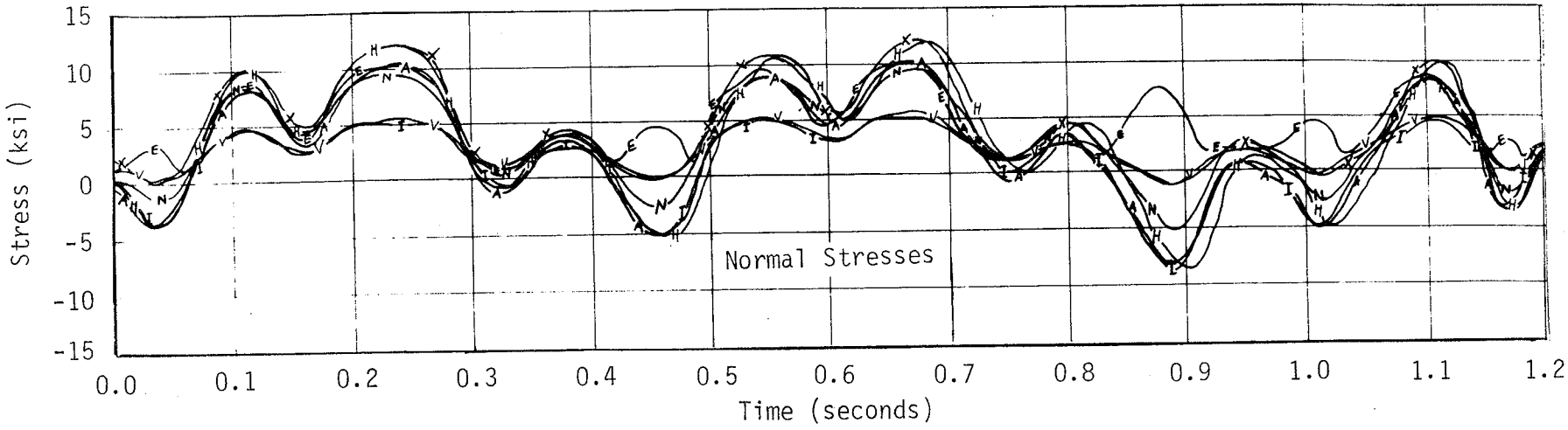

Normal Stresses (Range in ksi)

H = Horizontal Stress Component (20.18)

I = Minimum Principal Stress (13.63)

A = Approximate Stress (18.20)

V = Vertical Stress Component (6.57)

N = Normal Stress at a given Plane (14.08)

X = Maximum Principal Stress (13.1)

E = Effective Stress (9.12)

Shear Stresses (Range in ksi)

S = Shear Stress Component (1.34)

Σ = Maximum Shear Stress (3.38)

F = Shear Stress at a given Plane (6.80)

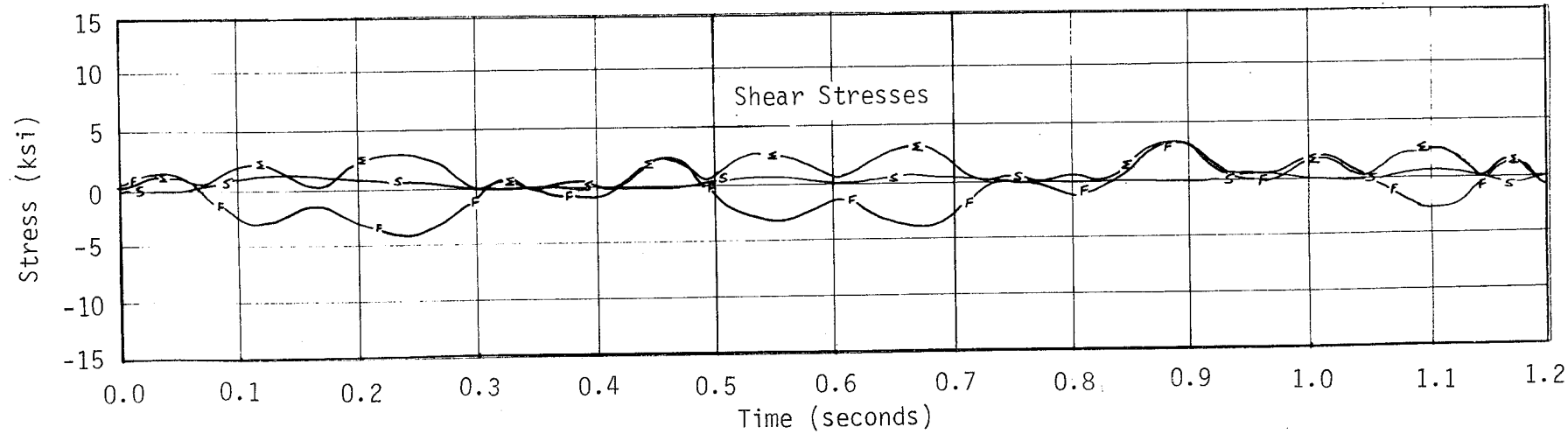

FIGURE A2.1. BIAXIAL STRESS COMPONENTS FROM ROSETTE STRAIN GAGES 7, 8, AND 9.
(Run #14 CCW at 42 mph, Near End of First Lap in FAST Section 07 at tie 0668)

the plate surface is 10 ksi, which is greater than the shear stress ranges on planes that are perpendicular to the plate surface. This confirms the selection of the horizontal stress component, or its corresponding simple approximation, as a satisfactory index of stress for fatigue evaluation. In this case, the range of approximate stress is 90 percent of the range of the actual horizontal stress.

Note that the range of "effective stress" is only 9.12 ksi. This is because (from the definition of effective stress) the positive square root of the sum of the squares of the principal stress differences is taken. So this quantity alone is not a reliable stress index in this instance.

The equations used to obtain the orthogonal stress components are for shear stress

$$\tau_{HV} = \frac{E}{2\ (1 + \mu)}\ [2\ \varepsilon_D - (\varepsilon_H + \varepsilon_V)] \qquad (1)$$

for horizontal normal stress

$$\sigma_H = \frac{E}{1 - \mu^2}\ [\varepsilon_H + \mu\varepsilon_V] \qquad (2)$$

and for vertical normal stress

$$\sigma_V = \frac{E}{1 - \mu^2}\ [\varepsilon_V + \mu\varepsilon_H] \qquad (3)$$

Where:

E is Young's elastic modulus
μ is Poisson's ratio
ε_H is the measured horizontal strain
ε_V is the measured vertical strain
ε_E is the measured strain on 45 degree diagonal

The effective stress, in terms of the orthogonal stress components, is

$$\sigma_{eff} = \sqrt{\sigma_H^2 + \sigma_V^2 - \sigma_H\ \sigma_V + 3\ \tau_{HV}^2} \qquad (4)$$

The principal stresses are

$$\sigma_{max} = \frac{\sigma_H + \sigma_V}{2} + \sqrt{\left(\frac{\sigma_H - \sigma_V}{2}\right)^2 + \tau_{HV}^2} \qquad (5)$$

$$\sigma_{min} = \frac{\sigma_H + \sigma_V}{2} - \sqrt{\left(\frac{\sigma_H - \sigma_V}{2}\right)^2 + \tau_{HV}^2} \qquad (6)$$

The expressions for the normal and shear stress on any plane that is perpendicular to the plate surface are:

$$\sigma = \frac{\sigma_H + \sigma_V}{2} + \frac{\sigma_H - \sigma_V}{2} \cos 2\phi + \tau_{HV} \sin 2\phi \qquad (7)$$

$$\tau = - \left(\frac{\sigma_H - \sigma_V}{2}\right) \sin 2\phi + \tau_{HV} \cos 2\phi \qquad (8)$$

where ϕ is the angle from the horizontal direction to the normal vector on the plane in question. For principal planes

$$\tan 2\phi = \frac{2\ \tau_{HV}}{\sigma_H - \sigma_V} \qquad (9)$$

As a closing cautionary note, it should be recognized that these biaxial stress observations are based on data from rosette gages at only one location. The state of stress at the top of the hitch plate, where maximum strains were observed (Gage #5), may well be different. However, since cracking was also observed in the rosette gage location, these observations do have some pertinence.

APPENDIX 3. LOAD AND ACCELERATION STRESS CONVERSION FACTORS

In order to relate selected accelerometer channel data as well as the lateral load bridge circuit channel (#20) to the fatigue critical stress, several analytical and/or experimental steps are necessary. First, the measured quantity must be related to the critical component load. Then the critical local stress must be related to this load. Generally, this is not a straight forward process. However, in order to illustrate this process in the simplest way, the "stress conversion factors" for these channels will be derived in an approximate manner in the following pargraphs.

Lateral Trailer Acceleration (Channel #24)

It is assumed that the lateral accelerometer in question (attached to the bottom of the trailer at mid-length) is actually located at the trailer center of gravity. Further, it is assumed that the lateral inertia of the trailer is resisted by the hitch and wheels in the same proportion as the static vertical load is supported. For a trailer weight (excluding tandems) of 60 kips, with CG 20 feet from the trailer front, a hitch located 3 feet from the trailer front, and a tandem centered 27 feet from the hitch--the lateral load on the hitch, H, may be shown to be

$$H = 10/27 \times 60 \times G = 22.22\ G \text{ kips}$$

where G is the lateral acceleration relative to the acceleration of gravity.

On the basis of the static lateral load tests, the 1 kip lateral load was found capable of producing a strain as high as 100 μ inches/inch in the critical gage (Channel #5). In terms of the approximate uniaxial stress, a 1 kip lateral load would then cause a stress of 3 ksi. Therefore, the stress conversion factor for Channel #24 would be

$$\text{Hitch plate ksi/G} = 22.22 \times 3 = 66.66.$$

Vertical Acceleration at the Car Center Plate (Channel #29)

It is known from the load/empty tests that the stresses induced in the hitch plate are relatively small for a 1G vertical load. So, instead of focusing on the hitch we propose to illustrate the conventional vertical dynamic car design evaluation approach and consider the stress in the car center sill at mid-length. From the static live load test the stress conversion factor is known to be

$$\text{center sill ksi/G} = 9.72.$$

Hitch Lateral Load Bridge (Channel #20)

Based on the static lateral load tests, the sensitivity of Channel #20 appears to have varied significantly with vertical load, unfortunately. The output strain varied from 8 μin/in for a 1 kip pull on the trailer to 20 μin/in for a 1 kip pull directly on the hitch. Let us simply use an average value of 14. Then, since a 1 kip hitch load can cause a 100 μin maximum plate strain or 3 ksi stress, the lateral load bridge stress/hitch stress conversion factor is

$$\text{Hitch plate ksi/lat. bridge strain} = 3/14 = 0.214.$$

Lateral Car Body Acceleration (Channel #30)

In the strictest sense, it is not possible to derive the hitch plate stress from this single measure of acceleration. Even if rigid body translation of the car is assumed, it is necessary to know the simultaneous motion of the trailer and the division of load between wheels and hitch in order to draw some conclusions about the force transmitted through the hitch. When the accelerating car body is considered in isolation, dynamic equilibrium requires the specification of force at the car/trailer interface as well as the car/truck interface. To avoid this complexity it is simply assumed, for illustrative purposes, that the lateral inertia of half the car is resisted only by the trailer and that the fraction resisted at the hitch relative to the tandem wheels is in the same proportion as the static weight distribution. For this "rough" approximation the car body light weight is taken as 60 kips. The lateral hitch force would then be

$$H = 10/27 \times 60/2 \times G = 11.11 \text{ kips.}$$

The corresponding stress conversion factor is

$$\text{Hitch plate ksi/G} = 3 \times 11.11 = 33.33.$$

This approach may well be thought conservative since higher stress than actual would be predicted.

APPENDIX 4. DESCRIPTION OF FAT II DATA BASE

All of the FAT II data were generated on the T-8 instrument car with the data acquisition GPAQ software, resident on the PDP 11/34 computer. The DEC-20 requires the data to be in 16-bit ASCII format. A program was originally written, though not completely documented, to convert data tapes, as received from TTC, to the DEC-20 system compatible ASCII format. However, this still left data in a somewhat hard to handle format. Technical Services then suggested the use of the 1022 Data Base System software, which is provided by Digital Equipment. This permitted the data to be stored and structured in accordance with the 1022 Data Base software. This software permits quick access, particularly for selected variables, and other statistical processing. Also, data files can be built for use with other programs with same ease. Tapes received from TTC in PDP 11/34 format were converted to ASCII and the data stored again on tape, in format compatible with the 1022 Data Base System. Where necessary, runs were broken into data blocks of 100K size. The longest run, Run 14 (33 channels, 100 samples/sec 7 to 10 minutes data) was stored as Runs 14A, 14B and 14C. Since the data were kept on tape, disk space requirements were minimized. This does somewhat inconvenience the analyst but is acceptable provided disk space is available for at least one segment, example Run 14A, of the run.

A listing of FAT II data tapes is shown in Table I.

Other programs were written for use with FAT II data, but are potentially useful for other data. These are:

a) FATSEE
b) FATPOS
c) FATACC
d) PSD Program
e) FATLEV

A very concise description is given here. A detailed program listing can be provided.

FATSEE

This is a program to examine the time history of a selected channel of data in graphical form and to provide minimum-maximum values.

FATPOS

This program provides a Percent Occurrence Spectrum for a selected channel of data.

FATACC

This (basically) extension of the FATPOS program permits accumulation of additional data to update the Percent Occurrence Spectrum of an existing data set. Individual FAST runs can be processed in parts, each from a different tape.

TABLE I. CATALOG OF FAT II CONVERTED DATA TAPES.

CAR	DIR.	SPEED	RUN#	VOLIDS*	FILES CONTENTS	NUMBER OF COMPUTER PAGES	NUMBER OF RECORD IN EACH DATA FILES	ACCESS TO RESTORE ON DISK
UNMO	CCW	25 MPH	R13	R13	R13.MAS	2		BETA:<DUMP>
					R13A00.DAT, DMS	8430, 3	100,000	
					R13B00.DAT, DMS	5232, 3	62,000	
	CCW	45 MPH	R14	R14A	R14.MAS	2		BETA:<ALP>
					R14A00.DAT, DMS	8438, 3	100,000	
					R14B00.DAT, DMS	8438, 3	100,000	
				R14B	R14C00.DAT, DMS	11425, 3	134,407	
			R15		R14D00.DAT, DMS	7584, 3	89,880	
	CW	25 MPH	R16	R16	R16.MAS	2		BETA:<ALP>
					R1600.DAT, DMS	12515, 3	148,320	
	CW	45 MPH	R17	R17A	R17.MAS	2		BETA:<ALP>
					R17A00.DAT, DMS	8438, 3	100,000	
					R17B00.DAT, DMS	8438, 3	100,000	
				R17B	R17C00.DAT, DMS	8316, 3	98,560	
			R18	R18	R18A00.DAT, DMS	8438, 3	100,000	BETA:<ALP>
					R18B00.DAT, DMS	2185, 3	25,880	
MODI	CCW	25 MPH	R20	R20A	R20.MAS	2		BETA:<ALP>
					R20A00.DAT, DMS	8438, 3	100,000	
					R20B00.DAT, DMS	8438, 3	100,000	
					R20C00.DAT, DMS	2757, 3	32,674	
	CCW	45 MPH	R21	R21A	R21.MAS	2		BETA:<ALP>
					R21A00.DAT, DMS	8438, 3	100,000	
					R21B00.DAT, DMS	8438, 3	100,000	
				R21B	R21C00.DAT, DMS	8438, 3	100,000	
					R21D00.DAT, DMS	5033, 3	59,640	
					R21E00.DAT, DMS	6952, 3	82,440	
	CW	25 MPH	R23	R23A	R23.MAS	2		BETA:<DUMP>
					R23A00.DAT, DMS	8438, 3	100,000	
					R23B00.DAT, DMS	3571, 3	42,320	
	CW	45 MPH	R24	R24A	R24.MAS	2		BETA:<ALP>
					R24A00.DAT, DMS	8438, 3	100,000	
					R24B00.DAT, DMS	8438, 3	100,000	
					R24C00.DAT, DMS	6453, 3	76,480	

* Volume Identification

PSD

This is a standard Power Spectral Density Program adapted for use on the DEC-20.

FATLEV

This program defines the occurrences per mile for crossing predefined levels of any single data channel. This program was developed to permit comparisons with previously obtained data on revenue track.

Use of "Quick Look" Programs on PDP 11/34 (at TTC)

Since the FATSEE program is not very efficient in scanning through data channels individually, TTC was requested to use the "Quick Look" programs, available on the T-8 PDP 11/34 computer as well as the PDP 11/60, to scan through all of the data runs to provide min/max/mean values. Additionally, static data plots (Force vs. Strain) were done using the "Quick Look" programs.

APPENDIX 5. SUMMARY OF DATA CONVERSION PROGRAM

The following programs provide a quick insight, as to scope and content, into the process of converting binary data into 16-bit ASCII data, for use on the AAR DEC-20 system.

1. Main Program: FAT II.EXE

Purpose: This program converts FAT II PDP-11 tapes to ASCII sequential files on disk. The FAT II.EXE skips header records and creates output files as described below.

Input files:

I PDP-11 tape file. One such file contains two record types: 1) header records and 2) data records.

II FAT II.CMD is a control file for FAT II.EXE with file specification and other parameters.

Output files:

I Runid.MAS
This contains records with header information and is appended to the 1022 Bundled data set Master.DMS. After appending file deleted.

II Runid.DAT: Data file
It contains information extracted from data record. An unbundled 1022 data set is generated for each of these. Because data sets are unbundled, the file must reside on disk when being accessed with 1022.

2. Main Program: 1022.EXE

Purpose: 1022.EXE is a software package that processes sequential file into data sets for fast retrieval of records.

Two types of data sets can be made:

1) Master.DMS is a bundled data set with all header records from all PDP-11 tapes. Records from specific files on tapes can be found by run identification number (RUNID) and tape file number.

2) Runid.DMS are unbundled 1022 data sets named by the user. One of these files is generated for every data file.

3. Main Program: Random.EXE and Random.FOR

Purpose: This program creates a random access file from a sequential data file that contains record information for a particular run.

The user must enter the name of the sequential data file and the output data file. The random access file may be given the same name as the sequential data file because a random access file must have records size specified in the open statement. This program can only create random access files with a record length <=99 characters.

The output file obtained from FAT II.EXE with name Runid.MAS should be randomized to run FATSEE, FATPOS, FATACC, and FATLEV.

APPENDIX 6. SUMMARY OF DATA REDUCTION PROGRAMS

1. Main Program: FATSEE

Purpose: This program allows the user to view the data on a specified channel for a given FAT II run. The user may view the entire file in one session or choose a particular portion of the file to view. In addition, the user may choose to print out a part of the file that is of interest.

Output: The file appears on the terminal or the print out as an "oscillogram". At the left is the time in hours, minutes, seconds, and milliseconds. Then, in the fifth column is the tachometer reading. The engineering values of the measurement on the specified channel are given in the sixth column. At the seventh column, the ALD marker appears with either the "!" or " " sign. A batch of " " signs indicates a real ALD marker on the track and with this information the user can find the location on the FAST track. Finally, on the right is the oscillogram itself which consists of a line at the left corresponding to minimum value of measurement, a line at the right corresponding to the maximum value of measurement, and a zero line (if zero falls between maximum and minimum values). The data point is plotted in this field. The user is required to have (RUNID.MAS) master file on disk each run to convert data into engineering units. Also, the input run file must be made in the following way:

RUN, SEC, SUB
example: R14A00

2. Main Program: STRSEE

Purpose: This program allows the user to view state of stress values instead of data in a FATSEE program for the specified lateral, diagonal, and vertical channel measurements.

The rest of the features are almost the same as in FATSEE. In this program, the user can also create a file on the disk an then may choose to print out. The user has to supply maximum and minimum values for the specified state of stress quality calibration factors from the RUNID.Master file to convert data into engineering units. The user can choose to view or to print any kind of state of stress one at a time from the following state of stress options (quantities expressed in psi unless otherwise stated below):

(i) Horizontal stress component
(ii) Vertical stress component
(iii) Shear stress component
(iv) Maximum principal stress
(v) Minimum principal stress
(vi) Principle direction (in degrees)
(vii) Equivalent stress
(viii) Normal stress component
(ix) Shear stress at any given plane

(x) Normal stress at any given plane
(xi) Effective stress at any psi
(xii) Maximum shear stress in psi

3. Main Program: FATLEV

Purpose: This program counts the number of level crossings (at specified levels about a specified base value) in a FAT II time history. The distribution of these counts is used for comparison with level crossing data from other tests.

This program has the same accumulation feature as in the case of FATPOS and FATACC. This program can allow the user to count the number of level crossings above and below the base level for a specified RUNFILE and a specified channel and also accumulate the previous RUNFILE/FILES and previous channel values of a number of level crossings. In this program one can select maximum numbers of level up to 20. This program requires master file (Runid.MAS) to convert data into engineering units.

4. Main Program: FATPOS

Purpose: This program counts the cycles in a selected portion of a FAT II run and generates the resulting percent occurrence spectrum. This program also calculates fatigue life in miles from percent occurrence spectrum.

Output: The following output file is generated by the program:

(i) RUNFILE.RNG: A normalized range distribution histogram (example Figure 23).

(ii) RUNFILE.POS: A percent occurrence spectrum of time history.

(iii) RUNFILE.MAP: An intensity map of the percent occurrence spectrum.

(iv) RUNFILE.TAB: The percent occurrence spectrum in tabular form. This will be used as input data file to FLAP.

(v) RUNFILE.NOS: A number occurrence spectrum of the time history.

This program has the option for accumulation for specified runfile and for a specified channel. To convert data into engineering units the Master file (RUNID.MAS) is required on disk. Also, this program has an option to calculate fatigue life for specified strength values, specified values of slope of S-N Curve and specified values of conversion factor (to convert strain into stress or acceleration to stress). Accumulation of run files is done by FATACC.

For more information refer to listing FATPOS.

5. Main Program: FATACC

Purpose: This program takes the accumulated range distribution and percent occurrence spectrum.

Output: Output file generated by the program has a name beginning with RUNID and all file extensions remain the same as in the case of FATPOS. This program has an option to calculate fatigue life with fatigue strength other than the previous selected fatigue limit. This program can be used after FATPOS.

For more information refer to listing of FATACC.FOR.

6. Main Program: FLAP

Purpose: To calculate fatigue life in miles for specified Road Environment Percent Occurrence Spectrum for a specified material properties.

This program is based on the Interim AAR Guidelines for Fatigue Analysis of Freight Cars. The output will show input stress spectra, material properties, and total expected fatigue life. This program has an option to print or to view output file. In our analysis, percent occurrence spectrum file in a tabular form (RUNFILE.TAB or RUNID.MAS) is used as a input to FLAP.

For more information refer to "Guide to Fatigue Life Analysis Program (FLAP)" Report No. R-273.

7. Main Program: PSD.FOR

Purpose: This program calculates the Power Spectrum Density (unit squared/Hz) and frequency in Hz for a specified channel data (number of data points used in our analysis = 4096) and plots the graph (PSD vs. Frequency) on the Tectronix terminal.

This program uses AVTEX.FOR subroutine to plot PSD versus frequency. To get a hard copy of the graph, the user has to use a copy command.

Logical Basis: The power spectral density function of random data describes the general frequency composition of the data in terms of the spectral density of its mean square value. The mean square value of a simple time history record in a frequency range between f and f + df may be obtained by filtering the sample record with a bandpass filter having sharp cut-off characteristics and computing the average of the squared output from the filter. This average square value will approach an exact mean square value as observation time T approaches infinity. In equation form,

$$\Psi_x^2 (f, \Delta f) = \lim_{T\to\infty} \frac{1}{T} \int_0^T x^2 (t, f, \Delta t)\, dt$$

where x (t, f, Δt) is that portion of x (t) in the frequency range from f to f + Δf.

For small Δf, a power spectral density function G_x (f) can be defined such that

$$\Psi_x^2 (f, \Delta f) \simeq G_x (f)\, \Delta f$$

$$G_x (f) = \lim_{\Delta f \to o} \frac{\Psi_x^2 (f, \Delta f)}{\Delta f}$$

The quantity $G_x (f)$ is always a real-valued, non-negative function. An important property of the spectral density function lies in its relationship to auto correlation function. Specifically, for stationary data, the two functions are related by a Fourier transform as follows,

$$G_x (f) = 2 \int_{-\alpha}^{\alpha} R_x (T)\, e^{-j2fT}\, dT = 4 \int_{o}^{\alpha} R_x (T) \cos 2\pi fT\, dT$$

where R_x is real part of complex number.

Subroutine: AVTEX.FOR

Purpose: To plot the specified quality of data on the Tectronix terminal.

In our analysis this subroutine was used to plot PSD vs. Frequency in the PSD.FOR program. In the subroutine, various other subroutines are used to draw axes, to find maximum and minimum, and to select scale, etc. All of these subroutines are in the area <FORT>.

Output: example in Figure 38.

Use of DEC 20 Data Base Structure

Use to select the portion of data and extract selected data or data information such as time, ALD marker, channels, etc. Also use to find maximum and minimum for specified channel(s) and to find actual ALD marker. The following program is used to locate the real ALD mark with data base structure.

TESTAC.DMC:

Print record numbers wherever real ALD mark occurs in the data.

Typ.DMC:

Will type on the terminal record the number, time in hours, minutes, seconds, and milliseconds, tachometer, ALD, etc.

After the ALD equal to 1 appears at least 4 times or a maximum of 6 times, and the tachometer value resets to minimum (2 or 3 or 4) from very high values, it shows the real ALD marker.